

Alma Mater Studiorum – Università di Bologna

DOTTORATO DI RICERCA IN
INGEGNERIA CIVILE, CHIMICA, AMBIENTALE E DEI
MATERIALI

Ciclo 33

Settore Concorsuale: 03/B2 – FONDAMENTI CHIMICI DELLE TECNOLOGIE

Settore Scientifico Disciplinare: CHIM/07 – FONDAMENTI CHIMICI DELLE
TECNOLOGIE

BIO-PLASTICS AND TECHNOLOGIES FOR ECO-
SUSTAINABLE PACKAGING

Presentata da: Emanuele Simonini

Coordinatore Dottorato

Prof. Luca Vittuari

Supervisore

Prof.ssa Nadia Lotti

Co-Supervisore

Prof. Maurizio Fiorini

Esame finale anno 2021

Abstract

Transmission welding tests on different eco-sustainable materials were performed using Thulium fiber laser radiation with 2 μm wavelength. All the samples were characterized via infra-red spectroscopy and DSC. The morphology of the materials and the relations between the laser process conditions and the quality of the seam were investigated by means of optical microscopy. Mechanical strength of the weld joints were measured via tensile tests, comparing some of them with different sealing methods and/or original tensile properties of the materials.

The morphology of the non-woven material especially plays an important role, compared to the continuous films, as well as the chemical nature of the samples. The experiments demonstrate new application areas of mid-IR fiber laser sources for materials processing.

Index

1. Introduction	4
1.1 Plastic Industry	4
1.2 Circular Economy	8
1.2.1 Plastics Recycling	9
1.2.1.1 Mechanical Recycling	11
1.2.1.2 Chemical Recycling	12
1.2.1.3 Other Processes	12
1.3 Bioplastics	12
1.3.1 Aliphatic Polyesters	14
1.3.2 Physical Properties	16
1.3.2.1 Structure of Polymers	16
1.3.2.2 Homopolyesters	19
1.3.2.3 Copolyesters	20
1.3.2.4 Thermal Properties	22
1.3.2.5 Mechanical Properties	23
1.3.2.6 Barrier Properties	24
1.3.3 Degradation	26
1.3.3.1 Chemical hydrolysis	27
1.3.3.2 Enzymatic hydrolysis	28
1.3.3.3 Composting	29
1.3.4 Applications	31
1.3.5 Starch-based polymers and blends	32
1.3.6 Cellulose-based polymers	34
1.3.7 Bio-polyesters	35
1.3.7.1 PBS	35
1.3.7.2 BioPBS and Copolymers (PBS BEPS, PBCE BEP CE)	36
1.3.7.3 PLA	39
1.4 Packaging	41
1.4.1 Nonwoven Materials	44
1.4.2 Polymer Welding	46
1.4.2.1 Heat Sealing	47
1.4.2.2 Ultrasonic Welding	48
1.4.2.3 Laser Welding	49
1.4.2.3.1 Laser Sources	49
1.4.2.3.2 Equipment and configurations	50
1.4.2.3.3 Laser-polymers Interaction	51

1.4.2.3.4 Laser welding techniques	53
2. Aim of the work	55
3. Materials and Methods	56
3.1 Materials	56
3.2 Methods	59
3.2.1 Polymer Characterization	59
3.2.1.1 Thermogravimetric Analysis (TGA)	59
3.2.1.2 Differential Scanning Calorimetry (DSC)	59
3.2.1.3 Infrared Spectroscopy (FT-IR)	60
3.2.1.4 Tensile tests	60
3.2.2 Laser welding tests	60
3.2.2.1 Laser system	60
3.2.2.2 Optical Microscopy	62
3.2.2.3 Laser Seal Strength Test	62
3.2.2.4 Heat Seal Strength Test	63
4. Results and Discussion	64
4.1 PLA nonwoven materials	64
4.2 PVA based water soluble film	70
4.3 Protein based water soluble film	73
4.4 PE/BVOHc/PE multilayer	76
4.5 PBSA + PBAT + PLA blend based film	81
4.6 PBSA + PCL + PLA blend based film	84
4.7 Cellulose Acetate + PLA multilayer	87
4.8 Cellulose Acetate + PBS multilayer	90
4.9 P (BCE BEP CE) copolymers	93
4.10 P (BS BEPS) copolymers	96
5. Conclusions	98
6. Acknowledgments	99
7. Bibliography	101

1. Introduction

1.1 Plastic Industry

Since 1950s, even if nitrocellulose was born at least 100 year earlier, plastics mass production changed our lifestyle with 360 degrees improvements; this is why we kept synthesizing plastic for 70 years, arriving worldwide at 359 Mtons in 2018 (Figure 1.1).

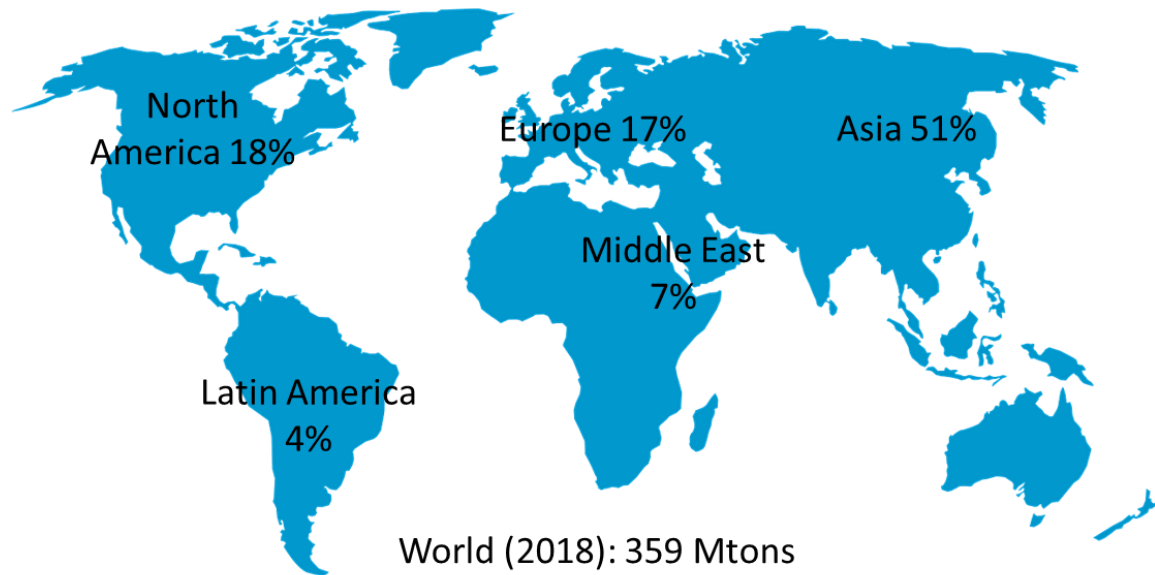


Figure 1.1: World and European plastics production 2018. [Source: Plastics Europe]

These successes are primarily due to their low cost, reproducibility and resilience to physical ageing and biological attacks [1]. The main reason is that fossil based plastic is durable, lightweight, strong, resistant to moisture, biologically inert, workable, and reasonably inexpensive.

More than 99 percent of these polymer products were derived from petrochemicals, but about half of them finish in the environment within a brief period of time. About 7 million tonnes of plastic waste was landfilled in Europe in 2018 (Figure 1.2). On the other hand, the trend is getting better: compared to 2016, in 2018 Europe landfilled 1.1% less plastics, increasing recycling by 5.7% and energy recover by 4.8%. We also increased post-consumer plastic collection by almost 20% since 2006 [Source: Plastics Europe].

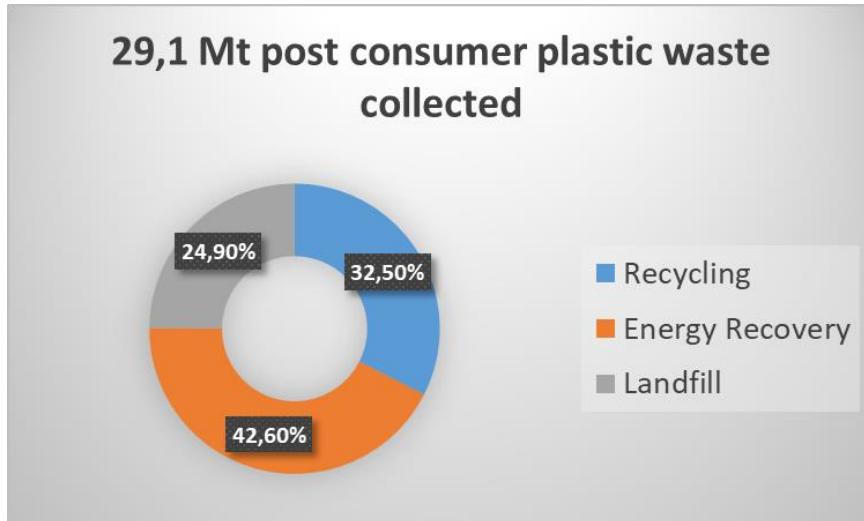


Figure 1.2: Treatment for post-consumer plastics waste in Europe in 2018. [Source: Plastic Europe]

Usually, the key sources of plastic waste are those areas where the largest disposal of plastic occurs. The contribution of numerous industrial fields to plastic use in Europe in 2018 is seen in Figure 1.4. Packaging is the greatest contributor to the market for plastics (39.9%), way ahead of building & construction (19.8 %) and "Others" (16.7%), which covers furniture, medical waste, etc. Automotive (9.9 %), electrical and electronic equipment (EEE, 6.2 %), are the remaining industries along with agriculture (3.4%) [Plastic Europe 2018].

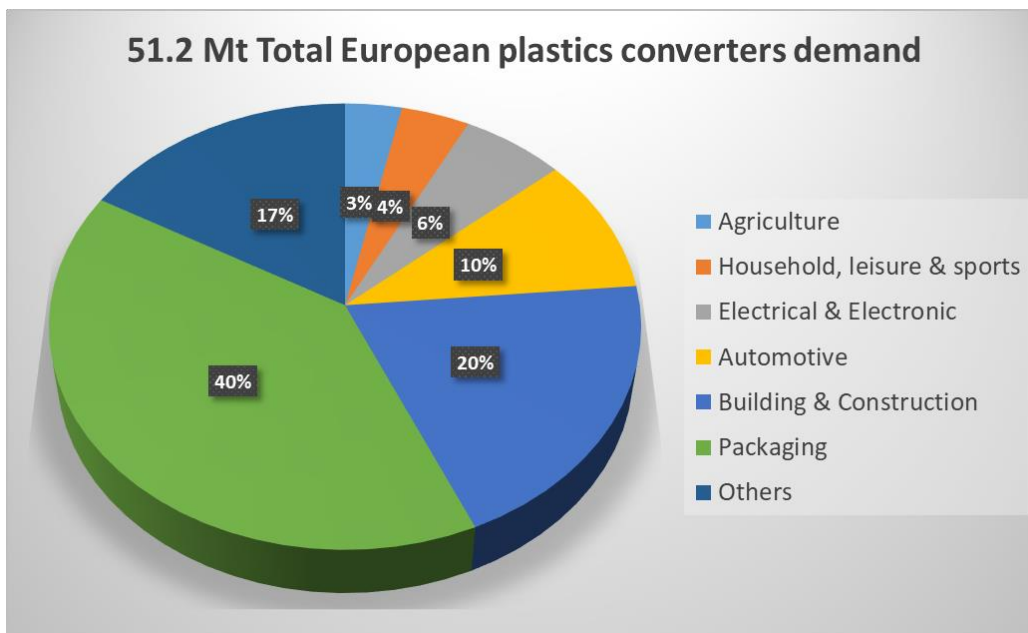


Figure 1.3: Distribution of European plastic demand by segment in 2018. [Source: Plastic Europe]

The biodegradation resistance of synthetic polymers, especially in those areas where they are used for a limited period of time before becoming waste, is becoming irreversibly

problematic. This is also the case in the areas of medicine, pharmacology, agriculture and packaging. Time-resistant polymeric wastes are no longer suitable in these areas, even if in certain fields these are not easily replaceable due to specific properties requirements.



Figure 1.4: Plastic waste pathway in our environment. [Source: OurWorldinData.org]

In tandem with the continuous rise in use of low biodegradable plastic materials, widespread littering is currently causing large-scale plastic accumulation in our environment (Figure 1.4). Plastic waste can pollute ground, rivers and oceans irreversibly. Living species, in particular marine animals, may also be restrained, as well as ingest plastic waste, or be exposed to plastic chemicals that cause biological function interruptions. Microplastics theme is strongly emerging as well, with first studies about their impact on our biology [2].

Right now, in the Pacific Ocean and collected by its currents, there is a plastic aggregate called Great Pacific Garbage Patch, with an estimated extension that easily surpasses the sum of territorial areas of France, Germany and Spain combined together (Figure 1.5).

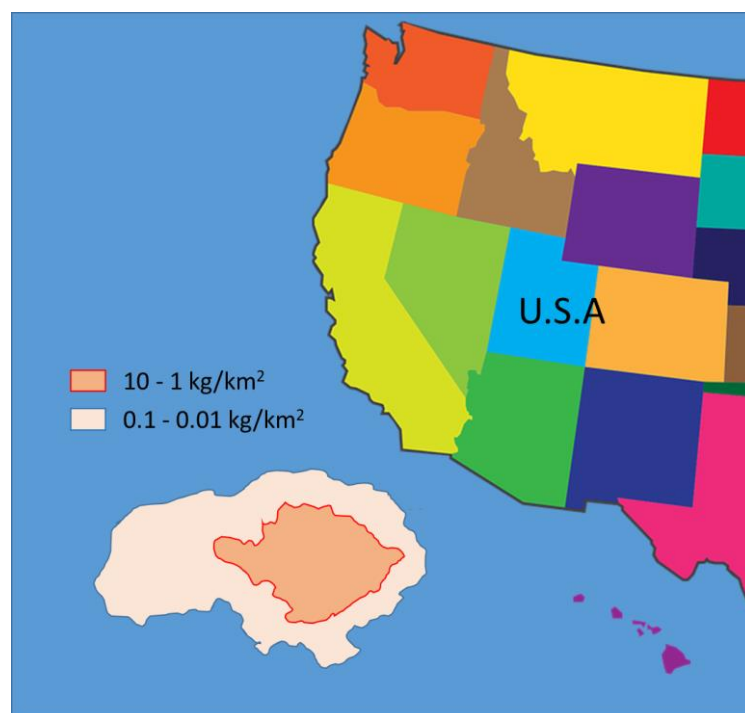


Figure 1.5: The Great Pacific Garbage Patch. [Source: International Marine Consultancy]

In order to protect our seas, coastlines, fresh water and the terrestrial habitats from plastic waste, urgent global intervention and initiatives to mitigate littering are vital. The shortening fossil fuel supplies and their price instability together with climate change, brings to a drastic scenario, which is the clear driver for states, industries and scientists to pursue alternatives to fossil-based polymers.

In particular, there is an immediate need to improve the production of partially or entirely biobased plastic materials, which are absolutely degradable in the environment for short-term and single-use applications.

Waste management failures and pollution (at least 8 Mtons of plastic per year finish in the ocean) led also to a vast social awareness that climaxed with the European Plastic Strategy in 2018 and Single-use Plastic ban by EU in early 2019.



Figure 1.6: Most common plastic objects found on European beaches.

1.2 Circular Economy

Even if the concept was there since 70s, only after the European Plastic Strategy the term “circular economy” really entered in public opinion vocabulary, with the aim to fight plastic pollution.

A circular economy is an economic structure which seeks to eliminate waste and make continuous use of resources. To build a closed-loop framework, minimizing the usage of resource inputs and the production of waste, deforestation and carbon emissions, circular systems employ reuse, sharing, maintenance, refurbishment, remanufacturing and recycling [3]. The goal of the circular economy is to continue the use of goods, facilities and infrastructure for longer, thus improving their efficiency [4]. The raw material of a process can come from the waste of another: as a by-product or resource recycled for another production process or as a regenerative resource for nature (e.g., compost). In comparison to the

conventional linear economy, which has a "take, make, dispose" pathway, this regenerative approach is, of course, circular [5].

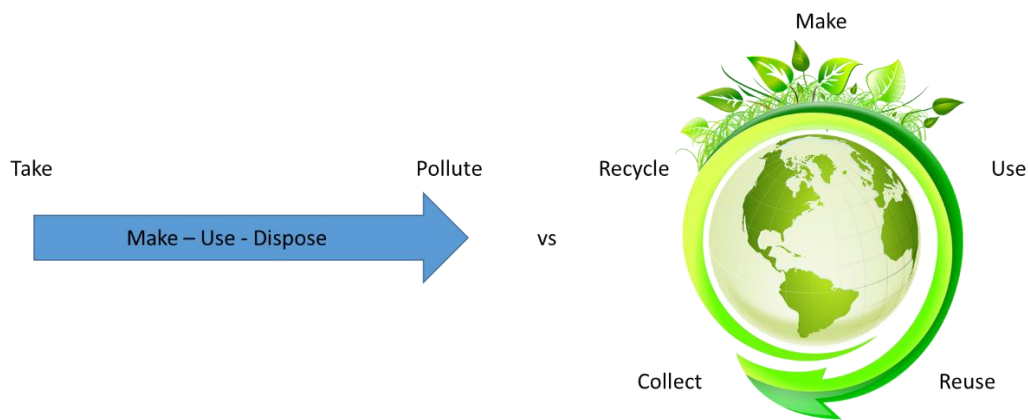


Figure 1.7: Linear vs circular economy.

Industrial sequential methods (take, make, dispose) and the society that rely on them, use finite resources to manufacture goods with a finite lifetime that end up in landfills or incinerators. On the other hand, the circular approach uses ideas from living systems. It assumes that our processes can behave like animals, processing nutrients that can be fed back into the cycle, whether biological or technological, thus the generally related "closed loop" or "regenerative" terminology (Figure 1.7). Several separate schools of thought may refer to or assert the circular economy, but all of them gravitate around the same core concepts.

Walter R. Stahel, an architect, economist, and a founding father of industrial sustainability, is one leading thinker on the subject. In the late 1970s, Stahel focused on creating a "closed loop" approach to manufacturing methods, co-founding the Product-Life Institute in Geneva, and was credited for the invention of the term "Cradle to Cradle" (as opposed to "Cradle to Grave", demonstrating our "Resource to Waste" way of functioning). In the United Kingdom in 1982, Steve D. Parker investigated waste as a resource in the UK agriculture industry, designing modern closed-loop processing processes. These processes mimicked the ecological environments they manipulated and interacted alongside them.

From plastics point of view, there are two main ways to "close the loop": recycling or biodegrade (compost). While the concept of recycling is directly closing the circle, since in the end new raw material is created (even if not always as good as virgin material), biodegradation closes the circle only if we consider a bigger picture. In facts, compost is not directly a raw material, but we can consider it as new ground in which we could grow plants to use for new biopolymers (thus, new raw material). Or, even a bigger picture, new ground is the raw material itself if we consider that human activity increased soil erosion/degradation (Figure 1.8) by 10% in 20 years (1993-2013, Source: FAO).

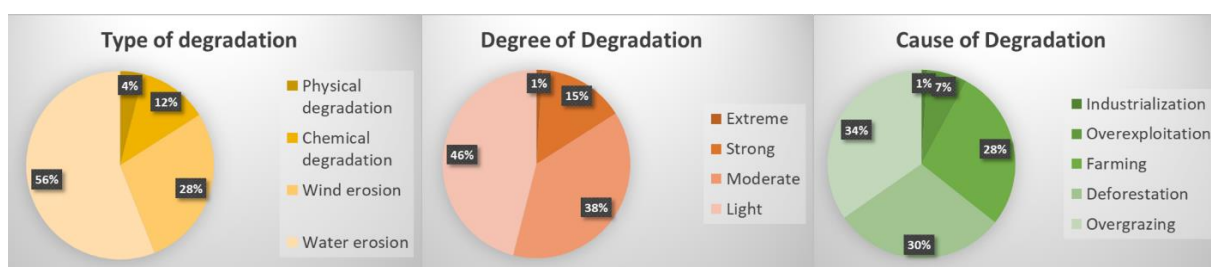


Figure 1.8: Types, degree and causes of global land degradation. [Source: 2013 Nature Education]

1.2.1 Plastic Recycling

The method of recovering scrap or waste plastic and reprocessing the material into usable items is called plastic recycling. Compared to profitable metal recycling and easy glass recycling, the recycling of plastic polymers is also definitely more problematic due to its low density and low economical value, meaning that great volumes and efficient methods are required to have a gain. When recycling plastic, there are still several technological challenges to tackle. It is the duty of materials recovery facilities to sort and handle plastics. Until 2019, these facilities have failed to make a significant contribution to the plastic supply chain due to constraints on their economic viability [6]. At least since the 1970s, the plastics industry has recognized that recycling of most plastics is impossible due to these constraints. However, as these businesses have continued to raise the volume of virgin plastic being produced, the sector has also united for the expansion of recycling, especially after economic incentives from EU Plastic Strategy [7].

When various types of plastics are melted together, they appear to be phase-separated and divide in layers, similarly to oil and water. The phase contact areas induce dimensional instability in the resulting material, ensuring that un-compatible polymer blends are typically usable in small applications only. This is also why the resin recognition codes have been produced by the plastics industry. This is how unfortunately behave the two most commonly created plastics, polypropylene (PP) and polyethylene (PE), reducing their usefulness for mixed recycling. Any time plastic is recycled, additional virgin materials are usually added to further enhance the purity of the compound. So, even recycled plastic has new plastic content mixed in. In most cases (nowadays), the same piece of plastic be recycled only around 2-3 times because of degradation caused by most recycling processes [8]. Thus, even though plastics have a resin code and are retrieved for recycling, only a limited amount of the content is eventually recycled (just 8% of US plastic has been recycled as of 2017) [9]. In Europe, it's estimated a more promising 42%, even if Plastic Strategy aims to reach a 55% by year 2030 (Figure 1.9).

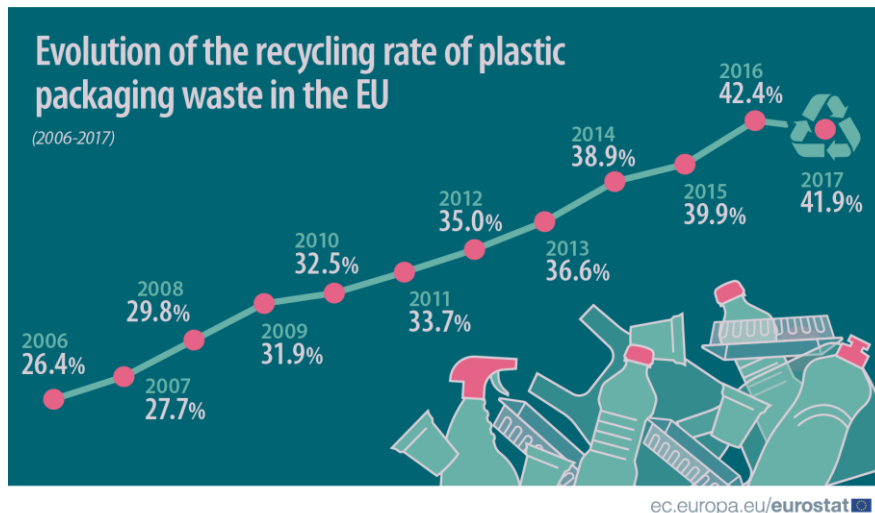


Figure 1.9: Evolution of the recycling rate of plastic packaging waste in EU. [Source: Eurostat]

There are two main types of plastic recycling in general: (1) mechanical recycling ('chop and wash'), where the plastic is cleaned, minced into powders/grains/scales and melted, and (2) chemical recycling, where the plastic is de-polymerized into monomers.

Many plastics are categorized according to their type of resin before recycling. The resin identification code (RIC, Figure 1.10), a method of categorization of polymer nature that was created by the Society of the Plastics Industry in 1988, was used by plastic reclaimers in the past. For example, poly(ethylene terephthalate), commonly known as PET, has a resin code of 1. Today, most plastic reclaimers do not rely only on the RIC: different sorting systems are used to classify the resin, from manual selection and picking of plastic products to automated mechanical processes including shredding, sieving, as well as density, air, liquid or magnetic separation, and advanced spectroscopic technologies, like UV / VIS, NIR, lasers, etc. [Source: Plastic Europe]. Before they are recycled, certain plastic items are often differentiated by colour.



Figure 1.10: Plastic Resin Identification Codes. [Source: Openclipart.org]

1.2.1.1 Mechanical Recycling

Since sorting, the plastic recyclables are then grinded in case of mechanical recycling. These shredded pieces then undergo processes (normally washes) to remove impurities including

paper labels (Figure 1.11). After that, they are melted and extruded into the shape of pellets that are then used for other items to be made. "Regeneration" can be referred to as the best quality purification [10].

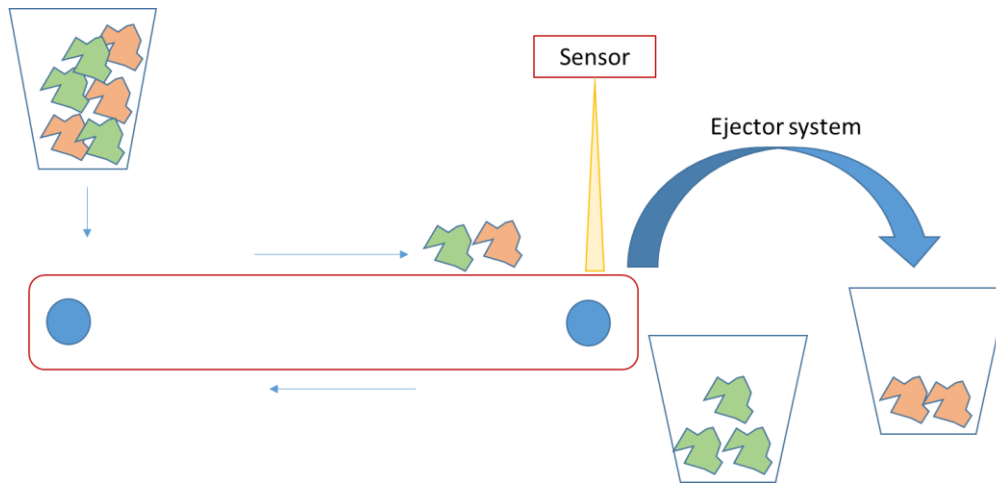


Figure 1.11: Plastic Waste Sorting Scheme.

1.2.1.2 Chemical recycling

Some polymers can be converted back into monomers, e.g. PET can react with an alcohol in presence of a suitable catalyst forming dialkyl terephthalate. In order to form a new polyester polymer, the terephthalate diester should be used with ethylene glycol, making it easier to use the pure polymer again. In 2019 it's esteemed that at least 60 companies are investing in chemical recycling [11].

For example, Eastman Chemical Company announced actions towards methanolysis of polyesters and polymer gasification to syngas in order to process a greater variety of different materials [12].

Always in 2019, Brightmark Energy in US started to build a factory to turn 100,000 tons of mixed plastic per year into diesel, naphtha blend stocks, and wax [13]. The company plans to expand and create another facility that will handle an additional 800,000 tons of plastic per year.

1.2.1.3 Other processes

There are also possibilities for improved processing of mixed plastics, eliminating the need for costly / inefficient plastic waste separation. Compatibilization, which utilizes specific chemical bridging agents called compatibilizers to preserve the consistency of mixed polymers, is one of such methods [14].

Lately, to address the problems involved with phase separation during recycling, the use of block copolymers as *molecular stitches* [15] or *macromolecular welding flux* has been proposed [16].

1.3 Bioplastics

Environmental problems and circular economy are the reasons why bioplastics are experiencing a renaissance, with a global bioplastics production capacity grown by 30% in 5 years (2014-2019) [17]. There is a steadily increasing industrial and academic interest in manufacturing a wide range of controlled life span materials on this basis; optimally engineered polymers must be resistant during their use and degrade at their end-life [18]. It is possible to narrowly classify biodegradable plastics into various groups depending on the sources of the raw materials (petroleum-based or biobased, Figure 1.12) and the methods used in their processing.

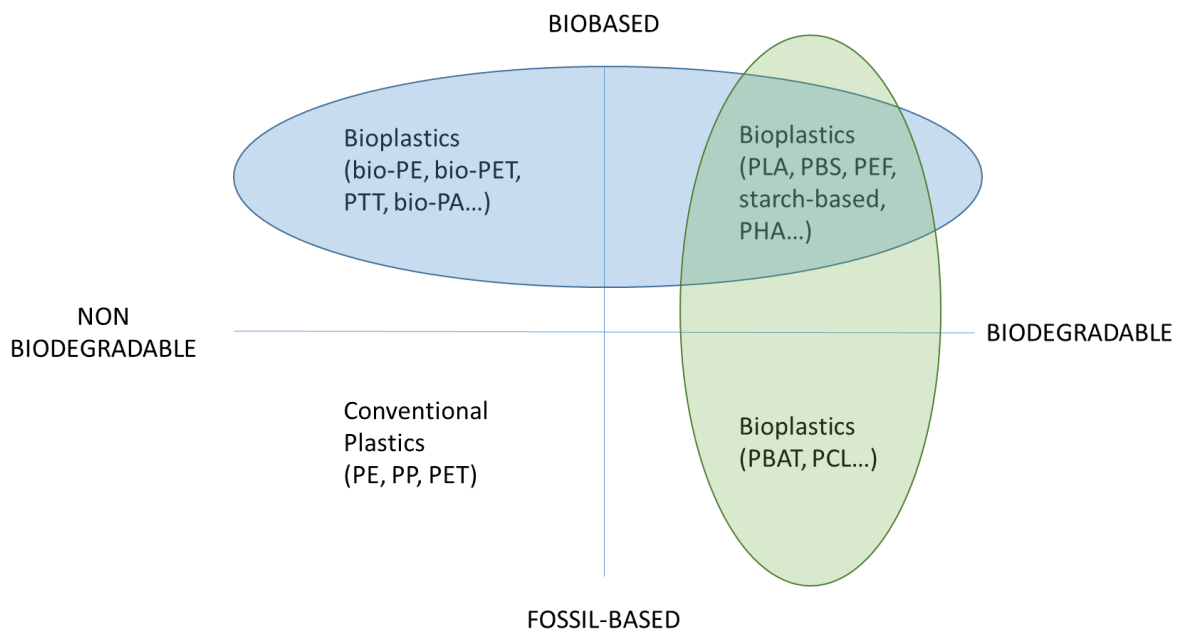


Figure 1.12: Bioplastic categories. [Source: European Bioplastics]

Worldwide in 2019 starch blends were the most produced bio-based plastics, followed by PLA and PBAT (Figure 1.13).

2.11 MTONS PRODUCED (2019):

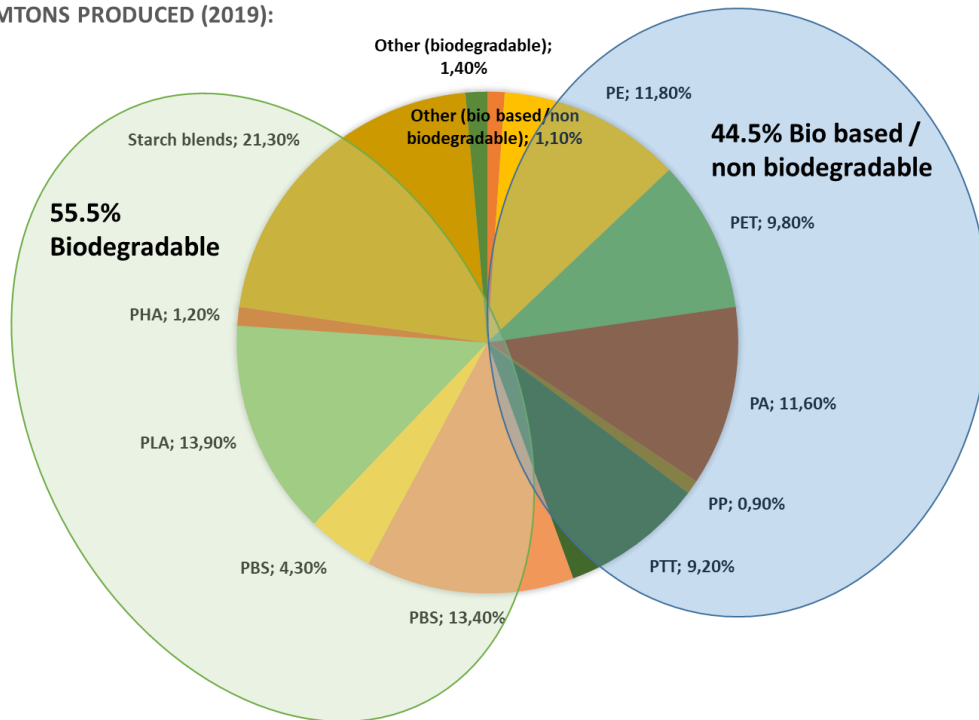


Figure 1.13: Global production capacities of bioplastics in 2019. [Source: European Bioplastics]

For the design of biodegradable polymers, four major methods can be employed. The simplest one is to add a biodegradable or photo-oxidizable part to cheap conventional synthetic polymers. Changing the chemical composition by the incorporation of hydrolysable or oxidizable groups in the main chain of non-degradable synthetic polymers is a more costly approach. The third solution is to substitute existing plastics with natural biopolymers such as starch, chitosan, chitin or their derivatives and, last but not least, to design different hydrolysable materials such as polyesters, polyanhydrides, polyurethanes and polyamides [19].

In the last two decades, research attempts to develop, synthesize and produce synthetic or renewable polymers have grown tremendously. In this way, some of the pitfalls of petrochemical polymers can be resolved, i.e. (a) diminishing oil and gas resources; (b) increasing oil and gas prices over recent decades; (c) environmental issues regarding their depletion or incineration and global warming; (d) uneconomic costs and cross-contamination of their recycling; and (e) risks of migration in food of their monomers or oligomers.

The enzymatic activity of micro-organisms such as microbes, fungi and algae consume the biodegradable polymers disposed of in bioactive conditions. Also, non-enzymatic processes such as chemical hydrolysis can break down their polymer chains. They are reduced to CO₂, CH₄, water, biomass and other natural substances through biodegradation. By biological processes, biodegradable plastics are thus naturally recycled.

The use of biodegradable plastics is of particular interest if, beyond simply "disappearing from view" by being buried in the soil or incorporated into the organic waste stream, the products can provide economic and/or ecological benefits. For example, if in a time-consuming process

conventional plastic garbage bags for organic waste are not separated from their contents, then incineration remains the only possibility for filled bags to be disposed. From an energy point of view, this makes no sense since organic waste is about two-thirds of water. However, if a biodegradable garbage bag is used, separation is no longer necessary, and the organic waste is disposed together with the bag. In the latter case, there are different possibilities: firstly, composting, secondly, anaerobic fermentation, during which biomass is converted into biogas (methane), providing an energy source. That is why biodegradable plastics not only represent a cost-effective solution for the disposal of organic waste, but can also make a significant contribution to the efficient management of organic waste. Target markets for biodegradable plastics include packaging materials (paper bags, laminated paper, food containers, film wrapping...), hygiene products (diapers, cotton swabs), consumer goods (razor handles, fast food tableware, toys, containers, egg cartons...) and agricultural tools (pots, mulch films)(Figure 1.14) [20].

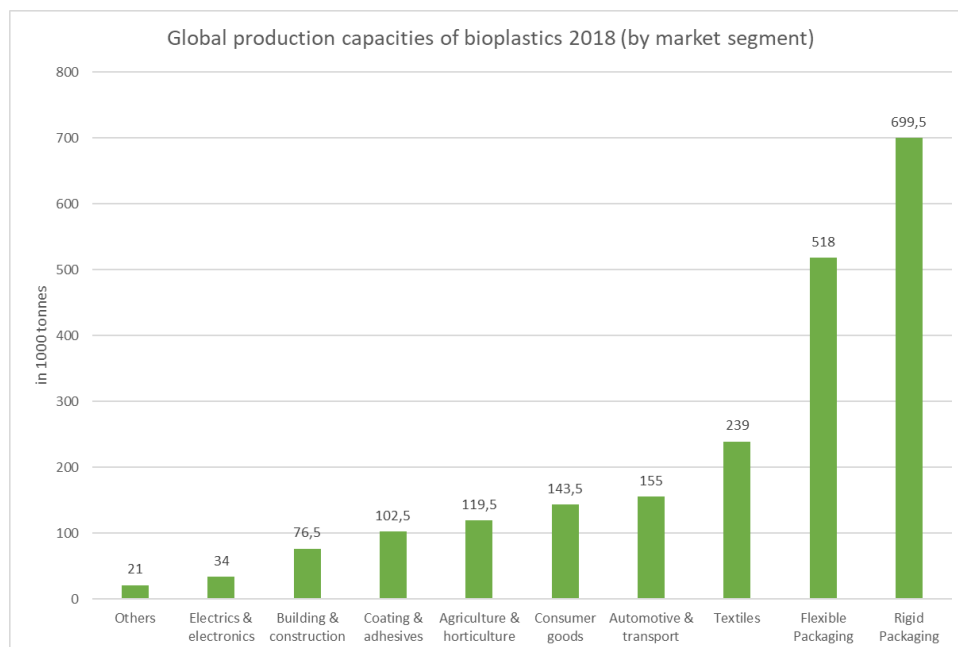


Figure 1.14: Global production capacities of bioplastics by market segment in 2018.
[Source: European Bioplastics]

1.3.1 Aliphatic polyesters

Aliphatic polyesters are a polymer class which contain an ester functionality along an aliphatic backbone (Figure 1.15).

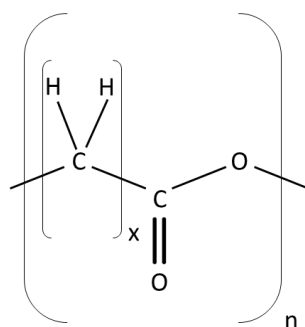


Figure 1.15 Chemical structure of aliphatic polyesters

Due to their advantageous biodegradability and biocompatibility characteristics, they constitute one of the most important classes of synthetic biodegradable polymers and are now widely available in a range of end-use types: pharmaceutical, medical and biomedical engineering, including drug delivery systems, artificial implants and tissue usable materials.

The history of aliphatic polyesters began in 1920s when, beginning with aliphatic diacids and aliphatic diols, the American chemist Wallace Carothers and his research group at DuPont made a ground-breaking work on the synthesis of polyesters in order to produce suitable polymers for fibre processing. Their work provided a solid basis for systematic studies of aliphatic polyester forming mechanisms [21]. This included in particular evidence of the high molecular weight nature of the polyesterification materials, the formulation of the so-called Carothers equation correlating the degree of conversion of the functional groups to the average degree of polymerization of the resulting linear polyester, and the significance in the polyester synthesis of ring-chain equilibria. Further experiments at Cornell University (Flory, a former assistant of Carothers, in 1936, 1939, 1942, 1953) contributed to the discovery of the concepts of polyesterification kinetics and distribution of polyester molar mass. However, only some low molecular weight soft materials with high susceptibility to hydrolytic degradation were made [22].

At that time, certain properties of aliphatic polyesters, such as hydrolytic instability, low melting temperatures and solubility in common organic solvents were considered to be detrimental from the practical point of view of application, resulting in a substantial delay in the production of these polymers. More recently, as environmental issues are gaining increasing attention along with the need for regulated life cycle materials, aliphatic polyesters have regained great interest because of their peculiar biodegradability; indeed, their use is being intensively researched as both biomedical and degradable consumer goods.

Biodegradable aliphatic polyesters are also found in nature, as in case of polymers such as polyhydroxyalkanoates (PHAs), which can be synthesized by certain kinds of microorganisms to store energy. Such examples include polyhydroxybutyrate (PHB), poly(hydroxyl valerate) (PHV), and their copolymers, which can be produced enzymatically from certain bacteria by feeding them with sugar or other nutrition (alcohols, alkanes, alkenes, etc.). Several businesses are commercially manufacturing such polymers by microbial fermentation. However, due to difficulties in extracting and purifying the polymer from microorganisms, its

cost is quite high. High-molecular polyesters, such as poly(butylene succinate) (PBS), poly(butylene succinate/adipate) (PBSA) and poly(lactic acid) (PLA), can now be prepared and marketed as biodegradable plastics for practical purposes [23].

1.3.2 Physical properties

The solid-state properties of aliphatic (and aromatic) polyesters are specifically associated with several variables, such as the degree of crystallinity, polar group presence, polymer chain mobility, molecular mass, branching presence, etc. For example, short-chain branches hinder crystallization, as stated in literature, while long branches decrease viscosity and confer plastic behavior [24]. In addition, by copolymerization the final properties can be further nicely modulated, acting on both composition and macromolecular architecture.

1.3.2.1 Structure of polymers

Polymeric materials can be categorized as amorphous, if totally disordered, and semicrystalline, if partially organized, as a result of the structure of the macromolecules (Figure 1.16). In certain cases, short-range order development can also occur, contributing to the creation of the so-called mesophase.

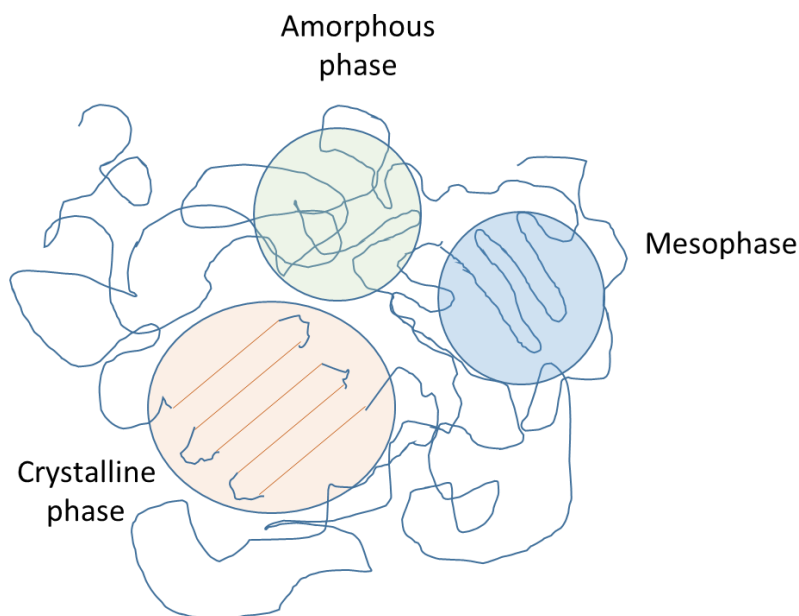


Figure 1.16: Graphical representation of amorphous phase, mesophase and semicrystalline structures.

A second order transformation, called the glass transition, characterizes amorphous polymers. This effect is defined as a kinetic process since the temperature at which the

transformation takes place depends on the rate of cooling: slowly cooling the melt creates a glass at a lower temperature than a rapid cooling will do. The temperature of the glass transition, T_g , is correlated with the key change in dynamic properties and is therefore also known as alpha relaxation. The material is rigid and fragile below T_g , a glass made of dense and less dense areas, established density variations, heterogeneities or defects [25- 27].

This less compact areas are mobile islands where it is still possible to allow local motions of chains or translational motions of trapped gas/small molecules. The mobility is however, limited to vibrational motions without involving the neighbouring atoms or molecules directly [28]. Considering their proximity to the glass transition, these phenomena are called "sub- T_g relaxations". In polymeric materials, various secondary sub- T_g relaxations can be detected, primarily β relaxations have been studied showing dependency on the Arrhenius law, with a characteristic activation energy (E_a) representing the degree of cooperative and non-cooperative movements.

A significant number of cooperative motions are possible when the material is heated above T_g , determining changes in the physical properties of the polymer (increasing heat power, entropy and thickness, and decreasing both rigidity and viscosity [29].

Amorphous polymers can be frozen in a non-equilibrium state using various cooling speeds, with the resulting entropy/enthalpy values and volume above those corresponding to the most stable situation [30]. Naturally, over the so called *relaxation time* and *enthalpy of relaxation*, the material will begin to relax into the equilibrium state. This mechanism happens slowly, however by raising the temperature its speed can be increased. In fact, increasing the temperature near T_g will dramatically decrease the relaxation time. Chain rearrangements and densifications can be detected from a microscopical point of view. As a result, the molecular organization is higher and reinforced interactions influence mechanical behaviour by increasing rigidity [31] and enhancing gas barrier properties, where diffusivity of the molecules across the substance is restrained [32].

Alongside the state of fully amorphous materials, the polymeric chains can arrange in crystalline 3D structure. Polymeric compounds are unlikely to achieve 100% of crystallinity due to the dimension of the chains. As a result, although constrained between crystals, an amorphous component is still present, but with the shift of T_g to higher temperatures than a fully amorphous state relative to the same polymer. The existence of the crystalline phase not only influences the T_g , but important changes in density, clarity and mechanical behaviour are observed. The temperature at which the 3D structure loses its order is called the melting temperature, T_m , and is defined as an endothermic effect by the subsequent mechanism (Figure 1.17).

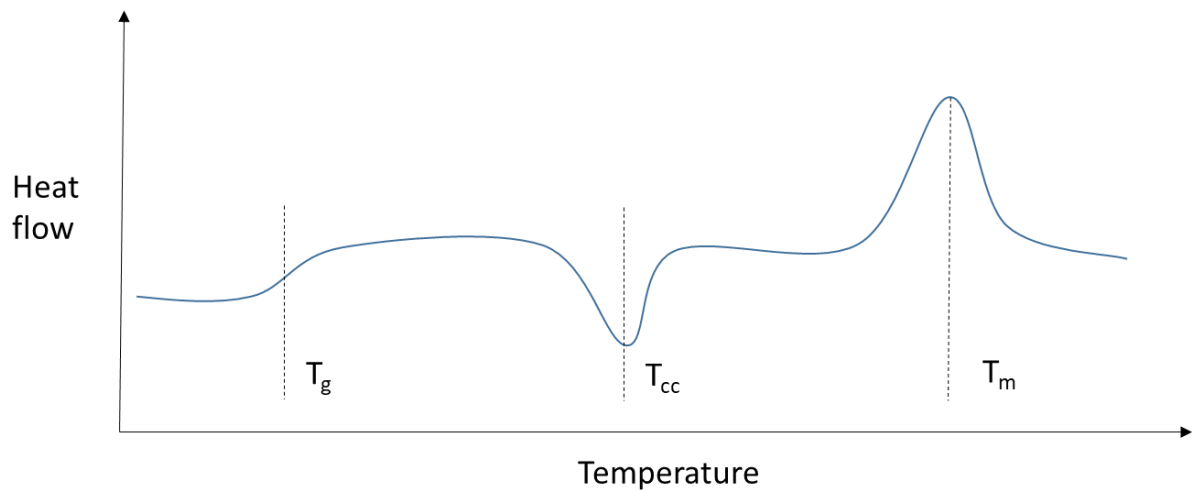


Figure 1.17: DSC analysis representation.

Crystallization is the process by which macromolecules are organized into a crystalline structure. The organization will start from the melt, explaining the process of "melt crystallization" and occurring at T_c (Figure 1.18) while also heating up the glassy substance, the so-called "cold crystallization" reported as T_{cc} .

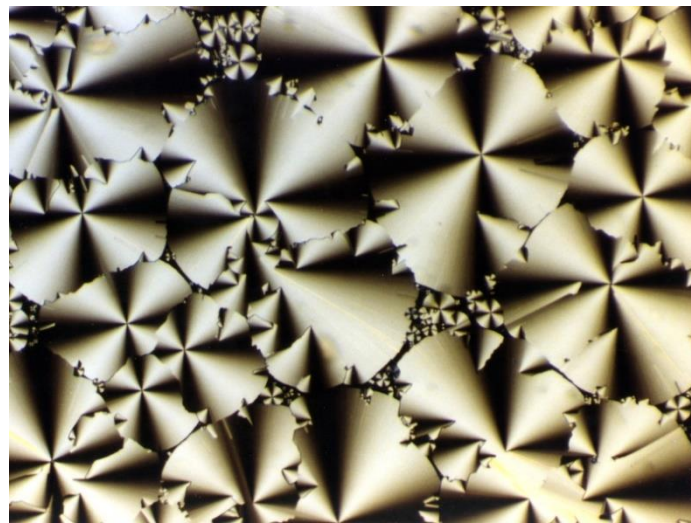


Figure 1.18: Crystallization process with spherulites growth. [Source: Minutemen, Wikimedia Commons]

The polymer has to be characterized structural regularity in order to be able to crystallize. The process, if possible, will occur in the range between T_g and T_m , with a rate specifically linked to the temperature, described as crystallization rate. The first step, if the polymer's specific structure is suitable, is the creation of nuclei, known as nucleation. Such process can occur either in *homogeneous conditions* or *heterogeneous conditions*. Without external force, the spontaneous nucleation begins with the arrangement of the macromolecules by themselves and therefore the crystallization rate can be quite low.

The standard methodology applied at industrial level is heterogeneous nucleation. There have been mentions of different techniques. One is to start by partially melting a polymer, using the crystalline fragments as self-nuclei during the successive cool-down. On the other hand, the addition of external nucleating agents is very effective as well. [33].

After the nuclei are born, they can grow at different rates in different conditions. The growth rate can be represented as a *bell-shaped* curve between T_g (restricted mobility = no more self organization in crystal form) and T_m (too much mobility = equilibrium between liquid and crystal).

Chemical structure, chain symmetry, stability and tacticity can influence glass transition temperature and melting temperature, as well as crystallization temperature. For instance, the presence of functional groups such as -O-, -COO-, OCOO- and -(CH₂)- promotes stability, whereas intermolecular bonding promoted by polar groups rises T_g and T_m and lowers T_c .

1.3.2.2 Homopolyesters

Linear aliphatic polyesters with x and y greater than 2 (Figure 4.8) have outstanding crystallization capability with a high degree of crystallinity, with a T_m about 40 ° - 90 °C and a temperature of glass transformation between -70 and -30 ° C.

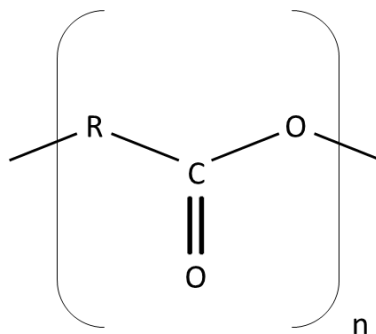


Figure 1.19: General chemical structure of polyesters.

Normally, the lower the ratio in the polymer chain between methylene and carboxylic groups, the higher the melting temperature: e.g. poly(butylene adipate) T_m is equal to 47 ° C, when $T_m = 116$ ° C is seen in poly(butylene succinate) [34-35]. Polyesters containing ether-linkages exhibit improved flexibility in terms of mechanical properties, e.g. poly(1,4-dioxan-2-one) properties are similar to the ones in human tissues [36-38] . Polymer blends and copolymerization, or modifying the macromolecular architecture (e.g. hyper-branched polymers, dendrimers or star-shaped polymers, etc) are all efficient tools to tailor the properties of these materials. [39]

1.3.2.3 Copolyesters

It is possible to describe copolymers as polymers with at least two different repeating units [40]. The purpose of the synthesis process, copolymerization, is to integrate all the various monomers into a single polymeric chain. Copolymerization makes it possible to have a wide range of possible final properties, enabling them to be fine-tuned according to the intended application. It's possible to act not only on composition, but also to modify the structure and architecture of the copolymers. Specifically, linear copolymers are formed by a single macromolecule, and four categories (Figure 1.20), can be identified depending on how the different monomers are lined up along the polymer chain [41]:

- random copolyesters: the co-monomeric units sequence is casual;
- alternating copolyesters: units A and B alternate regularly along the chain;
- block copolyesters: constitute of two or more homopolymers linked by covalent bonds.
- graft copolymers: branched copolymers in which the side chains are structurally distinct from the main chain;

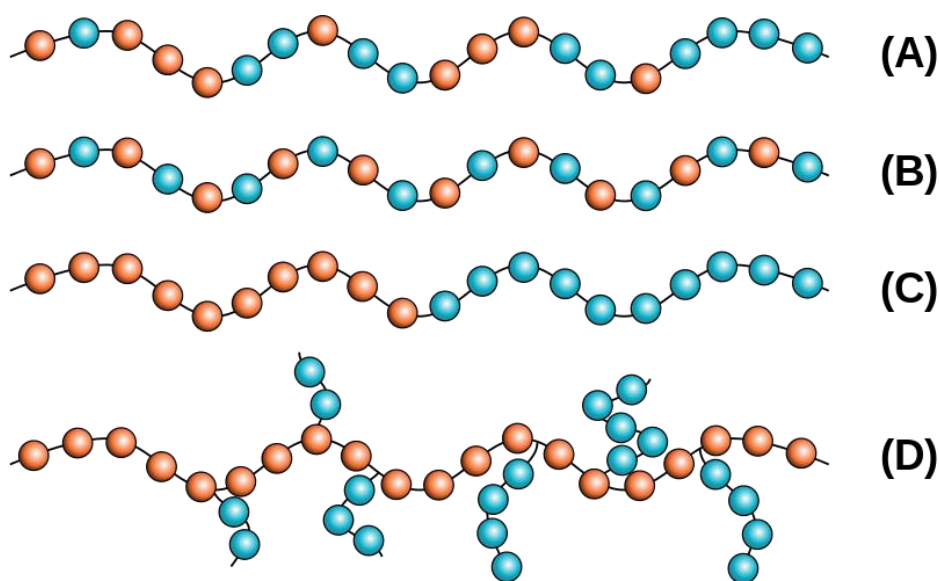


Figure 1.20: Copolymer architectures: (A)Random; (B) Alternate; (C) Block; (D) Graft.
[Source: Minihaa, Wikimedia Commons]

The final properties of the substance are described by the subunits' physico-chemical properties, but also by the copolymer's composition and architecture. Molecular weight and its distribution, ramifications, cyclic structure, or crosslinks often play an important role.

Block copolymers are complex macromolecules capable of containing two or more distinct homopolymer chains, resulting in broad architectural possibilities: - linear di-block A-B; - linear tri-block A-B-A; - multi-block or segmented (AB)_n; - star di-block (AB)_nX. Linear A-B-C, B-A-C and A-C-B triblock copolymers can be prepared where a third monomer is involved [42].

In nature, block copolymers are not available: they have to be synthesized. Pluronics, a surfactant made up of propylene oxide and poly(ethylene oxide), is one of the first examples of a commercial block copolymer. In 1959, Du Pont launched Spandex, an elastomeric polyurethane, the first product built on the concept of soft and hard blocks. Due to two different self-organization mechanisms competing against each other (microphase separation and crystallization), the process of crystallization is complex. Considering a di-block copolymer in which only one of the two blocks can crystallize, both blocks influence the thermal transitions. When two or more blocks can crystallize, the thermal behaviour is more complex. If the two blocks have different melting temperatures and the microphase-separated melt is quenched at a certain temperature below T_m , one block can predominantly crystallize, but the crystallization of the other block can affect this phenomenon, depending on several parameters (crystallization temperature, molecular weight of the blocks, etc.)[43].

1.3.2.4 Thermal properties

It is important to classify plastics in thermoplastics and thermosets, depending on their thermal and mechanical properties [44]. Thermoplastics are materials that, due to the presence of secondary bonds that can reversibly soften without any chemical transformation, can be softened by heating, formed and hardened by cooling many times. Saturated polyesters, polyamides or polycarbonates are some examples. Instead, thermosets are products that irreversibly harden after heating. Chemical groups or double bonds undergoing cross-link reactions, like in unsaturated polyesters, resins or polyurethanes, characterize these polymers. Thermal deterioration, due to the high temperature involved, is one of the key problems that arise during synthesis and processing of polymeric materials. In the macromolecular structure, heat induces thermal degradation and consequent chemical changes, such as breaking bonds and the creation of reactive materials, changing the final properties. For this purpose, the determination of thermal stability is important in order to determine the maximum temperature that can be achieved, preventing polymer degradation.

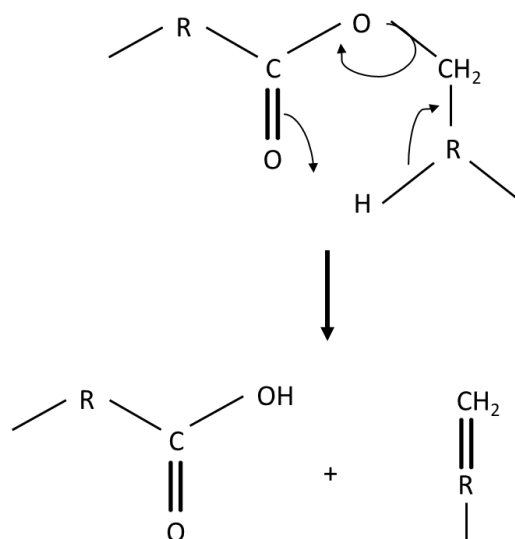


Figure 1.21: β -scission mechanism.

The mechanism of thermal degradation has been widely studied and includes two separate reactions at the same time. Random bonding break is responsible for decreasing molecular weight, while volatile sub-products are created by chain-end splitting of Carbon-Carbon bonds, also known as the depolymerization reaction. This happens at the gas-liquid interface of the system, when bonds in the main chain are weaker than those of the side groups [45]. Typically, it begins from the end of the chains, releasing monomeric units gradually. In comparison, any bond along the chain will break with a random body scission. In polyester β -scission is one of the most common processes of spontaneous degradation (Figure 1.21), arising in the presence of β -hydrogen atoms in the sub-unit of diol [46]. Hydrogen bound to a carbon atom is removed in the β position of the carbonyl group, splitting the O-CH bond [47]. The degradation process shapes terminal groups-COOH and $\text{CH}_2 = \text{CH}$ -. In aliphatic and aromatic polyesters, the presence of the methylene group raises the chances of chain splitting [48]. That is why PBT or PPT degrades faster than PET, the latter possessing a lower number methylene groups; for the same reason poly(butylene succinate) (PBS) is less thermally stable at high temperatures than poly(ethylene succinate) (PES). Thermal degradation produces various sub-products such as H_2O or CO_2 or acetaldehyde, formaldehyde, acetic acid and formic acid. Traces of acetaldehyde in food packaging plastics, in particular, is a major concern not only because of the coloured by-products that can be produced, but also because of its high toxicity.

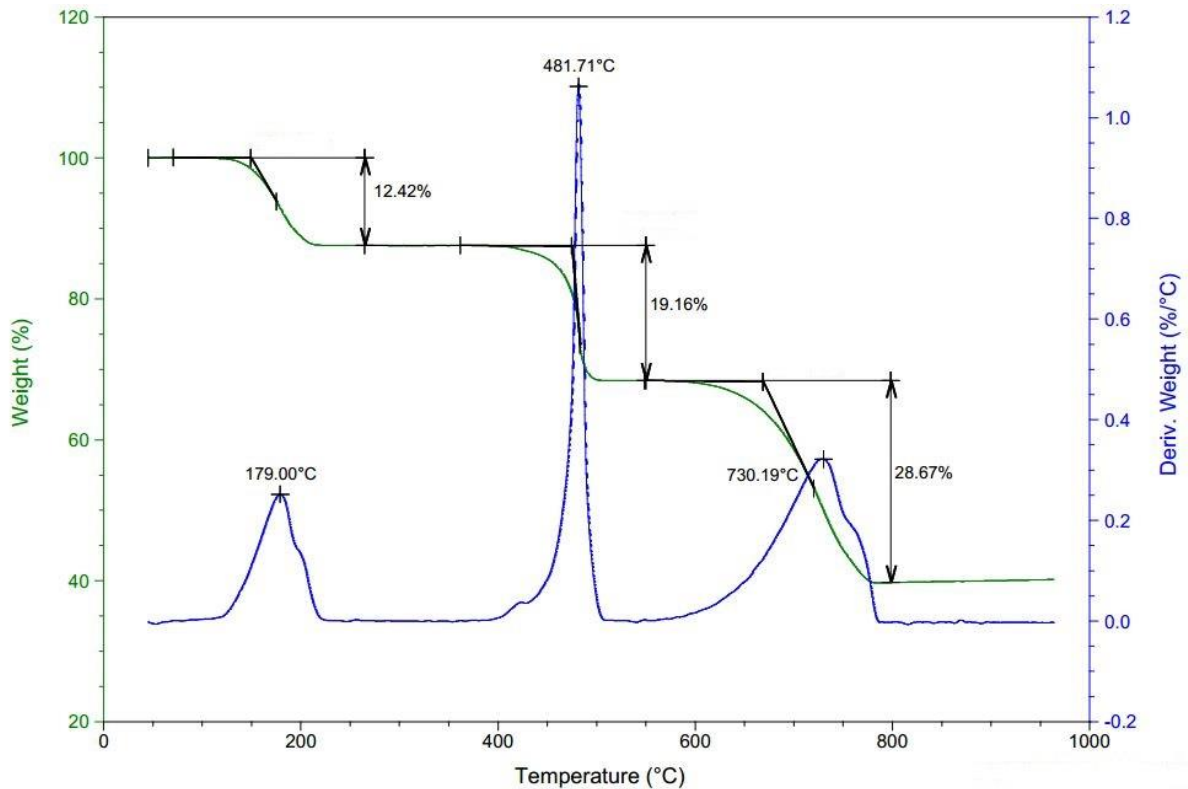


Figure 1.22: Example of thermal gravimetric analysis (TGA). [Source: DocMatSte, Wikimedia Commons]

Thermogravimetric analysis is one of the major methods for studying thermal degradation phenomena. The mass loss can be tracked during the test as a function of the temperature under a regulated and defined rate of heating or in isothermal conditions, for example retaining a constant temperature. In a typical polyester thermogram obtained under non-isothermal conditions (Figure 1.22) the substance shows the major mass loss in one level. In other cases, the degradation of low molecular weight residues such as unreacted monomers, oligomers, catalysts or water is responsible for smaller mass losses at lower temperatures. It is possible to equip the instrument with a mass spectrometer or Fourier Transform Infrared Spectrophotometer to collect information on the thermal degradation process.

1.3.2.5 Mechanical properties

Polymers are known as viscoelastic materials because they can exhibit both elastic and plastic behaviour. These materials can be deformed and, depending on the load applied, revert to the original shape after stress removal (elastic behavior) or can be deformed irreversibly (plastic behaviour). It is possible to run mechanical experiments of various geometries and loads (static and dynamic) [49]. The stress-strain test is commonly used (Figure 1.23); in this test the strain, defined as the change in the sample length divided by the original length, is determined in response to the stress, defined as the force applied to the structure divided by the cross-sectional area, applied at a constant rate.

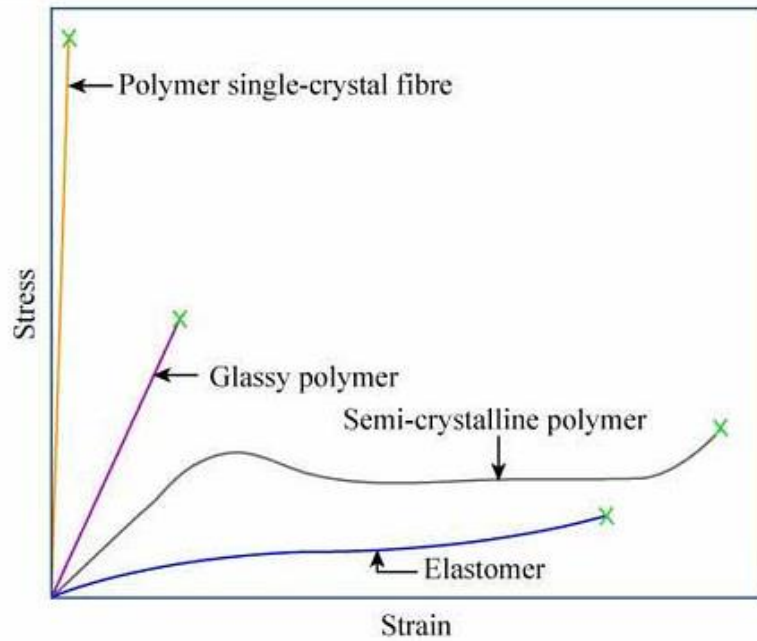


Figure 1.23: Stress strain curve of different types of polymers. [Source: MIT OpenCourseWare]

From stress strain curves, several experimental data can be deduced: toughness, defined as the ability of a material to absorb energy and deform plastically without fractures and identified as the area under the stress-strain curve; elastic modulus (E), calculated through the slope of stress-strain curve in the initial linear part (elastic region); stress (σ_y) and elongation (ϵ_y) at yielding, identified as the point of passage from the elastic region to the plastic one; stress (σ_b) and elongation (ϵ_b) at break, the point of fracture (X).

A variety of considerations related to the chemical structure of macromolecules are specifically bound to the mechanical properties of polymers. Molecular weight, degree of crystallinity, chain mobility and molecular architecture are the most important characteristics. In particular, in order to obtain an acceptable final mechanical behaviour, the molecular weight of the polymer needs to be high enough. In addition, crystallinity raises the polymer's rigidity and brittleness, with a consequent decrease in elongation at break; otherwise the absence of crystals favours greater elongation at break and decreases the elastic modulus. Moreover, the temperature at which the test is carried out is important because of its effect on the mobility of the chain: polymers in the glassy state are distinguished by low elongation at break and high elastic modulus; otherwise, if the chains easily move (rubbery state), elongation at break increases [50].

1.3.2.6 Barrier properties

Due to the different nature of the packed products, plastics used for food packaging applications require tunable barrier properties. For instance, oxygen can react with lipids,

altering the colour of edibles, while freshness of food can be affected by increasing humidity; on the other hand, CO₂ inhibits the proliferation of a wide variety of micro-organisms and can prolong the shelf life of fresh meat, so it is added and must be retained in the pack [51]. Contemporarily, the migration of lipids and the release of additives (antioxidants, dyes/pigments and antimicrobial agents) must be limited [52].

Barrier properties are based on materials' ability to hinder the movement of substances of low molecular weight, such as gases or organic molecules [53]. Two distinct factors influence the passage through the film: solubilisation and diffusion (Figure 1.24) [54]. The phenomenon can be summarized in three parts: (1) molecular adsorption: small compounds dissolve in the surface exposed to the gas (upstream surface); (2) molecular diffusion: the compounds cross the film with a given gradient; (3) molecular desorption: low molecular weight compounds exit from the opposite side of the film (downstream surface).

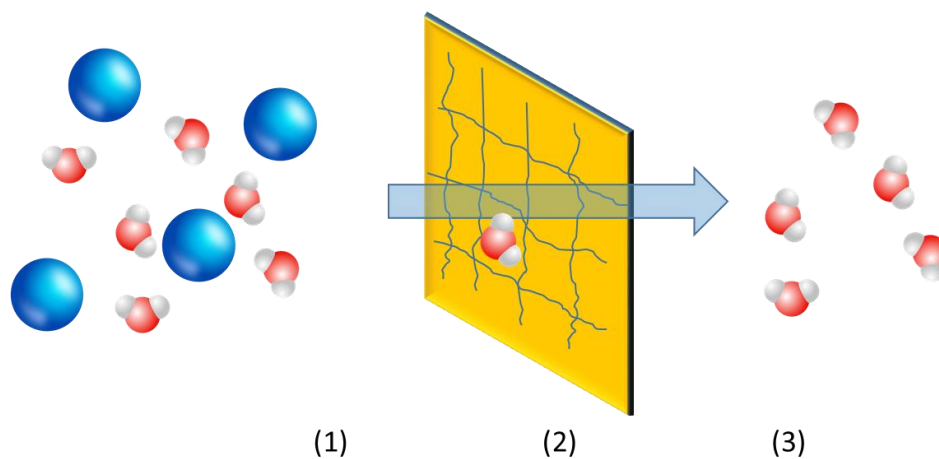


Figure 1.24: Solution-diffusion mechanism.

The solution-diffusion mechanism depends on several factors, such as penetrating molecule condensability, polymeric chain cohesive energy density, and polymer-permeant molecule interactions. High barrier properties are guaranteed by low fractional free volume and high intermolecular cohesion [55]. Indeed the molecules migrate through the free volume elements (FVEs) within the polymer matrix during the diffusion process. FVEs are thermally produced nanometric voids and are not stable, appearing and disappearing continuously. Until another chain motion happens nearby, the penetrating molecules can fill these voids, which are called free volume in the amorphous phase [56]. Thermal treatments are an effective method for changing the free volumes in polymers in the glassy state, in particular slow cooling reduces void formation.

In addition, the free volume can also be influenced by the molecular structure, for example polar groups with low particular volumes can minimize the presence of FVEs and favour chain packing [57]. Furthermore, affinity with the future penetrating molecule is also influenced by the chemical structure. The permeability would also be low if the solubility is low, even if the diffusion kinetics are favourable. Another critical element, crystallinity, influences processes of solubility and diffusion. In facts, compared to amorphous phase, these regions are more

ordered and denser, impeding the adsorption of molecules. Crystals serve as a buffer, extending the distance that the permeant should travel. Specific mechanical stretching can also change the barrier properties by influencing chain orientation. This influence is attributed not only to the development of aligned lamellar structures, but also to the crystallization caused by stress and the consequent amorphous component orientation [58]. Depending on the temperature at which they occur, permeation processes have a different effect: if the test temperature is higher than the T_g of the sample, the free volume rises since the motions of the chains are increased, thus the penetrating molecules can easily cross through the polymer.

1.3.3 Degradation

For all plastics, polymer degradation play a key role. Therefore, the distinction between degradable and non-degradable polymers is not clean-cut and is simply subjective, since all polymers can degrade in general. The relation between the time-scale of degradation and the time-scale of the operation is what makes the difference between degradable and non-degradable polymers. We typically allocate the "degradable" attribute to materials that degrade during, or directly after, their use. Non-degradable polymers are those that need a considerably longer degradation time than their period of use [59]. Polymer degradation happens primarily by breaking of the polymer molecules' main chains or side-chains, caused by thermal or mechanical activation, oxidation hydrolysis, photolysis or radiolysis.

In biological conditions, certain polymers undergo degradation in presence of living cells or microorganisms. These systems include all the Earth's lands, oceans, rivers and streams, as well as the human body. These polymers are considered polymers that are biodegradable.

With regard to the solid environments in which those polymers biodegrade, the two main categories considered in the technical literature, in the standards and on the market are: (1) materials that biodegrade under composting conditions (compostable materials) and (2) materials that biodegrade under soil conditions (biodegradable in soil materials).

Only polymers that can degrade by enzymatic hydrolysis in these biological conditions are considered biodegradable, not those that are subjected to thermal oxidation, photolysis, or radiolysis. Strictly speaking, a polymer that loses its weight inside a living body over time should be classified as absorbable, resorbable or bioabsorbable, no matters of its degradation by chemical or enzymatic hydrolysis. Thus, the term biodegradable should be used only for those polymers which have been produced to protect the earth's environment from plastic waste [60].

The processes involved in polymer biodegradation, and in the case of polyesters in particular, are complex. They can be split into chemical and enzymatic hydrolysis, with water involved in the process in both cases. Which degradation process is dominant depends on the polyester structure as well as the environment. Aliphatic polyesters have ester bonds that can be cleaved by enzymes such as lipases due to their mobility, with the produced chain fragments eventually dissolving in the water phase surrounding them.

The degradation can take place both at the surface (homogeneous) or in the bulk (heterogeneous) and is regulated by a broad variety of compositional and property factors, such as matrix morphology, chemical structure, chain orientation, stereochemistry, molecular weight and distribution, monomer sequence. Also presence of residual low-molecular-weight products, size and shape of the specimen, and degradation environment, (humidity %, microorganisms, oxygen, enzymes, temperature and pH) have a strong impact on the process [61].

The polymer's hydrophilicity and degree of crystallinity play an important role in determining its degradability, significantly affecting the accessibility of polymer surfaces. The accessibility of water is limited in the crystalline regions and permits degradation mainly in the amorphous phase, although highly crystalline starch and bacterial polyester have been reported to rapidly hydrolyze [62].

1.3.3.1 Chemical hydrolysis

Polymers must contain hydrolysable covalent bonds such as esters, orthoesters, ester amides (urethanes) anhydrides, ethers amides, carbamides (ureas) and so on in order to be degraded by water [18]. The type of bonds present in the polymer main chain determines the hydrolysis rate: anhydride and orthoester bonds are the most reactive, followed by esters and amides. Similarly, hydrophobic polymers are unable to absorb large quantities of water and are therefore characterized by a low rate of degradation. In contrast, hydrophilic polymers take up large quantities of water and degrade quite rapidly as a result [59].

In drug delivery systems, the absorption of water is particularly significant. For example, hydrogels may experience significant swelling, which is a crucial drug release regulation parameter, which may be more critical than polymer degradation. There are two major mechanisms by which polymer bonds can be broken: (1) bulk erosion, if water diffusion through the polymer is faster than polymer bond degradation, and (2) degradation limited to the polymer surface, if polymer bond degradation is faster than water diffusion [63]. In aliphatic polyesters the hydrolytic degradation happens in bulk: the penetration of water causes the chemical polymer degradation, leading to the formation of monomers and oligomers. Many factors are involved: absorption of water, fracture of ester bonds, neutralization of surface carboxyl end groups, within autocatalysis, oligomer diffusion and solubilisation [64].

The reaction is:



Acid or basic compounds catalyze the chemical hydrolysis reaction. Via autocatalysis, the acid byproduct, RCOOH, is able to speed up the hydrolysis. This hydrolysis takes place in two stages from a macroscopic point of view: first, a spontaneous cleavage of the backbone of the polymer chain occurs with a concomitant major decrease in molecular weight, consequently decreasing mechanical properties such as tensile and impact strength and ultimate

elongation, while weight losses are marginal [65]. The molecular fragments are solubilized in the intermediate to the last degradation stage and weight losses are measured [66].

1.3.3.2 Enzymatic hydrolysis

In comparison to chemical hydrolysis, the biological hydrolysis reaction is catalysed by enzymes. Depending on the form of bond that would be hydrolyzed, a wide variety of different enzymes are involved. They are in general called depolymerases. This kind of reaction affects ester bonds, glycosidic bonds and peptide bonds. It is well known that lipases and PHA-depolymerases cleave the ester bonds of aliphatic polyesters [67]. The reaction products are the same as those for enzymatic hydrolysis or chemical hydrolysis.

Biodegradation is successful in a biological system when the enzyme adapts to the stereochemical conformation of the substrate molecule. This behaviour is defined as being similar to a key fitting into a lock (Figure 1.25), and one chemical function is performed by each enzyme.

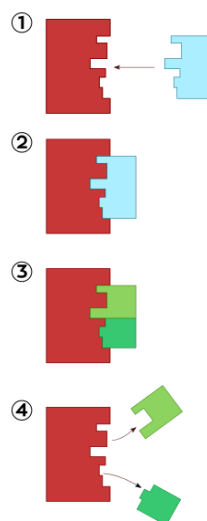


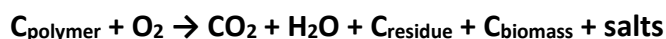
Figure 1.25: Key-lock mechanism of enzyme-substrate fitting and reaction. [Source: Wikimedia Commons, CC by 4.0]

Enzymatic degradation happens only on the solid substrate surface, followed by both surface corrosion and weight loss, since the polymer matrix cannot be penetrated by the enzyme. Thus, the polymer weight decreases with enzymatic hydrolysis and the distribution of molar mass and molecular weight scarcely varies, unlike chemical hydrolysis [66]. Then the surrounding aqueous environment solubilize the low molecular weight degradation products from the substrate.

1.3.3.3 Composting

Biodegradability is defined as the ability of a material to undergo decomposition into carbon dioxide, methane, water, inorganic compounds and biomass, with hydrolysis and enzymatic action of microorganisms as the predominant mechanisms, according to standard specifications (ASTM D6400, ASTM D6868 , ASTM D 7081, or EN13432) [68]. Ultimately, biodegradation catalyzed by microorganisms that may occur in the presence of oxygen (aerobic) or in the absence of oxygen (anaerobic) results in the formation of carbon dioxide (or methane in presence of oxygen), water and new biomass (Figure 1.26). The following equations can summarize the chemical process:

Aerobic conditions (C = carbon):



Anaerobic conditions:

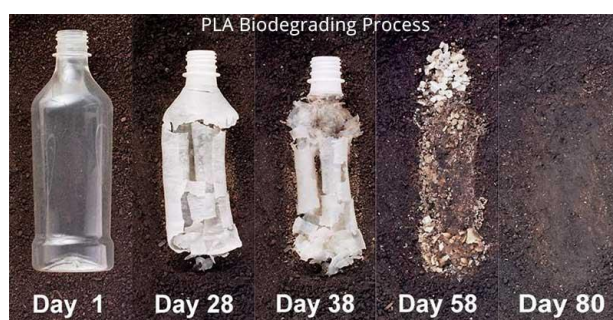


Figure 1.26: PLA biodegradation.

When no trace remains, complete biodegradation (or mineralization) occurs, i.e. when the original substance is fully transformed into gases and salts [66].

The biodegradability of a material buried in a compost medium where moisture, temperature, and aerobic environment are controlled is defined compostability. Additional criteria relating to the latter represent the difference from biodegradable polymers. In addition to biodegradation into carbon dioxide, water, inorganic compounds and biomass, compostable polymers must meet other requirements, such as compliance with the composting process, no adverse effects on compost quality, and degradation rates compatible with other established composting materials must be met.

In order to bestow "biodegradable" labels, numerous worldwide standardized tests have been created. Nowadays, ISO and ASTM norms define the purposes of "biodegradable and compostable" in detail.

For example, the ASTM D6400 standard lays down criteria for the labelling as “compostable in municipal and industrial composting facilities” of materials and goods, including packaging made from plastics:

- Conversion to carbon dioxide, biomass and water in the form of powder, film or granule under micro-bacterial action of the test polymer sample;
- Ninety percent of the conversion to carbon dioxide and less than 10 percent with a scale of 2 mm or less of the remaining material;
- The same biodegradation rate as that of natural materials (grass, leaves, paper, and food waste);
- Biodegradation time of less than 180 days;
- Nontoxicity of the resulting compost to the ecosystem.

Composting is characterized by ASTM standards (ASTM D 6400-04; ASTM D 6002-96) as a regulated process that controls the biological decomposition and conversion of biodegradable materials into a humus-like substance called compost: the aerobic mesophilic and thermophilic degradation of organic matter for the production of compost, the conversion of biologically decomposable material through a controlled bio-oxidative process. Special conditions are needed for composting, particularly temperature, humidity, pH, aeration and carbon to nitrogen (C/N) ratios, which are linked to optimum biological activity at different stages of the process.

Waste degradation into compost proceeds in three phases according to ASTM standard [69]:

1. The first mesophilic phase

Mesophilic bacteria and fungi degrade soluble and readily biodegradable organic matter compounds, such as monosaccharides, starch, and lipids, at the start of composting. Organic acids are formed by bacteria and the pH decreases to 5-5.5. When heat is released from exothermic degradation reactions, the temperature begins to spontaneously increase. Protein degradation leads to ammonia release, and the pH rises rapidly to 8-9. The length of this stage is from a few hours to a few days.

2. Thermophilic phase

When the temperature exceeds 40°C, the compost goes into the thermophilic phase. Thermophilic bacteria and fungi take over and the waste rate of degradation grows. Microbial activity and diversity decline drastically if the temperature reaches 55-60°C. The pH stabilizes to a neutral level following peak heating. The thermophilic process will last between a few days and a few months.

3. Cooling and maturation phase

The compost continues to cool after the easily degradable carbon sources have been consumed. The compost is stable after cooling; mesophilic bacteria and fungi reappear, which is followed by the maturation process. However, most species vary from those of the first mesophilic phase species. Biological processes are now sluggish, but the compost is humidified further and matures.

The length of the phases depends on the organic matter composition and the process efficiency, which can be determined by the consumption of oxygen [70].

The degradation of polymers in compost can be tracked by measuring changes in molecular weight due to bond cleavage or by measuring weight loss due to low molecular weight content depletion [71]. Other criteria, such as loss of mechanical strength, complete degradation into monomers or their release, have been suggested as a criterion for degradation in addition to loss of molecular weight.

1.3.4 Applications

The availability of monomers used in polyester synthesis makes it possible to prepare a wide range of products possessing unique characteristics for a broad variety of applications.

Aliphatic polyesters, thanks to their mechanical efficiency, biocompatibility and biodegradability, are used, for example, in the manufacture of various medical devices such as prosthetics, bone screws, artificial skin, pins, dental implants, vascular grafts, stents and temporary internal fracture fixation plates [72-73]. Since they are to be used for a limited period of time, degradable polymers are needed in all these cases to fulfil the elimination after use criterion.

Aliphatic polyesters are also used for environmental applications in addition to the biomedical field. In a certain way, biomedical implants can be compared to applications such as packaging, crop defence coatings, mulching films, chewing gums, agricultural staples, cigarette filters, cartridge and so on. Materials are used for a limited period of time in these fields as well and produce waste after use. In addition, conventional polymers are not biodegradable and accumulate in our ecosystem. For this purpose, in many applications degradable polymers are essential. In agronomy, for instance, polymeric systems are used to distribute pesticides, fertilizers, insecticides, etc (localization, time, and rate control of the delivery; higher efficiency; lower toxicity; ...).

Sadly, the available materials themselves are unable to provide solutions to the potential applications mentioned. As a result, science and technology will be developed by polymer scientists and industrialists to take advantage of the outstanding potential provided by polymeric systems to comply with material properties and application requirements, namely copolymerization and additive formulation [1].

Biopolymers may have properties similar to conventional ones, depending on the manufacturing process and on the source. In general, they can be split into three major groups: polymers based on starch, polymers based on cellulose and polyesters.

1.3.5 Starch-based polymers and blends

Starch, an inexpensive biodegradable resource produced annually from maize and other crops, is one of the biopolymers found in nature. In packaging industry starch has received extensive attention for the development of commercial thermoplastic polymers [74-76]. It is possible to use starch-based packaging for fresh cut beef steaks or whole fresh celery and is already used for milk chocolates and organic tomatoes [77].

Atmospheric CO₂ trapped by starch-producing plants is recycled during the biodegradation of starch items. They can degrade in 5 days in the aqueous aerobic systems, in 45 days in managed compost and in water, depending on the type of thermoplastic starch content [78].

Varying the starch source, all starches contain certain ratios of amylose and amylopectin (figure 1.27)

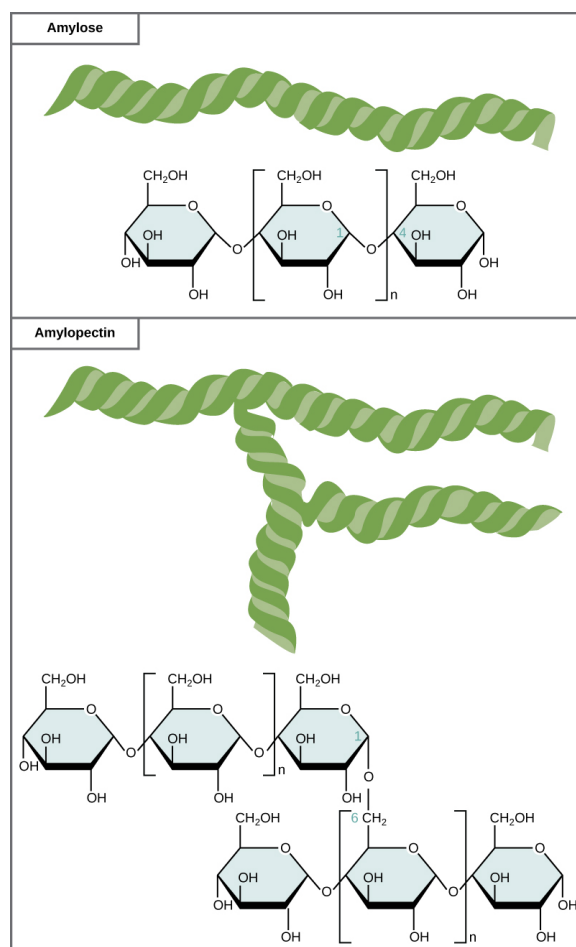


Figure 1.27: Chemical structures of Amylose and Amylopectin [Source: CNX OpenStax, Wikimedia Commons]

In hot water, amylose forms a colloidal dispersion, while amylopectin is fully insoluble. The amylose/amylopectin ratio affects the physical properties of starch. The starch granules swell during gelatinization and form gel particles. In general, the swollen granules are enriched with amylopectin, while the linear amylose diffuses from the swollen granules and outside the granules forms a continuous phase. Normally, before it melts under applied heat, a starch granule degrades because its molecular structure has strong inter- and intra-molecular hydrogen bonds that result in high glass transition (215-238 ° C) and melting temperatures (267-277 ° C) [79].

However, compared to their synthetic equivalents, natural polysaccharides have many drawbacks, including decreased thermal stability, moisture absorption and limited mechanical efficiency, which prevents their straightforward application in virgin form for advanced material systems. Polysaccharides are thus typically used in a derivatized form and/or in conjunction with other biobased polymers, requiring blends and composites of this kind to be compatible. [80-81].

Humidity absorption leads to the slow recoiling of gelatinized molecules of amylose and amylopectin back into their native helical configurations or into a new conformation of a single helix. As it improves crystallinity and decreases film elongation over time, retrogradation is undesirable. This limits their ability to be used for the production of biodegradable packaging materials as a fundamental raw material. Mixtures with other materials, such as plasticizers, crosslinking agents or other polymers, have been studied in order to improve the properties of the starch film. As a plasticizer, glycerol may be applied to boost the mechanical properties of the film, increasing its flexibility [82].

In order to enhance their functionality, the addition of other thermoplastic polymers to form mixed starch films will modulate the properties of the films. Hydrophobic synthetic polymers, such as aliphatic polyesters, could give adequate solutions among all commercially available biodegradable polymer materials if blended with thermoplastic starch (TPS), a non-crystalline de-structured starch developed by heat application and working in the presence of a plasticizer [83-85].

The inadequate interfacial adhesion between the hydrophilic starch and the hydrophobic polyester is the greater difficulty in producing starch/Polyester blends. Multifunctional compounds, such as maleic anhydride (MA) and citric acid (CA), are added to solve this problem in order to facilitate esterification/transesterification (crosslinking) reactions at the interface between polymeric chains in order to enhance their compatibility. According to literature, this reality has been successful in several polymeric systems for morphological regulation [86-88].

The properties can be easily and effectively controlled by adjusting the synthetic polymer component, even playing on the morphology of the blend. Under the trade name Ecostar[®], LDPE-starch blends were commercialized in 1993. Bioplast[®] (from Biotec GmbH), NOVON[®] (from NOVON International) and Mater- Bi[®] are other commercial trade names (from Novamont). Both products are transformed predominantly into films and sheets.

For foaming and injection molding, blends of more than 85 percent starch are used. Foams may be used as loose-fill instead of polystyrene; loose fills based on starch have an average density of 6 to 8 kg/m³, compared to 4 kg/m³ for loose filling with extended polystyrene. Biopur[®] (from Biotec GmbH), Eco-Foam[®] (from National Starch & Chemical) and Envirofill[®] are the commercial trade names (from Norel). In general, loose-fill materials from starch are water sensitive. If the packaging material is exposed to water, this is a concern, but a benefit when quick disposal is required. Rigid and dimensionally stable injection molded products result from combining thermoplastic starch with cellulose derivatives.

1.3.6 Cellulose based polymers

One of the most available organic materials on earth, cellulose (Figure 1.28) is a polysaccharide consisting of a linear chain of many hundred to several thousands of β -connected D-glucose units which has an interesting combination of different properties. Every natural fibre is cellulosic in nature, whether it is wood or non-wood. This implies that cellulose is a natural polymer that exists in the cell walls of all plants. Although humans can eat edible plants, the human digestive system does not digest the cellulose inside them and is rejected by the body. On the other hand, parts of them can normally or accidentally be discarded during the time of planting through the harvesting of plants and turned into agricultural waste.

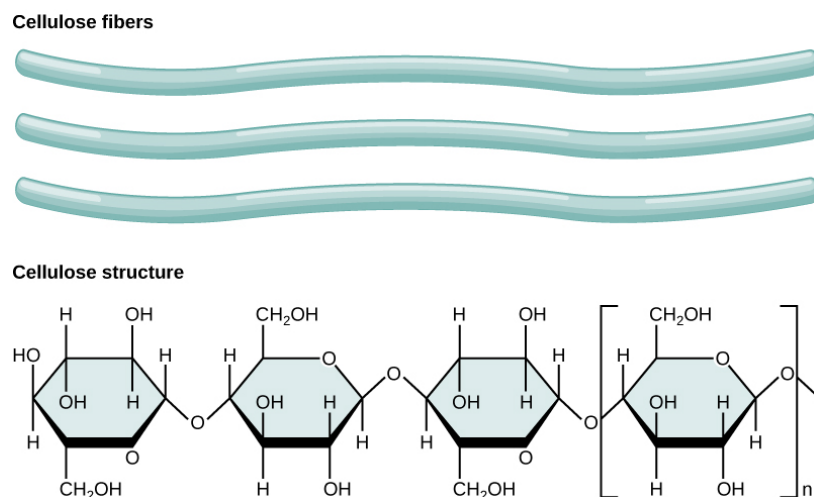


Figure 1.28: Chemical structure of cellulose [Source: CNX OpenStax, Wikimedia Commons].

Cellulose applications can be grouped into three major topics in the packaging industry. The first is to remove and directly use cellulose from plants to prepare composites. The second is to manufacture cellulosic plastics such as cellulose acetate, which are the best examples of renewable resource-derived biopolymers. The third is to prepare materials for the coating, such as edible and non-edible films [89].

In addition, a relatively new research area is the subject of cellulose-based nanocomposites: in developed and developing countries there is now a growing interest in biopolymer-based nanocomposites, especially if nanocomposites are based entirely on renewable raw materials [90-91].

A special interest is dedicated to PLA/cellulose nanocomposites, since both poly(lactic acid) matrix and cellulose have very abundant and renewable raw materials [92]. Cellulose is widely used in nanocomposites in form of nanocrystals, CNC, which are the crystalline regions extracted from cellulose microcrystals, mainly through strong acid hydrolysis at elevated temperatures. Those materials have the peculiar properties of high aspect ratio, high surface area, high mechanical strength, and a liquid crystalline nature [93].

1.3.7 Bio-Polyesters

Aliphatic polyesters are undoubtedly one of the most promising groups for packaging applications among biodegradable polymers because they combine interesting properties with proven biodegradability and reasonable production costs.

Unfortunately, at present biopolymers must contend with existing common and inexpensive materials in terms cost and efficiency. This is incredibly challenging because in order to be economically viable, modern processes require extensive analysis and substantial capital costs and must be scaled-up. The commercialization of biodegradable plastics will continue to increase on the basis of both economic and environmental considerations, especially in markets where goods have a relatively short lifetime of use. Despite that, many biodegradable polyesters are on the market or at an advanced development level.

1.3.2.1 Long chain aliphatic polyesters

As mentioned above, synthetic polymers, derived from petrochemical resources, are the most widely used polymers in packaging applications. Polyethylene (low density (LDPE), linear low density (LLDPE), and high density (HDPE)) are undoubtedly the most widely used in these applications.

Their great success is due to the low cost and excellent physical-mechanical characteristics of their products. Sadly, as is well-known, in conditions where they are disposed after their work has finished these materials are not readily degraded. For this purpose, since the 80s, both academic and industrial researchers have devoted their efforts to the design of biodegradable polymers with chemical and physical properties very similar to PE or other polyolefins. Due to the large number of methylene units along the macromolecular chain, long chain aliphatic polyesters well mimic the Poly(Ethylene) backbone.

Recently, numerous studies have focused on the synthesis and characterization of HDPE and LDPE aliphatic long-chain polyesters [94-100].

Unfortunately, the biodegradation rate of these polymers remains very low due to the low number of hydrolyzable ester bonds along the polymeric chains.

1.3.7.1 Poly(buthylene succinate) PBS

Poly(butylene succinate) (PBS, Figure 1.29) [101] and its copolymers are a family of biodegradable polyesters that are useful in a broad range of applications among bioplastics [102-105]. Since 1993, PBS has been commercially available, among other popular cases. It is manufactured by Showa-Denko under the tradename Bionolle™ and by Mitsubishi Chemical Corporation under the tradename GS Pla™ [106-107]. Its key uses include environmental purposes, such as compostable bags, mulching films, catering goods and foams, nonwoven sheets and textiles.

The monomers used in the PBS synthesis are succinic acid (SA) and 1,4-butanediol (BD), which are widely obtained and readily available on the market from fossil resources. Interestingly, from fermentation both SA and BD can also be produced. Different microorganisms have been screened and tested for succinic acid production through biotechnological processes in recent years, with good yields [108].

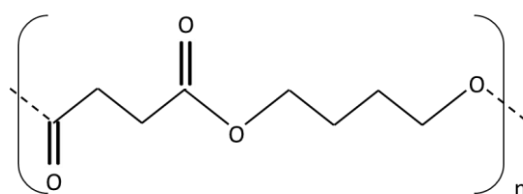


Figure 1.29: PBS structure

By hydrogenation, the obtained SA can then be converted into 1,4-butanediol [109]. This will result in a fully bio-based PBS. Companies such as Succinity (a joint venture between BASF and Purac), Reverdia, BioAmber and Myriant are involved on an industrial scale in the manufacture of biosuccinic acid.

PBS's popularity as a thermoplastic material is due to its characteristics. In fact, PBS is a semicrystalline polymer with a high capacity for crystallization (crystallinity degree = 35-45 percent) [110] and one of the highest melting temperatures among poly(alkylene dicarboxylate)s [111-112]. The temperature of the glass transition is far below room temperature, so PBS has a wide range of processability that enables extrusion, injection molding and thermoforming [113-115].

Concerning mechanical properties, the presence of small amounts of diisocyanates, usually hexamethylene diisocyanate, used as chain extenders is strictly influencing them. Synthesized high molecular weight PBS without chain extensors demonstrates a fragile behavior, with very short elongation at break, whereas the use of isocyanates greatly improves its elongation, up

to values equivalent to polyolefins [116]. Unfortunately, due to its high degree of crystallinity and rigidity, the use of PBS is limited in those applications where rapid degradation rate and flexibility is needed [117].

1.3.7.2 BioPBS and Copolymers

Biodegradable and bio-based plastics are the most preferred option in this context: bio-based poly(butylene succinate) (BioPBS), which has been manufactured industrially by PTT MCC Biochem Company since 2016, belongs to this class because it can be extracted from natural resources such as cassava and maize sugarcane and is naturally compostable into biomass, carbon dioxide and water without the need for specialized co-operation. In addition, it can be manufactured without any additional investment using the current extrusion coating machines, blown film extruders and injection molding machines used for LDPE; it has excellent heat sealability; and it has been certified for food touch [118-119].

Since 2009, many block and random PBS copolymers has been analyzed: the barrier efficiency of PBS and some of its statistical copolymers have only recently been investigated [120-122]. As is well known side alkyl groups, randomly distributed along the main linear chain, help to increase the flexibility of the material, reducing the capacity of the macromolecular chain to crystallize [123-124].

As previously said, PBS is too rigid for flexible food packaging: copolymerization with a glycol containing sufficiently long side alkyl groups may be an effective method for improving mechanical properties. Prof. Lotti and coworkers recently synthesized and investigated thermal, mechanical and gas barrier properties of high molecular weight random copolymers of PBS containing alkyl side groups, successfully obtained by one pot-solvent-free process. The chemical formula is shown in Figure 1.30 [125].

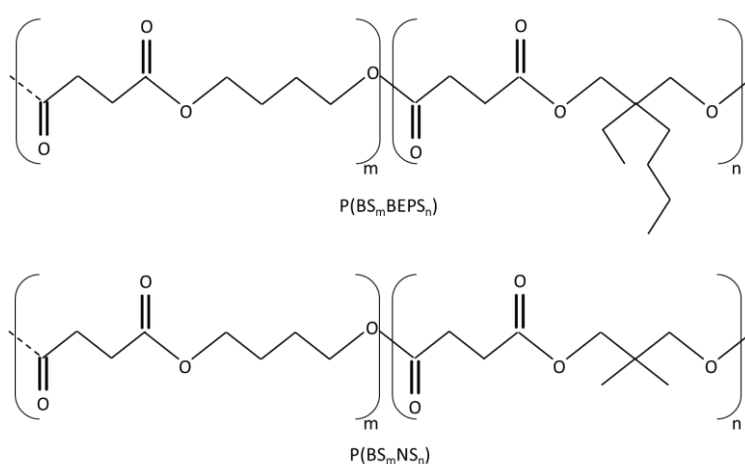


Figure 1.30: new poly(butylene/2-butyl,2-ethyl-propylene succinate) (P(BS_mBEPSt_n)) and poly(butylene/neopentyl succinate) (P(BS₇₀NS₃₀)) random copolymers.

Thermal stability, a key element during material production, was not worsened by copolymerization. The PBS crystallizing ability is greatly reduced by long pendant groups: a dramatic reduction in the degree of crystallinity is indeed observed. With the shortest methyl side groups included in the PBS crystal lattice, such an effect is not so marked.

The mechanical properties are greatly affected by the long alkyl pendant groups, reducing and increasing the elastic modulus and elongation at break, respectively. The introduction of 30 percent of BEPS co-units along the polymer chains of PBS gives elastomeric activity to the final material.

In view of the desired packaging use, gas permeability properties can be nicely adapted, acting both on pendant group duration and on copolymer composition. In particular, due to a decrease in the degree of crystallinity, a decrease in barrier efficiency was observed with an increase in the BEPS co-unit material. The rise in GTR values was more associated with the CO₂ gas test, while the N₂ test was more moderate. These lie in between with respect to the O₂-GTR value variations.

In order to choose the required headspace gas composition, such findings are of fundamental importance to MAP technology. An atmosphere that is low in O₂ and high in CO₂ slows down the metabolism of packed products or the activity of spoilage, preserving or prolonging the shelf-life of the desired product [126-127].

N₂ gas, on the other hand, allows the creation of an inert atmosphere that prevents the collapse of the set. It is critical, therefore, that its internal percentage remains constant. Finally, with respect to LDPE, which is commonly used in flexible food packaging, the barrier performance of certain copolymers appears to be comparable or even superior.

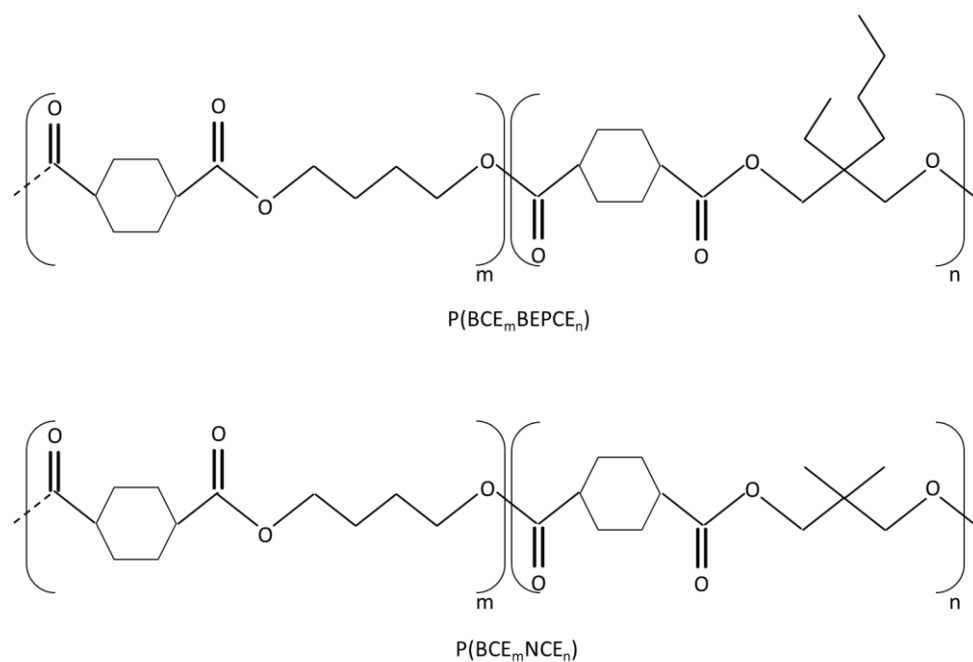


Figure 1.31: poly(butylene/2-butyl-2-ethyl-propylene trans-1,4-cyclohexanedicarboxylate) (P(BCE_mBEPCEn)) and poly(butylene/neopentyl trans-1,4-cyclohexanedicarboxylate) (P(BCE₈₀NCE₂₀)) random copolymers.

New high molecular weight poly(butylene/2-butyl-2-ethyl-propylene trans-1,4-cyclohexanedicarboxylate) (P(BCE_mBEPCE_n)) and poly(butylene/neopentyl trans-1,4-cyclohexanedicarboxylate) (P(BCE₈₀NCE₂₀)) random copolymers containing side aliphatic chains of different lengths (Figure 1.31) were also synthesized [128].

The two copolymers most rich in BEPCE co-units, characterized by elastomeric behaviour and exceptional barrier properties to oxygen and carbon dioxide, are especially interesting for packaging application. It is hypothesized that the outstanding barrier properties are related to the presence of mesophase, especially important for the copolymer P (BCE₅₀BEPCE₅₀). In spite of being amorphous and having a T_g below room temperature, this latter material can still be processed as a freestanding flexible film. Its barrier efficiency is substantially higher than that of two bio-based high performance barrier materials, poly(ethylene 2,5-furanoate) and poly(propylene 2,5-furanoate) [129-134].

Many other co-polymeric systems have been developed, starting from studies on PBS copolymers, leading to interesting tuning ability on a wide range of final packaging application properties [135-142].

1.3.7.3 Poly(lactic acid) (PLA)

Biodegradable, recyclable and biocompatible: PLA is one of the most promising bio-based polymers, requiring low production energy, good processability, high transparency and resistance to water solubility [78, 143-144]. Such properties combined with favorable market costs, made it one of the first biopolymers commonly used in the packaging of fresh products to be commercially available. Today, PLA is manufactured on a large scale by companies around the world, such as Mitsui Chemicals Inc. (Japan), NatureWorks Llc (USA), or Futerro (Belgium).

Carothers pioneered the manufacture of lactic acid polyester in 1932 and Dupont and Ethicon improved it further [145]. Until the late 1980s, prohibitive manufacturing costs limited the applicability of this polymer outside the medical sector. Since then, significant breakthroughs in process technology have led to the commercial-scale manufacture of lactic acid plastics for non-medical uses, combined with reduced costs for biologically produced lactic acid. This combination of biotechnology and chemistry is a significant technique that will be critical for improving many other chemical processes in future.

Two chemical routes for the conversion of lactic acid to high molecular weight PLA have been established. A solvent-free continuous process and a new method of distillation are used by Cargill Dow LLC [146]. Mitsui Toatsu, on the other hand, transforms lactic acid directly into high molecular weight PLA through a solvent-based azeotropic process (where vapor and liquid have the same composition at some stage in distillation) by distilling water elimination.

Chemical monomer synthesis is based on heavy acid hydrolysis of lacto-nitrile, giving rise to a racemic blend of D- and L-lactic acid. Catalyzed sugar degradation, propylene glycol oxidation, acetaldehyde reaction, carbon monoxide and water at high temperatures and pressure,

chloropropionic acid hydrolysis and propylene nitric acid oxidation may be several synthetic methods.

Interest in the microbial fermentative processing of lactic acid has grown in order to use renewable resources instead of petrochemical ones, and to obtain an environmentally friendly monomer. Sugar in pure form (glucose, lactose, sucrose) or sugar-containing materials such as whey, sugar cane bagasse and cassava bagasse, tapioca, potato, barley, wheat, etc. may be the carbon source for the microbial production of lactic acid. To minimize the cost of raw materials, food/agro-industrial by-products or residues may be used as a cheaper alternative [147]. A direct polycondensation reaction could be used to produce the corresponding polyester because both a hydroxyl and a carboxylic group are present in the lactic monomer. In this case, the addition of acidic catalysts is required to obtain high molecular weights and decrease the polymerization time and temperature, with a moderate yield of relatively high molecular weight polymer.

A good alternative is the step-growth polymerization, starting from lactic acid or by ring-opening polymerization (ROP) of lactide (LA), that is the ring-formed lactic acid dimer [148]. Thanks to the chiral nature of Lactic acid, it exists in three different forms: L,L-LA, D,D-LA, and D,L-LA (mesolactide), as well as a 50/50 mixture of L,L-LA and D,D-LA referred to as racemic lactide (Figure 1.32).

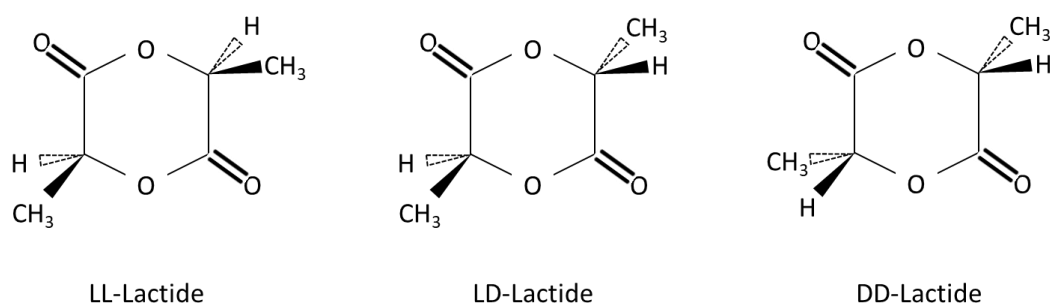


Figure 1.32: Chemical structures of LL-, meso- and DD-Lactides.

The properties of the PLA material depend on the type of isomer (D-, L-, DL-lactide), molecular weight, temperature of processing and annealing time. The stereochemical structure has a powerful effect on the melting point and the ability to crystallise of the polymer [149]. PLLA has a 37 percent crystallinity, a 50 to 80 ° C glass transition temperature, and a 173 to 178 ° C melting temperature. The introduction of stereochemical defects (meso-lactide or D-lactide) decreases these parameters compared to pure PLLA but has a slight effect on the temperature of the glass transition [150]. When D-lactide is copolymerised with L-lactide, similar effects are observed. It is possible to modulate their degradation rate by adjusting the degree of crystallinity of the polymers. The higher the percentage of crystallinity, the lower the rate of biodegradation. In addition, degradation has been found to rely on a number of variables,

such as temperature, molecular weight, pH, purity, terminal carboxyl or hydroxyl group presence, plasticizer, water permeability and additives [151].

PLA degrades mainly by hydrolysis, not microbial aggression, upon disposal [145]. It is also unlikely to experience contamination of high molecular weight PLA by mould, fungi, or other microbes even at high humidity. This unique aspect of a bioplastic is desirable for applications where it is in close contact with food for long periods of time. This is why PLA is currently used in packaging for applications like films, thermoformed containers, and short-shelf life bottles.

As a packaging material, PLA's certified compostability and compliance with the food contact safety regulations [148] makes it desirable because it meets the compostability criteria of EN13432 [EN 13.432, 2005], thus alleviating the issue of plastic waste.

Even though PLA can be considered a valid substitute for many non-biodegradable polymers, its brittleness and barrier properties make it less appealing.

However, by altering its chemical composition and varying its molecular characteristics, its physical, mechanical and barrier properties can be tuned. The mixing (both blending or copolymerization) of PLA with other polymers is also possible, making it a good biodegradable alternative to conventional polymers for use in plastic packaging and other special applications (e.g medical scaffolding). Some examples are represented by multiblock biobased copolymers, nanocellulose biocomposites (and NC grafting), blends with PHB, keratin reinforcing etc. [152-161].

1.4 Packaging

Packaging is the largest category of plastic applications, representing approximately 40% of the European converter market alone (Figure 1.3). Petrochemical plastics such as polyethylene terephthalate (PET), polyvinylchloride (PVC), polyethylene, polypropylene (PP), polystyrene (PS) and polyamide (PA) have been widely used as packaging materials due to their relatively low cost availability and good mechanical efficiency such as tensile strength and tear resistance, good oxygen and carbon dioxide barrier. Their use has been limited in recent years for the reasons already explained above.

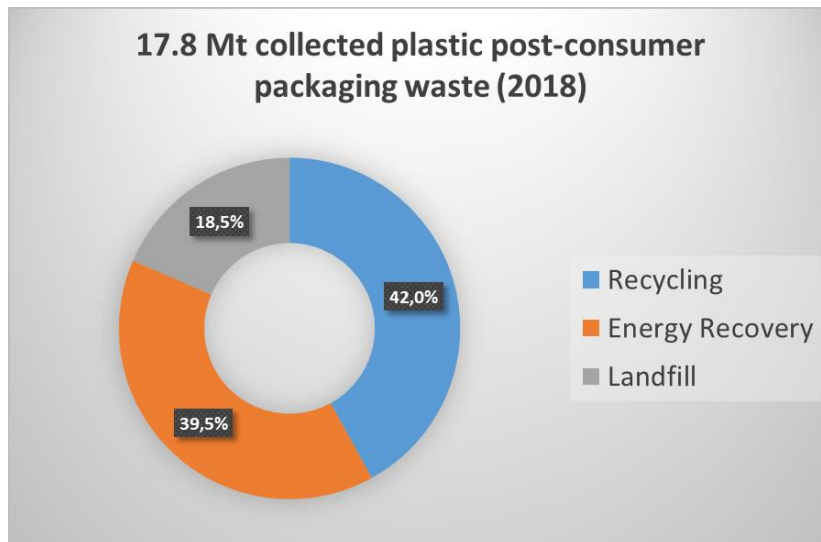


Figure 1.33: Packaging waste end-life in Europe. [Source: Plastics Europe]

In 2018 in Europe 17.8 Mt post-consumer packaging waste were collected from household, industrial and commercial packaging, and still almost 20% is landfilled, and almost 40% is burned (Figure 1.33). In order to replace their non-degradable counterpart, new bio-based food packaging materials have been designed [162]. It is well known that high manufacturing costs of biodegradable materials are an obstacle, with synthetic materials being an important drawback. The production of eco-friendly products, however, is justified because they ensure environmental protection. This means the safety of non-renewable sources and the prevention of contamination problems associated with the final disposal of non-degradable materials [163]. In addition, the production of unique performance packages requires safer, healthier, and high-quality foods with longer shelf life [164].

Even thin plastic film packaging with a thickness of just a few microns will increase the shelf life of goods while reducing food waste, energy consumption and emissions of greenhouse gases. Food packages should have customised properties, such as mechanical, optical and barrier properties that depend on the structure of the polymeric packaging material, in order to perform these functions. To ensure their handling without any food product damage, materials must be tough and versatile enough. In addition, package tightness related to barrier properties is another important concern, because organoleptic and microbial food qualities rely on the effectiveness of the package to regulate the exchange of gases.

A package system's specific barrier requirement depends on food characteristics and expected end-use applications. Water vapour and oxygen are two of the main gases studied in packaging applications as permeants; they disperse through the film, altering the consistency and shelf life of the product. For ones whose physical and chemical degradation is linked to moisture content, the water vapour barrier property of film packaging is significant [165]. A low gas transmission rate is important for oxygen gas, as this gas promotes many mechanisms of food degradation, such as corrosive phenomena, oxidation, and modifications to organoleptic properties [166].

The key problems restricting the shelf-life for fresh fruits and vegetables are the high breathing rate, acidification, development of off-flavors, loss of firmness and decoloration, high production of ethylene, and microbial spoilage [167-169]. By reducing the rate of breathing by limiting O₂, the shelf life of fruits and vegetables is prolonged by delaying the oxidative breakdown of the complex substrates forming the product. O₂ concentrations below 8 percent decrease ethylene development, a key component of the process of maturation and maturation [170].

Modern technologies for food packaging include modified atmosphere packaging (MAP), active packaging and smart packaging designed to improve food safety and quality in the most natural way possible [171]. The atmosphere is modified according to the ambient atmosphere under controlled conditions, and these conditions are maintained throughout storage. This method desirably generates an atmosphere low in O₂ and high in CO₂, which affects the metabolism of the packaged product or the activity of microorganisms that cause food spoilage, which ultimately leads to increased storability and shelf-life [172] MAP hinders spoilage processes, as well as decreases breathing, delays maturation, decreases production of ethylene and sensitivity [173-175].

In addition, it is important to study the changes in the characteristics of plastics that may occur during the time of food interaction [176]. Last but not least, food compatibility plays a key role in this type of application; in fact, it has been recognised as a potential source of loss of food quality properties [177]. Disposable cutlery, drinking cups, salad cups, plates, overwrap and lamination film, straws, stirrers, lids and cups, plates and containers for food dispensed in delicatessen and fast-food establishments are included in the field of application of biodegradable polymers in food contact articles. Especially after single-use plastic ban. These articles will be in contact with aqueous, acidic and fatty foods dispensed or maintained at or below room temperature or dispensed at temperatures as high as 60 ° C and then allowed to cool down to or below room temperature [178].

To date, for all these reasons, only a limited quantity of biodegradable polymers has suitable properties and can be used in food packaging applications. For other packaging types, more solutions have been found.

Speaking of packaging types, there is a main classification of packaging (Figure 1.34): primary, secondary, tertiary, and eventually ancillary.



Figure 1.34: Packaging types examples.

Packaging in direct contact with the product itself is primary packaging and is sometimes referred to as consumer or retail packaging. Primary packaging is primarily intended to protect and/or preserve, contain and inform the consumer.

There are different examples of primary packaging, and for one product, there can sometimes be several components. For beer, for example, the liquid-containing bottle and the label are both classified as primary packaging. For gift and luxury products such as in the technical and cosmetic industries, corrugated primary packaging is often used.

The primary purpose of secondary packaging is for branding and logistical functions. As well as protecting and collecting individual units during storage, they are often used for displaying primary packs on shelves by the beverage, food and cosmetic industries and are sometimes also referred to as grouped or display packaging. Secondary packaging also provides packaging designed to display several product units for sale that speeds up replenishment from storeroom to shelf, including retail packaging (RRP), shelf-ready packaging (SRP) or counter-top display units (CDUs).

Secondary packaging is primarily corrugated cardboard packaging printing finished to a high standard, such as litho printed with branding and design due to the integral part of the marketing funnel that it has to play.

Tertiary packaging makes it easier for a set of sales units or secondary packaging to be protected, treated and shipped in order to group it into unit loads during transit. The customer seldom sees this form of packaging.



Figure 1.35: Tea bag packaging.

Among food packaging we can have for example tea/coffee bags (Figure 1.35), which are mainly made of nonwoven materials or filter paper, in order to permit the hot water passage during the infusion. Those bags are then possibly wrapped in single pouches or directly put in their secondary packaging (normally paper boxes), depending on the chosen shelf life strategy, and finally stored in a tertiary packaging (cardboard box).

1.4.1 Nonwoven materials

More than what the material is, the term "nonwoven" defines what a material is not. The word has never been able to adequately reflect this particular sector, but efforts have not been successful in changing the name or classification. In the beginning, nonwovens were less regarded than woven and often were used as cheaper replacements for woven materials [179]. However the nonwoven textile industry is currently highly profitable and has stable annual growth rates. In the textile materials industry, nonwovens are the fastest growing market, and there is a demand for nonwovens, especially in the area of disposable products, but also among the most valuable non-disposable products. The market for nonwovens in the United States alone is expected to grow to \$7.1 billion in 2016 with a 5.7 percent annual increase. [180].

The manufacturing systems for nonwoven are divided into drylaid, wetlaid or spun (Figure 1.36). Drylaid materials have their origins in textiles, wetlaid materials in the production of paper and spunlaid products in polymer extrusion and plastics. Therefore it is possible that the term "nonwoven" applies to different companies, which rarely have anything in common. Due to the use of different types of raw materials, technology, fields of research and development, products and/or business models, the differences among companies can vary. Nonwovens are often split into groups such as consumer products, medical, automotive or civil engineering industries and so on, depending on their end-use applications.

Nonwoven paper-based fabrics are made from mixed suspensions, where liquid fibres are manipulated. The three stages of the production of nonwovens with the wetting method are: (1) fibre swelling and dispersion in water; (2) transport suspension by filtration on the screen, where the web formation takes place; (3) web drying and bonding. One benefit of this process is that almost anything including Kevlar, leather and even stainless steel, can be the fibres used. The negative side of the wetlaid process is that it consumes large volumes of water and that the process is capital intensive. EDANA determines the distinction between wetlaid nonwovens and wetlaid paper (the European Nonwovens and Disposables Association). The fibrous content of a nonwoven material must meet certain requirements, according to EDANA. These requirements mean that the length/diameter ratio must be greater than 300 for 50 percent of the fibres, or that the density must be less than 0.40 g/cm^3 for 30 percent of the fibres.

The end-use applications in the production of "fabric-like" nonwovens are surgical products, hospital supplies, bed linen, napkins and towels. Nonwoven products from Glassbases include roofing, flooring, circuit printing mats, batteries, philtres and decorative materials. In filtration (dust, air and liquid), laminate, wood flooring, teabag paper, plug wrap and sausage skin paper, etc., specialty papers can be used.

There is a relatively limited life cycle of a large number of nonwovens, which contributes to problems with disposability. In recent years, the environmental effect of disposable goods has become a major concern and a subject for discussion. Many disposable products, including polyester (PET), polypropylene (PP), polyamide (PA), polyethylene (PE) and polycarbonate(PC), are produced from conventional thermoplastics [181].

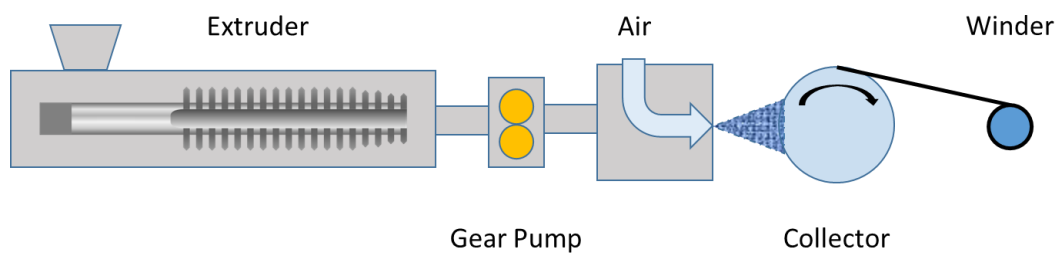


Figure 1.36: Typical polymeric nonwoven process (melt blowing spinning).

Biodegradable nonwovens may also be a solution to the increasing quantity of consumption waste, although they also have a limited life span. As a result, there is a growing effort both in academia and in industry in the field of biodegradable nonwovens in design, research and production [182].

Biopolymers such as PLA have helped expand the market and to become more flexible. Combined with natural fibres or other biodegradable resins, this polymer is also used. The industry is currently developing new ways of manufacturing bio-based nonwovens, which can minimise fabric costs and provide more sustainable, environmentally friendly consumer goods. Another topic of industrial research is to speed up the process and eliminate non-conformities in the finished product, which ensures that packaging materials and machines have correct, consistent interactions. In the welding stage of the development of packaging, this aspect is especially significant.

1.4.2 Polymer Welding

Plastic welding is a welding process for semi-finished polymeric materials and is defined in ISO 472 as a process for the union of softened material surfaces, typically by means of heat (except solvent welding). Thermoplastics welding is conducted in three sequential steps, namely surface preparation, heat and pressure application, and cooling. For the jointing of semi-finished plastic materials, various welding methods have been established. Welding methods for thermoplastics can be categorised as external and internal heating methods on the basis of the process of heat generation at the welding interface [183]. External Methods include Thermal ones (e.g. Heat Sealing and Laser welding), while Internal are divided in Mechanical (e.g. Ultrasonic welding) and Electromagnetical (e.g. Microwave welding).

On industrial machines, whether sealing in a vertical or horizontal configuration (e.g. on a form-fill-seal – FFS- machine), there are two widely accepted ways of creating a seal: by applying heat or generating friction via ultrasonics.

1.4.2.1 Heat sealing

To make a seal with a set of crimp seal heating bars, standard heat sealing systems use a combination of heat, time, and pressure. A layer of plastic is melted as the jaws come together, which binds the two layers of film together.

This technology is reasonably inexpensive to use at high speed on a variety of materials, including foil, poly-coated Kraft paper bags, OPP and laminates. Impulse sealing, which uses Teflon-coated heated sealing wires that are activated when the sealing bar is pressed tightly, is a variant of traditional heat sealing. Impulse sealing is primarily used where a barrier is not critical for PE applications.

There are four types of sealing jaw essentially, with the main difference between them being the time in which jaws come into contact with the sealing area.

- Rotary jaws

Primarily used on both horizontal and vertical machines for applications such as sweets, biscuits and confectionery, rotary jaws contra-rotate 360 degrees and meet in the centre to shape the seal. The sealing time is very low, making this a very high-speed technology, but one that does not guarantee a hermetic seal of high integrity.

- D-cam

In theory, this jaw assembly is similar to a rotary jaw design, but rather than adopting a circular movement pattern, D-cam jaws adopt an elliptical D-shaped pattern, which ensures that the jaws meet for longer in the seal region (the length of the 'D' stem). For high-speed applications where a hermetic seal is needed, D-cam revealed to be the most suitable jaws.

- Long-dwell

Long-dwell jaws do not rotate, in comparison to D-cam and rotary jaws, they shift instead with the pack, resulting in increased sealing time compared to rotating designs. Product height is limited to ensure clearance due to the 'up-down' motion of the jaws. For MAP packaging products, such as cheese, baked goods and cooked meats, this technology is very common.

- Box motion

Compared to other jaw designs, sealing time is considerably improved by only rotating the film while it is in contact with the jaw. This sealing unit is reserved for MAP and hermetically sealed applications involving, for example, cheese, very thick films where lots of pressure, heat and dwelling time are needed.

These are the jaw settings that can be used to generate the end seals (also known as the top and bottom, transversal or cross seals). A separate sealing device, comprising two, three or four hot and/or cold rollers, is needed for the fin or longitudinal seal (the seam which runs

down the length of the bag joining the right and left side of the originally flat film). The thickness and sealing properties of the film will determine the exact arrangement.

FFS can be continuous or intermittent. The packaging film is still as the longitudinal seam is covered on an intermittent machine, while the material is moved without stops on a continuous machine. The key advantage of continuous operation is higher productivity. Moreover, the film can travel through the machine at a slower pace than on an intermittent machine, leading to less technical problems.

1.4.2.2 Ultrasonic Sealing

Increasingly, packers and producers are migrating to ultrasonic sealing systems especially those in the salad bags industry. In order to produce heat only in the region between two film layers, this cold sealing device relies on friction generated by an oscillating device (a transducer coupled with a sonotrode). Vibrations for friction generation are induced at frequencies of 20-40kHz by ultrasonic energy.

Ultrasonic sealing requires less energy than heat sealing, and as the seals at the longitudinal and transverse seams are narrower, tangible material savings. The most important reason for ultrasonic sealing choice, however, is the degree of resistance and quality of the seal which can be achieved.

Ultrasonic sealing will reduce by 80% the leaky bag rates, by being able of sealing through any substance that may have been inadvertently deposited in the weld region. This method on VFFS (vertical type fill seal) machines is increasingly prevalent, but it is still in its infancy for horizontal applications due to geometrical problems.

1.4.2.3 Laser welding

Laser welding has been an emerging process for joining polymers since the mid-nineties of the last century. A wide range of thermoplastics can be processed today with a wide range of suitable laser sources using this contactless technology which enables effective, space-selective energy deposition. Continuous research efforts in laser polymer welding concentrate on process optimization [184], development of novel processing methods [185] and laser sources [186], and various material aspects of polymer joining [187], considering its general acceptance and usage in mass production and high-precision assembly for a broad range of industrial applications.

1.4.2.3.1 Laser sources

CO₂ lasers, Nd:YAG lasers, Diode lasers and fibre lasers are among the types of lasers used for welding polymers. Because of the high energy absorption coefficients of most plastics, CO₂ lasers are often applied to weld thin films. Nd:YAG lasers and Diode lasers generate short

wavelength radiation that transmits unpigmented polymer over several millimetres [188]. They are used in the techniques of transmission laser welding.

Carbon dioxide lasers have a 10.6 μm wavelength that is easily absorbed by most polymers. The processing of plastics using CO_2 can be carried out quickly with low laser power due to high energy absorption coefficients. For direct welding of polymers or cutting, this form of laser can be used. The penetration of CO_2 lasers, however, is less than 0.5 mm and is mainly applicable to thin film and surface heating welding. Since the beam cannot be transmitted by silicon fibre, mirrors normally deliver the beam, making the system quite hindering [189].

Nd:YAG lasers have a wavelength in the 0.8 - 1.1 μm range, with the most common being 1064 nm. The high beam efficiency of these lasers allows for small spot sizes. It is possible to deliver this form of beam by fibre optic cable.

Usually, diode laser wavelength is in the wavelength range of 780 - 980 nm. Diode laser has a superior energy efficiency compared to Nd:YAG laser and CO_2 laser. In semicrystalline plastics and further in unpigmented amorphous plastics, the high-energy light wave can penetrate a thickness of a few millimeters. Either fibre delivered or local to the weld position can be diode lasers. The relatively small size makes it possible to assemble arrays for larger footprints.

Generally, fibre lasers have wavelengths ranging from 1000 to 2100 nm. The extended range of wavelengths has allowed transmission welding to be obtained without absorbing additives for certain polymers [190]. Thulium lasers are part of this category and were first developed for medical applications: since they are part of the thesis, they will be described in Chapter 2.

1.4.2.3.2 Equipment and configurations

There are many options in system setup; however, in most of the machines five components are included: generator/power supply, control interface, actuator, lower fixture and upper fixture.

A generator part converts the voltage and frequency obtained from the laser source into the corresponding voltage, current and frequency. The two most widely used systems for laser welding are diode lasers and fiber lasers [191].

The control interface is an interface for controlling device operations between the user and the computer. Logic circuits are designed to transmit machine status information and welding parameters to operators. It can vary the parameters that are allowed to change based on various laser modes.

The actuator portion is a pneumatic and electrical power enabled press. To contact the components in the lower fixture, it compresses the part in the upper fixture and applies pre-

determined loads during welding processes. Displacement controls are applied to actuators to reliably track movements.

A structure that hosts the lower part of a joint is the so called lower fixture. This offers places and alignments that ensure the welding of components with close tolerances. In the whole scheme, the upper fixture is the most complex and critical part. The laser beam is shot to heat up the welding joints in this component. The upper fixture configuration also differs from laser sources and modes of heating. For instance, optical fibers are sometimes used to provide mobility when a YAG laser or a diode laser is used as the heat source [192].

Via a range of configurations, the laser beam energy can be distributed to the appropriate areas. Contour heating, simultaneous heating, quasi-simultaneous heating, and masked heating are the four most common approaches (Figure 1.37).

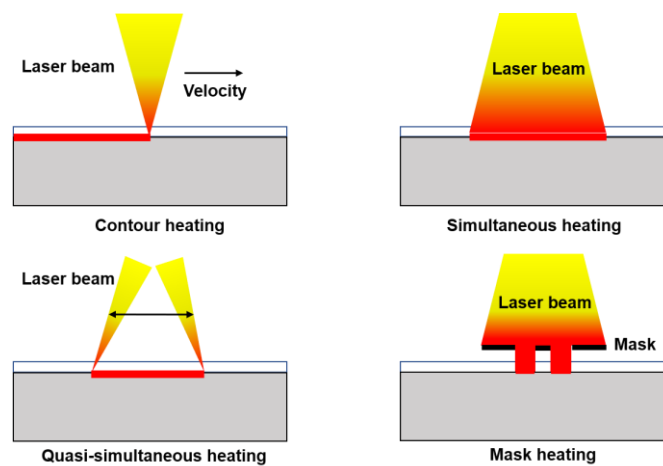


Figure 1.37: Laser application configurations [Source: based on Benatar, Avraham (2017). Applied Plastics Engineering Handbook (Second Edition). William and Adrew. pp. 575-591 CC BY-SA 4.0]

A laser beam of fixed dimension passes through the target area with the contour heating (laser scanning or laser moving) process to create a continuous weld seam. The laser source is moved to scan at a rapid rate by a galvanic mirror or a robotic lens system. The *pro* of contour heating is that the weld can be done with a single laser source that can be reprogrammed for different applications; however, uneven contact between welding components can occur and form weld voids due to the localized heating area. The essential parameters for this include: laser power, laser wavelength, crossing speed, and polymer properties.

A beam spot of sufficient size is used in the simultaneous heating method to irradiate the entire weld region without any relative movement between the work piece and the laser source. Multiple laser sources can be combined to create a weld with a wide area by melting a selected region simultaneously. In the case of welding vibration-sensitive materials, this technique can be implemented to replace ultrasonic welding. Laser wavelength, heating time,

laser strength, clamp pressure, polymer properties and cooling time are main processing parameters for this method.

In quasi-simultaneous heating configuration the use of scanning mirrors irradiates the work area. The mirrors quickly pass the laser beam over the surface, producing a region that is melted simultaneously. The important parameters are similar to the simultaneous heating ones.

Masked heating is a laser line scanning through a surface procedure, with a mask that ensures that when the laser passes through, only the selected areas can be heated. Masks can be obtained from laser cut steel or other materials that block laser radiation efficiently. This method is capable of producing micro-scale welds on parts with particular geometries. Also in this case, laser wavelength and intensity, heating and cooling time, clamp pressure, and polymer properties are main processing parameters for this approach [193].

1.4.2.3.3 Laser-polymers interaction

There are three kinds of interactions between laser radiation and plastics that can be observed: reflection, absorption and transmission. The extent of individual interaction depends on the properties of the material, laser wavelength, laser intensity and velocity of the beam [194]. In most polymers, reflection of incident laser radiation is typically 5 to 10 percent, which is low compared to absorption and transmission [195].

Processes such as transmission welding are possible due to the transmission of laser energy through certain polymers. Moreover, the laser beam is refracted when the laser beam travels through the interfaces of different media, unless the path is perpendicular to the surface. As lasers pass through multi-layers to enter the joint zone, this impact must be taken into account [190]

As the laser moves through the thickness of semicrystalline plastics internal scattering takes place, where there is a different refraction index for the crystalline and amorphous phases. Scattering can also occur with reinforcement (e.g. additives, colorants, glass fiber...) in crystalline and amorphous plastics. In transmission laser welding, this effect can reduce the laser radiation's effective energy towards the joint region and limit the part thickness.

Laser absorption can happen on the surface of plastics or through the layer during transmission. Laser wavelength, polymer crystallinity and absorptivity, and additives influence the quantity of laser energy absorbed by a polymer [191]. There are two possible ways of surface absorption: photolytic and pyrolytic. At short wavelength radiation (less than 350 nm or ultraviolet (UV)), the photolytic process takes place, when the photon energy is sufficient to sever chemical bonds. At long wavelength radiation (larger than 0.35 μm), the pyrolytic process occurs. This method requires the production of heat that can be used for welding and cutting applications.

The heat distribution inside a laser welded polymer is described by the Bouguer–Lambert law of absorption:

$$I(z) = I(z=0) e^{-Kz}$$

where $I(z)$ is the laser intensity at a certain depth z , $I(z=0)$ is the laser intensity at the surface, K is the absorption constant [195].

As stated before, polymers may contain additives to influence certain properties (e.g. strength, color, absorption, etc.). The laser interaction with the polymer portion can be deeply influenced by these elements.

Various fibers are included in polymeric matrices to manufacture composites with higher mechanical strength. Glass, wood, carbon fibre, etc. are some common fiber materials. Laser beam can be dispersed or absorbed when it interacts with these materials that alter the optical properties of the base polymer. A transparent reinforcement material can absorb or dilute the energy beam further in laser transmission welding, affecting the quality of the junction [192]. High glass fiber content increases the dispersion of the beam inside the polymer and increases the required laser energy input for welding a certain thickness.

Colorants (dyes or pigments) are added for several purposes, including aesthetics and practical specifications (like in optics). The laser weldability of a polymer may be adversely affected by such color additives, like titanium dioxide. Titanium dioxide provides polymers with white coloring, but it makes difficult to weld them due to laser energy scattering effects. A very efficient energy absorber is another color additive, carbon black, which is sometimes added to improve weldability. The effective welding area can be controlled by regulating the concentration of carbon black within the absorbing polymer [196].

1.4.2.3.4 Laser welding techniques

Four separate laser welding techniques for plastic joining were developed based on various interactions between laser and thermoplastics. In most thermoplastics, CO_2 lasers have strong surface absorption, so they are used for *direct laser welding* and *laser surface heating*. The deep penetration of laser beams is needed for *through transmission laser welding* (TTLW, Figure 1.39) and *intermediate film welding*, so the most popular sources for these techniques are YAG lasers and diode lasers. However, by being directly absorbed without bulky devices typical of CO_2 lasers, new generation fiber lasers can reunite the advantages of both YAG and CO_2 sources.

In direct laser welding, the polymer's surface is heated to obtain a melt zone that joins two components together, similarly to laser welding of metals. With complete penetration, this approach can be used for butt joints and lap joints. Due to their high absorptivity in polymers, laser wavelengths between 2 and 10.6 μm are used for this process [194].

Intended to create a molten surface layer, laser surface heating is similar to non-contact hot plate welding, where mirrors are placed between components. The duration of exposure is

generally 2-10 s. Then the mirror is retracted and a joint is formed by pressing the components together. The laser output, wavelength, heating time, change-over time, and forging pressure and time are process parameters for laser surface heating.

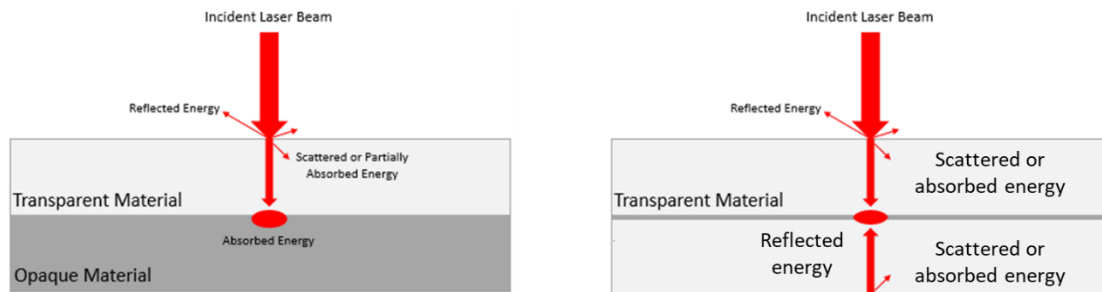


Figure 1.38: Through transmission laser welding [Source: Chojnacki.8, Wikimedia Commons].

A technique for forming a joint at the interface between two polymer components with different transparencies for laser wavelengths is called transmission laser welding. The upper component is usually transparent to laser wavelength from 0.8 μm to 1.05 μm , and the lower component is either naturally opaque or tuned by adding pigments that facilitate laser radiation absorption. Carbon black, which absorbs most electromagnetic wavelengths, is a standard colorant. The transparent layer lets the beam pass with minimal loss when the joint is irradiated, while the opaque layer absorbs the laser energy and heats up [193].

To control alignment, the two components are held by the lower fixture and a small clamping force is applied to the upper portion to form intimate contact. At the interface between the two parts and consisting of a mixture of the two plastic materials, a melt layer is then formed. Transmission laser welding, such as quick welding speed, good cosmetic properties, flexibility and low residual stresses, can provide many advantages. Laser welding can be obtained in the pre-assembled conditions from the manufacturing perspective, eliminating the need for complex fixtures; however this approach is not ideal for highly crystalline plastics due to refraction and geometric limitations [192].

Intermediate film welding consists in placing a film between incompatible polymers to join them. Laser radiation passes through the transparent parts, similarly to transmission welding, and melts the intermediate layer to create a joint. This layer can be made of an opaque thermoplastic, viscous fluid, solvent or other substances that heat up when exposed to laser energy [191].

In summary, the key advantages of laser welding of polymers are the following:

- Weld strength capable of matching the parent material tensile strength
- Neat, esthetically pleasing appearance of junctions

- Enabling the technique of “cut and sew” sealing to be merged into one
- High energy enables elevated processing speeds
- Contactless welding enables the entire process to remain clean from debris and overheated material.
- Flexibility represented by different beam delivery methods allow for easy switching from one part to the next.
- Laser light is very easy to control and allows the right amount of energy to be delivered accurately.
- Easy automation, since lasers can be integrated on-line with an automatic control robot.

2. Aim of the work

As explained in the Introduction Section, socio-political awareness led to increased market demand of new eco-friendly materials. Many of those are being studied and sometimes commercialized. An important step towards a widespread sustainable packaging is to explore as many industrial applications as possible in order to increase the fields of viable development.

Among those, welding of different materials represents a key topic when the potentiality of new eco-friendly materials for food packaging applications is evaluated. Surely, laser transmission welding is an interesting tool for joining materials, especially suitable when the realization of efficient welds and avoiding the contact between the thermal source and the processed materials are important [197].

Noteworthy, a new class of high-power fiber laser systems [198], such as Thulium-doped fibers pumped by 793nm laser diodes with high brightness. In contrast to the visible and near-infrared wavelength ranges, the emitted laser radiation has a wavelength around 1940 nm, which allows new process windows for laser welding of polymers based on various absorption properties. In addition, laser radiation emitted by Tm-doped fiber lasers provides high output powers of continuous wave and good beam quality that can be absorbed directly into the material. Finally, in the so-called "eye-safe" spectral region, the wavelength of 2 microns can support the general acceptance of Tm-fiber lasers in the industrial environment. This is due to this spectral region's high absorption of laser light in the eye's cornea that protects the extremely sensitive retina from laser light penetration [199].

In this PhD's work, we present a process evaluation for transmission welding of different eco-friendly materials, using Thulium fiber laser radiation.

The research activity here presented consisted of the following steps:

- careful bibliographic research to get the state of the art on the subject;
- molecular, physico-chemical and mechanical characterization of the tested materials;
- optimization of the laser system setup;
- laser welding tests of different materials, with optical and mechanical evaluation of the seam.

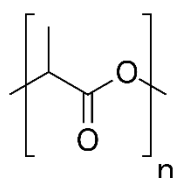
3. Materials and Methods

3.1 Materials

Most materials are commercially available and have been obtained in film or nonwoven form. Characterization of the materials was part of the work.

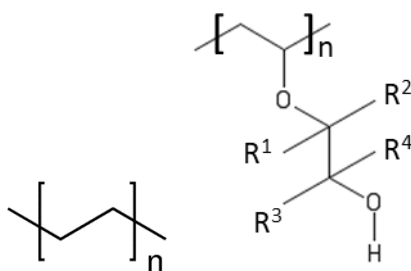
PLA nonwoven materials

Poly lactic acid (PLA) nonwoven samples has been tested. The PLA used for those materials was both virgin or with infrared-absorbing additives. Kindly supplied by IMA spa.



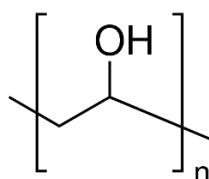
PE/BVOH/PE multilayer

In this film Polyethylene was coextruded with a Butanediol Vinyl Alcohol co-Polymer, a water soluble, compostable alternative of ethylene-vinyl alcohol (EVOH), in order to achieve good barrier properties. This film was also studied in order to evaluate its recyclability. Kindly supplied by IMA spa.



PVA based water soluble film

A water soluble polyvinyl alcohol based film was taken into account. Kindly supplied by IMA spa.

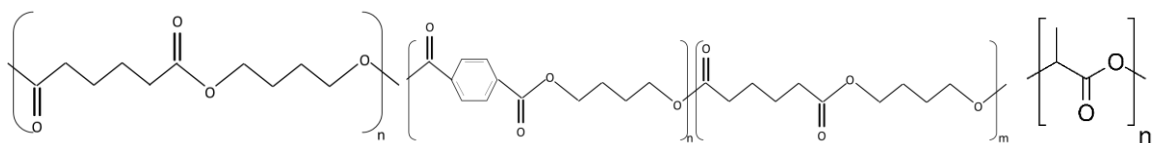


Protein based water soluble film

A film based on protein, possibly mucin, which is water soluble and possibly edible Kindly supplied by IMA spa.

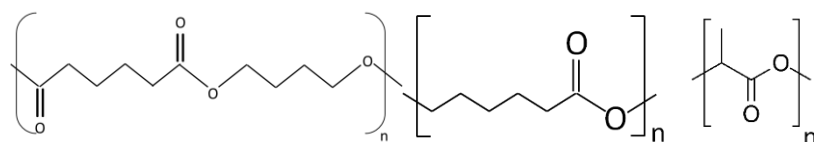
PBSA + PBAT + PLA blend based compostable monofilm

Polymeric film based on a blend of PLA, poly butylene succinate adipate (PBSA) and poly butylene adipate terephthalate (PBAT), which are all compostable. Kindly supplied by IMA spa.



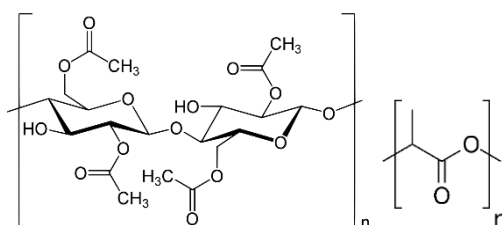
PBSA + PCL + PLA blend based monofilm

Polymeric film based on a blend of PLA, poly caprolactone (PCL) and poly butylene succinate adipate (PBSA), which are all compostable. Kindly supplied by IMA spa.



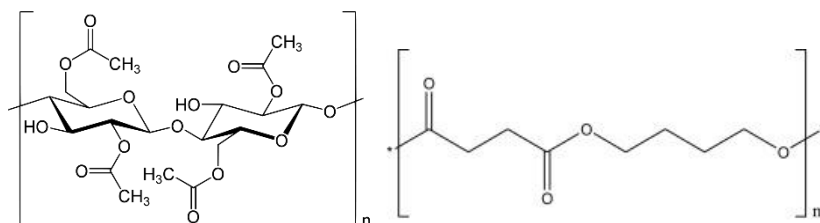
Cellulose Acetate + PLA multilayer

Two-layers multimaterial film: external layer of cellulose acetate, sealing layer of PLA. Received from IMA spa.



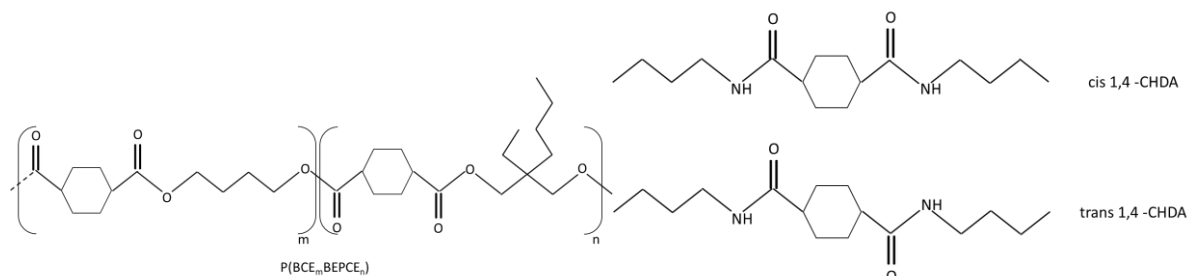
Cellulose Acetate + PBS multilayer

Two-layers multimaterial film: external layer of cellulose acetate, sealing layer of PBS.
Received from IMA spa.



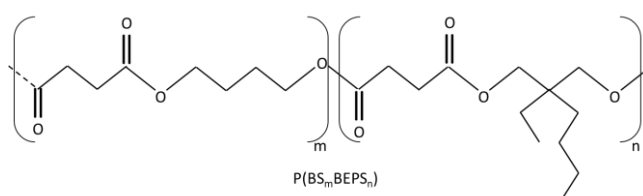
P(BCE BEP CE) copolymers

Poly(butylene/2-butyl-2-ethyl-propylene trans-1,4-cyclohexanedicarboxylate) random copolymers with different composition were considered. M and n represent mol% of BCE and BEPCE comonomeric units, respectively. M ranges from 100 to 60 mol%. Also, a copolymer containing cis/trans isomers of cyclohexane dicarboxylate units is taken into account, with m=65. The copolymers were synthesized and characterized by Prof. Lotti's research group (see REF 128).



P(BS BEPS) copolymers

Random poly(butylene/2-butyl,2-ethyl-propylene succinate) copolymers characterized by different molar ratio of BS and BEPS co-units were taken into consideration: m ranges from 100 to 70 mol% of BS co-units. The copolymers were synthesized and characterized by Prof. Lotti's research group (see REF 125).



3.2 Methods

Instruments and techniques were used in LAMAC, materials engineering laboratory of DICAM, Bologna, and OPENLAB, IMA spa laboratory network, in Ozzano dell'Emilia (BO).

3.2.1 Polymer Characterization

3.2.1.1 Thermogravimetric Analysis (TGA)

Thermal stability tests were conducted in nitrogen atmosphere (gas flow: 40 mL/min), by using a Perkin Elmer TGA7 (Waltham, MA, USA) apparatus. The test method requires heating the sample (10 mg) from 40°C to 800°C at 10 °C/min. The output of the test is a thermogram in which is possible to determine weight losses of the sample over time.

3.2.1.2 Differential Scanning Calorimetry (DSC)

A Mettler Toledo DSC 3 (Columbus, Ohio, USA), accessorized with the cryogenic cooling adapter Huber TC100, was used for calorimetric analyses. The calibration was carried out using indium of high purity. Samples of ca.6 mg were closed in aluminum pans of 40 µl and inserted next to the reference (empty aluminum pan) within the instrument. The internal system was constantly purged with 50 ml/min Nitrogen flow.

The method on the samples is the following:

- 1st scan: -70 °C to 220 °C at 20 °C/min
- Isotherm of 5 min at the final temperature
- 220 °C to -70°C at 20 °C/min
- 2nd scan: -70 °C to 220 °C at 20 °C/min

These temperatures were chosen to avoid the risk of degradation of the low temperature melting biopolymers, especially important to have an effective insight during the second scan.

The glass-transition temperature (T_g) can be estimated in the thermogram as the midpoint of the heat capacity increase (Δc_p) associated with the glass-to-rubber transition; Δc_p can be measured at the glass transition temperature from the vertical distance between the two extrapolated baselines. It is possible to determine the cold crystallization temperature (T_{cc}) as the peak minimum of the reported exothermal transition, and the corresponding crystallization heat (ΔH_{cc}) can be determined taking into account the total peak area. The highest value and the underlying region of the endothermal peak were measured to determine melting temperature (T_m) and the corresponding fusion heat (ΔH_m) respectively.

3.2.1.3 Infrared Spectroscopy (FT-IR)

Infrared spectroscopy was performed in the range between 4000 and 450 cm^{-1} (NIR Near Infrared), using a Perkin Elmer Spectrum Two FT-IR spectrometer with both the attenuated total reflectance (ATR) accessory (diamond crystal) and the transmission accessory (where applicable). 16 scans with 4 cm^{-1} resolution were performed to obtain the final data. Those spectra help to evaluate the absorption of IR radiation within the molecules, giving insight of their chemical structure.

3.2.1.4 Tensile tests

Tensile tests were performed using an Acquati AG/MC2 tensile testing machine (Arese, Milano, Italy), equipped with rubber coated metal clamps and a 10 daN load cell. The polymeric film samples were cut following a stencil (15 mm wide and 200 mm long) and their thickness was evaluated using a Mitutoyo S112XB Digital comparator (Kawasaki, Kanagawa, Japan). The sample was fixed with the clamps at 100 mm distance and 50 mm/min clamp separation speed was adopted, following ASTM D882 "Standard Test Method for Tensile Properties of Thin Plastic Sheet". All the samples were conditioned by resting several days at controlled temperature and humidity (23°C – ca. 30% RH).

3.2.2 Laser welding tests

The laser welding tests include the laser welding process and the welding quality measurement. The latter was evaluated via qualitative/quantitative optical microscopy (see section 3.2.2.2), welding strength test and eventually comparison with traditionally heat sealed test strength.

3.2.2.1 Laser system

The Thulium laser system is an IPG-TLR-100WC (Oxford, Massachusetts, USA) with the following characteristics:

Wavelength	1940 nm
Average Power	108 W
Focal length	170 mm
Beam quality (M^2)	1,06
Spot diameter	0,08 mm
Rayleigh length	3.7 mm
Working distance	192 mm

The scanning head is a Raylase SS-III-10 [1940] (Weßling, Germany) controlled via Weldmark software, with a telecentric f-theta lens Sill S4LFT3162-159 (Wendelstein, Germany).



Figure 3.1 Laser system setup.

Figure 3.1 represents the system setup (without the IPG laser generator), with curved aluminium sample holder (with adjustable working distance) in order to be able to fix the material with tape and apply more tension than a planar surface. The best working distance was found to be ca. 190 mm, with a 2 cm defocus.

The standard laser test procedure was the following:

- 1) Cut two stripes of the material of 35 mm width and 50 mm length;
- 2) Overlap the stripes, with eventual sealing layers facing each other;
- 3) Fix the overlapped stripes to the sample holder with paper tape;
- 4) Set on the marking software the shape of the laser path (a 30 mm single line);
- 5) Define on the marking software the power and speed of the laser path;
- 6) Shoot the laser.

The test were normally conducted from 20% to 100% laser Power, with 20% steps, while the marking speed was checked at 50-100-200 mm/s... and moving up 100 by 100 mm/s until no more sealing was observed.

3.2.2.2 Optical Microscopy

A Leica DM2700M (Wetzlar, Germany) optical microscope equipped with 5x-10x-20x-50x objectives and a MC170 HD camera was used to capture magnified images of the samples. The software LAS was then used to elaborate the results and perform measurements.

3.2.2.3 Laser Seal Strength Test

Seal strength tests were performed using an Acquati AG/MC2 tensile testing machine (Arese, Milano, Italy), equipped with rubber coated metal clamps and a 10 daN load cell. The polymeric film samples were cut following a stencil (15 mm wide and 200 mm long) and their thickness was evaluated using a Mitutoyo S112XB Digital comparator (Kawasaki, Kanagawa, Japan). The sample was fixed with the clamps at 25 mm distance and 200 mm/min clamp separation speed was adopted, following ASTM F88/F88M “Standard Test Method for Seal Strength of Flexible Barrier Materials”.

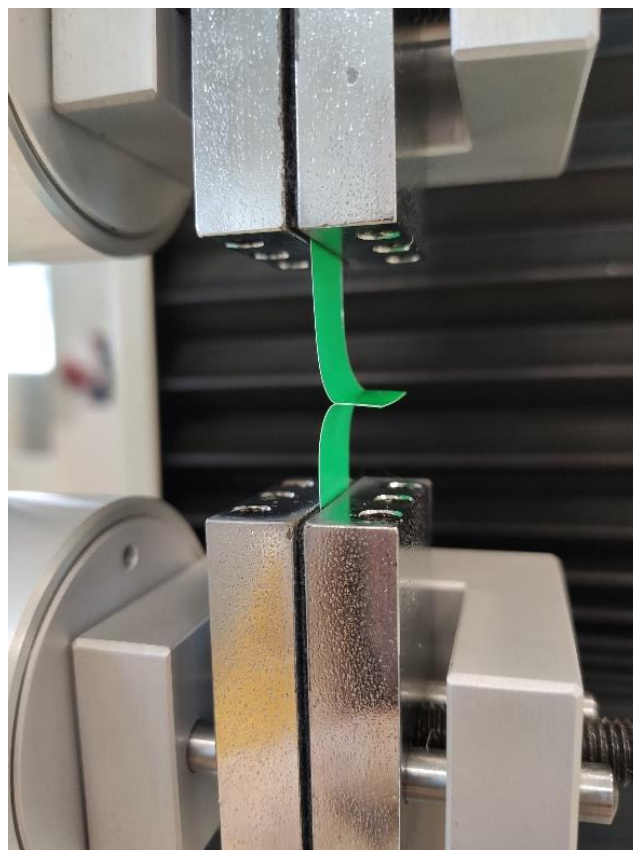


Figure 3.2: Example of the seal strength test setup.

3.2.2.4 Heat Seal Strength Test

Heat seal strength results were obtained using a J&B Hot Tack 5000 MB tester (Vived Management, Lanaken, Belgium). The instrument performs a heat sealing with a couple of 10x50 mm seal bars, followed by a sealing strength test with a 40N load cell. Sealing was performed at variable temperatures, fixing the bars contact time at 0.5 s, bars contact pressure at 0.5 N/mm² (5 bar) and cooling time before strength tests at 3 seconds. Samples were fixed with the clamps at 25 cm distance and 200mm/min clamp separation rate.



Figure 3.3: Example of the heat seal strength test setup.

4. Results and Discussion

4.1 PLA nonwovens

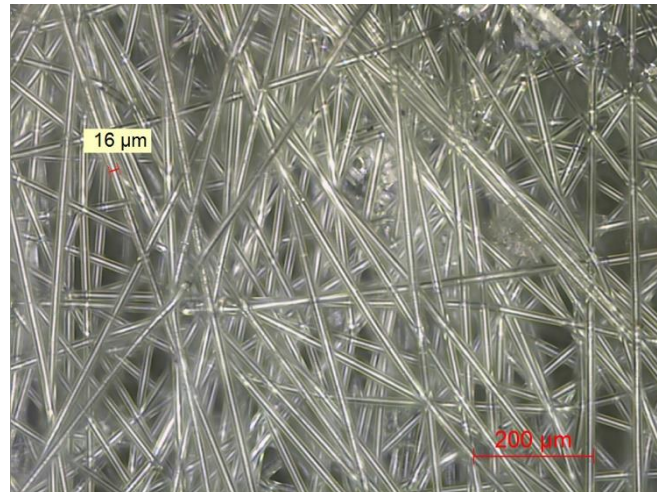


Figure 4.1: Example of surface Optical Microscopy of PLA nonwoven samples.

Preliminary characterization permitted to evaluate morphology and thermal behaviour of PLA nonwovens. Fibres diameter was measured for different samples and found characterized by a distribution range between 15 and 20 microns. It is hard to define a thickness of the layer, which can be estimated around 80 microns, where the grammage of the samples is roughly 20 g/m².

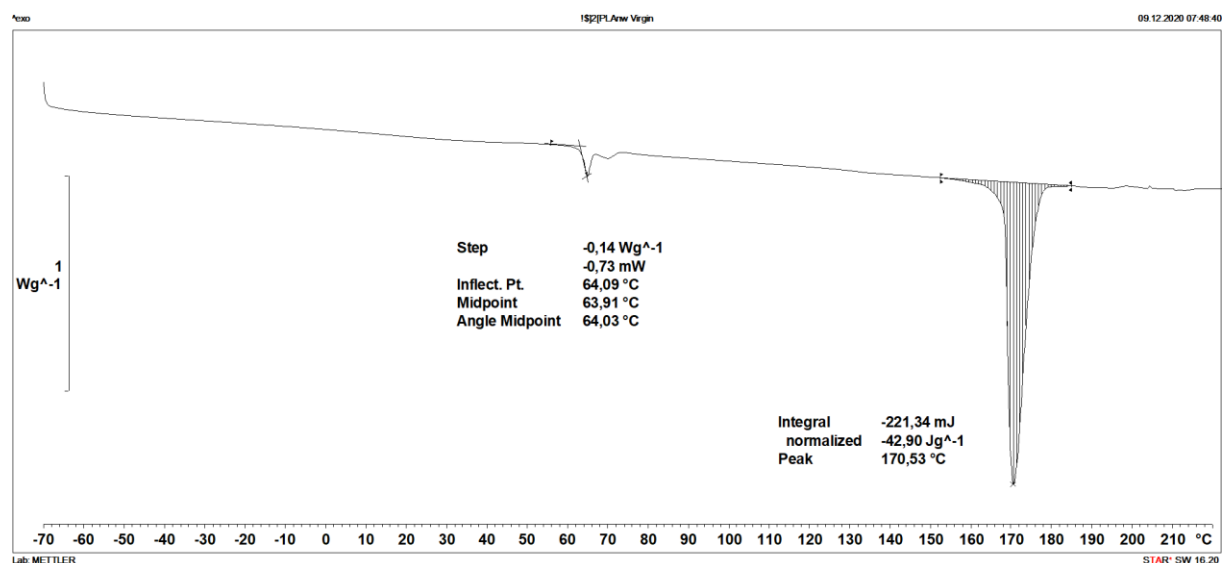


Figure 4.2: DSC curve of virgin PLA nonwoven (I scan).

DSC analysis shows a similar thermal behaviour (Table 4.1) between the “virgin” PLA nonwoven samples and the one with additive (* additive remain undefined for industrial privacy).

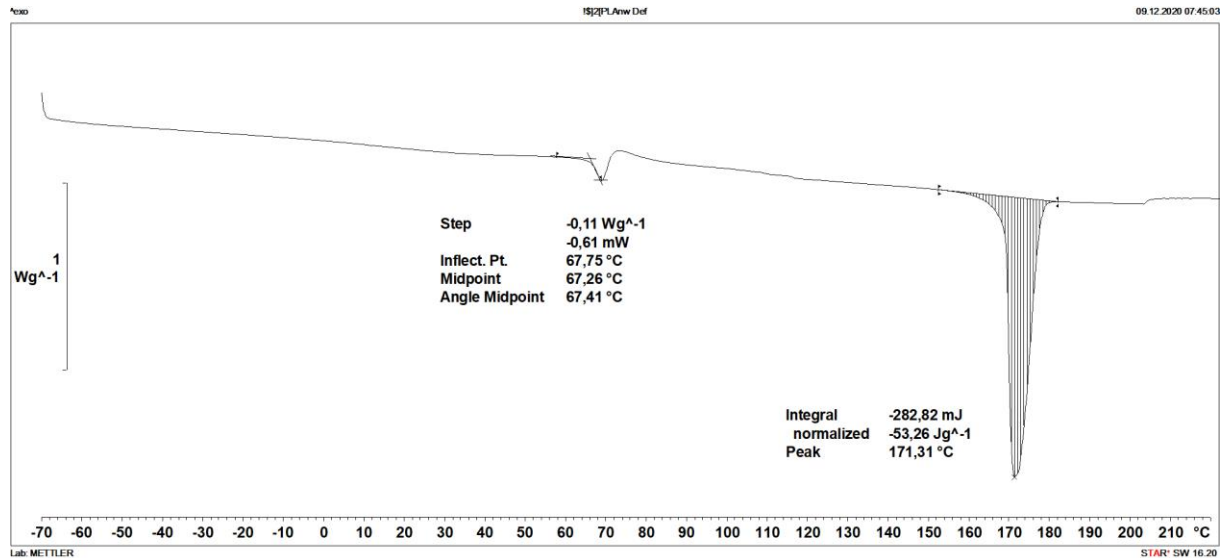


Figure 4.3: DSC curve of PLA nonwoven with IR absorber (I scan).

Sample	T_g (°C)	T_m (°C)	ΔH_m (J/g)
PLA Virgin	65 ± 2	171 ± 1	43 ± 1
PLA+Additive*	67 ± 1	172 ± 2	52 ± 2

Table 4.1: DSC results for PLA nonwovens.

Laser welding performance tests are reported as histograms in which y axis contains the sealing tested strength, while x axis shows the marking speed. Columns are grouped by Power (%) of the laser used for the test, and different powers are reported. This leads to group of columns: for every group, a certain column colour represents a certain marking speed.

Moreover, a red dashed line was added to represent the acceptability threshold for the seal. The choice of the threshold is supposed to be related to the final application, since there is no such thing as a “standard” seal strength. For this reason, for nonwoven materials and water-soluble materials it has been taken as reference the usual strength suitable for tea bags applications: between 1 and 1.5 N.

Another important observation is that in all cases of laser welding tests of virgin materials, the acceptable sealing strength always corresponded to **welding and cut** results.

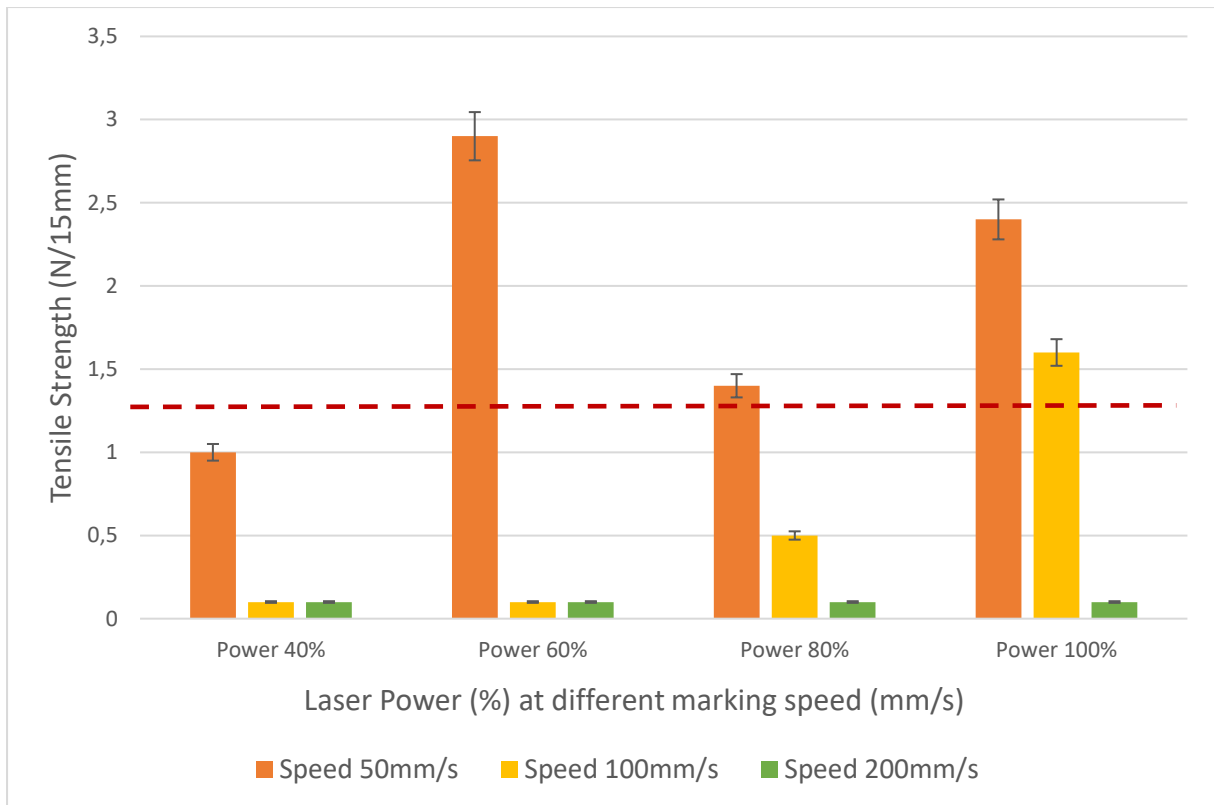


Figure 4.4 Laser welding performances of PLA virgin nonwoven.

As seen in Figure 4.4, PLA nonwoven virgin samples reach their maximum acceptable welding speed at 100% laser power and 100 mm/s.

This result was compared to heat seal strength test (Figure 4.5) revealing that acceptable performances are obtained by heating the sealing bars at 160°C, with higher seal resistances resulting from this approach. After this temperature, the material completely collapses.

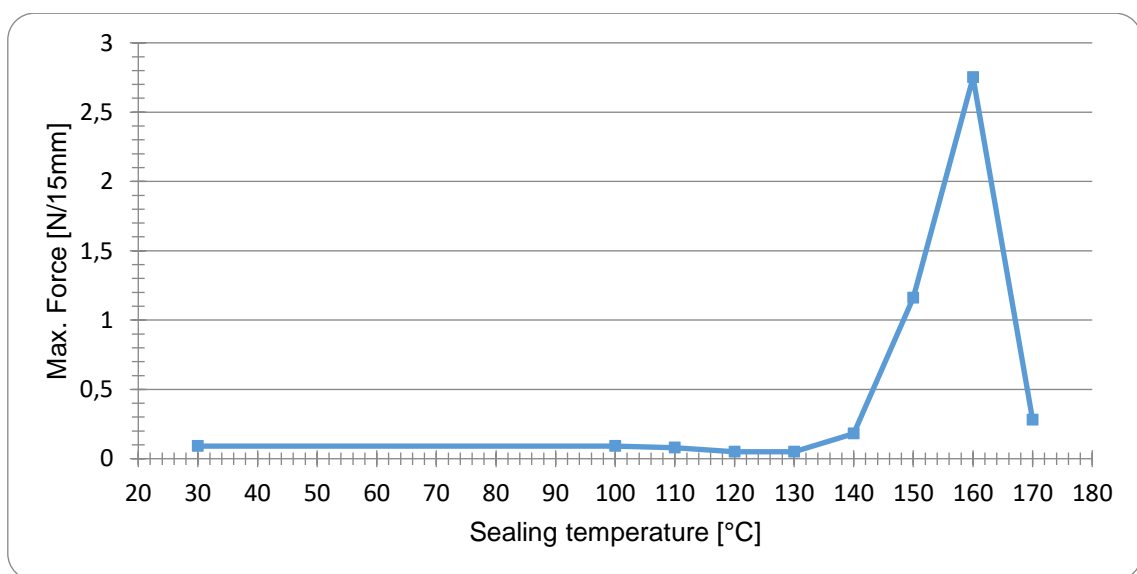


Figure 4.5: Heat seal strength test of PLA virgin nonwoven.

As shown in Figure 4.6, acceptable results are still observed around 1000 mm/s, with a great improvement in speed performances due to the IR-absorber additive.

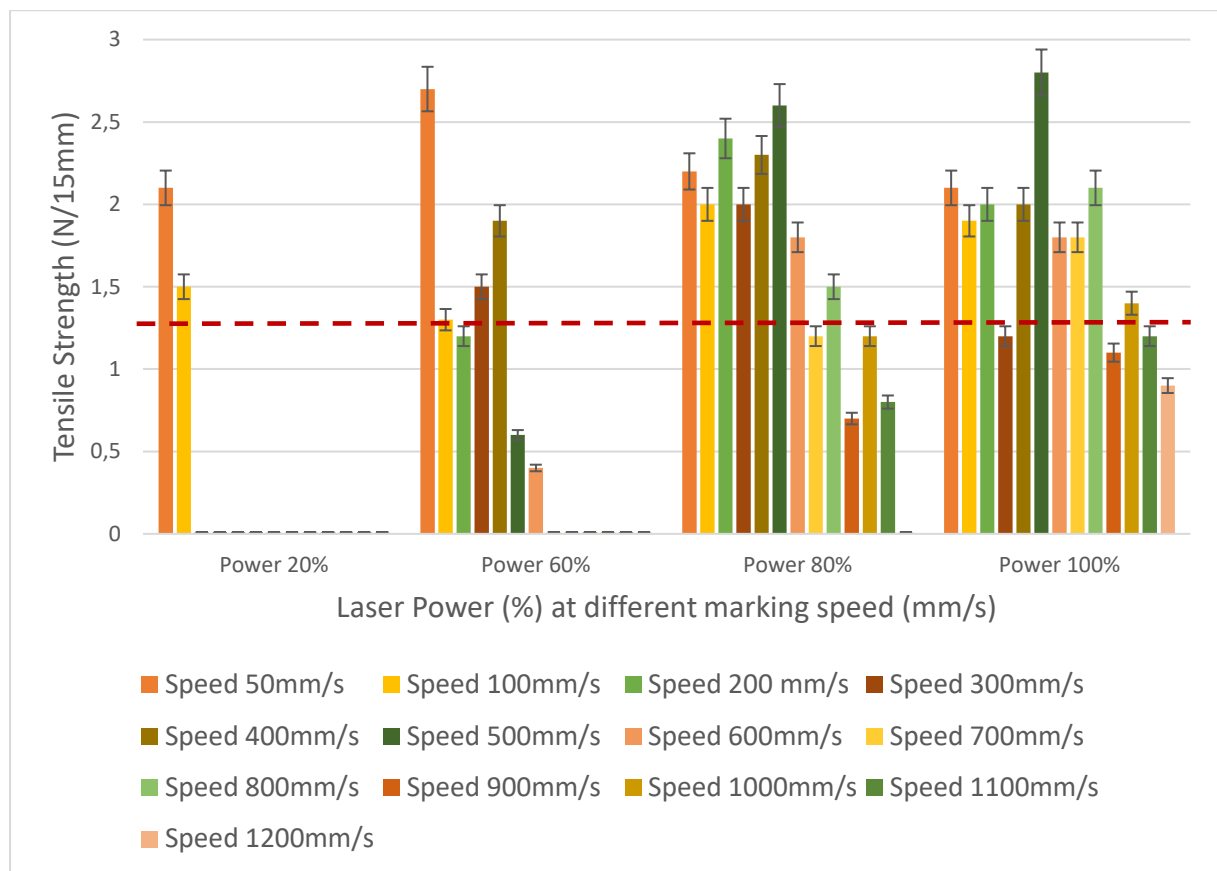


Figure 4.6: Laser welding performances of PLA with IR absorber nonwoven.

In this case, a comparison with Hot Tack Tester analysis (Figure 4.7) was made: in this case higher temperatures are necessary for the seal bars to weld the material. Moreover, the maximum strength is lower, more comparable to the forces obtained in laser tests. The same IR-absorber that boosts laser welding results could have caused a worsening of the response to heat sealing by introducing discontinuities in the material that could conduce heat more poorly than the polymer.

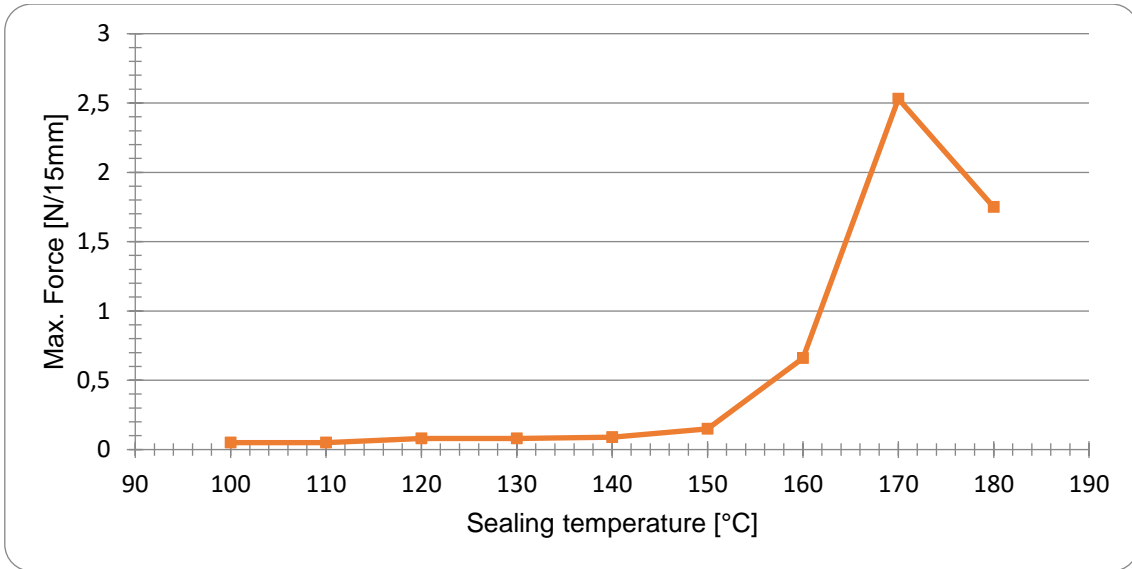


Figure 4.7: Heat seal strength test of PLA with IR absorber nonwoven.

This time, it is important to specify that welding and cut results are observed until 500 mm/s welding speed. At higher speeds, the sealing is still acceptable, but the material remains in one piece. Examples of welding and cut or only welding results are shown in Figure 4.7, corresponding to optical microscopy junction evaluation.

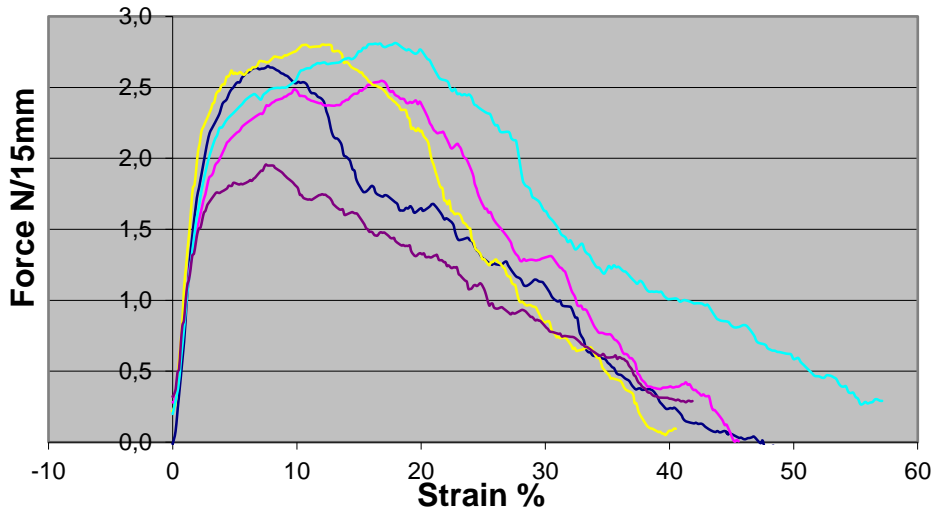


Figure 4.8: Tensile strength tests of PLA nonwoven with additive.

It is interesting to underline that the max load for the material itself is around 2.5 N, so any welding that could match this strength can be considered perfect since there is no distinction between the resistance of a welded area and any other region of the sample.

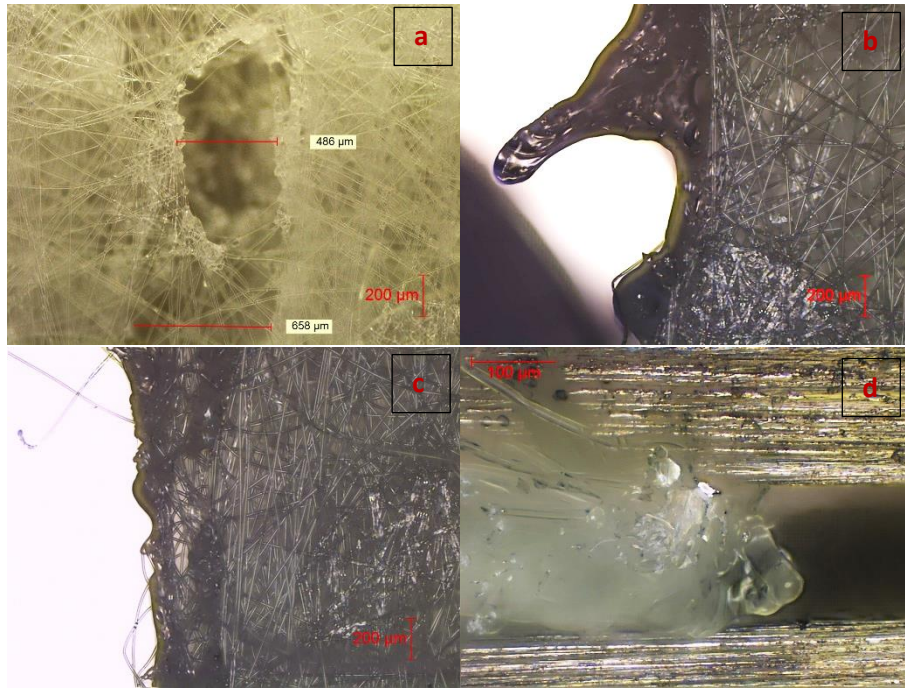


Figure 4.9: optical microscope images of (a) welded (without cut) region; (b) welded and degraded region; (c) welded and regularly cut region; (d) section of joined and cut PLA region.

We observed different phenomena depending on laser power and marking speed, thus on the quantity of energy transferred to a single point of the polymer: weld without cut (only a superficial incision; Figure 4.9a); cut and weld, with a regular junction line (Figure 4.9c); cut and weld, with a degraded junction line (Figure 4.9b). In any case, it's possible to observe clusters of melted polymer (Figure 4.9d), with the exception of non-welding situation, when the energy is not enough to melt the material.

Despite the size of the laser spot, which has 80 micron diameter, it's important to notice that the marking of the laser passage reaches in this kind of material a width around 500 microns. This means that there is a part of the material at the centre of the beam which is vaporized. In addition, the morphology of the sample is important to explain the cut phenomenon: the random distribution of the fibres with empty spacing means that when they start to melt they need to retract, shorten, to find other melting material to weld with.

4.2 PVA based film

Concerning the water-soluble poly-vinyl alcohol film, a cross section image was captured via optical microscopy. Both this technique and digital comparator confirmed a thickness of 40 microns of the film.

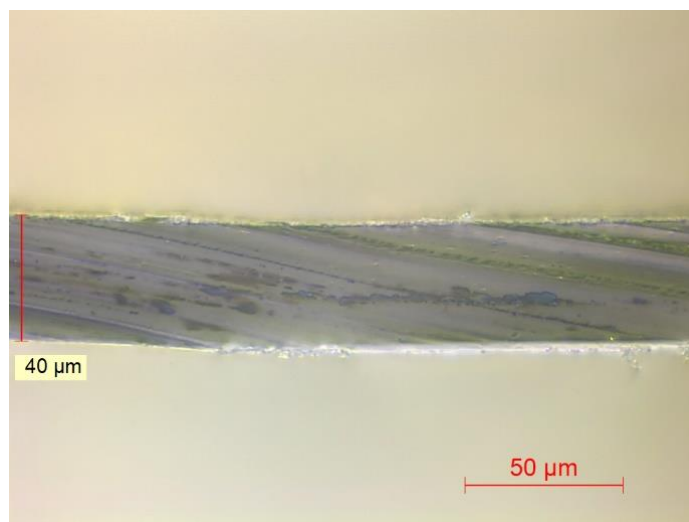


Figure 4.10: Optical microscope image of the section of the PVA based film.

Characterization also included thermal analysis, in order to confirm polymer nature along with FT-IR spectroscopy. DSC curves exhibit the typical behaviour of a wet PVA (melting temperature around 200°C, with a big humidity peak around 90°C). We did not consider dry samples, even because usually at industrial level wet PVA is used. Similarly to cellulose, -OH groups of the polymer could trap intimately water molecules, in which case a vacuum oven could be the only way to remove humidity from the sample. The second scan was obtained after cooling the molten material at controlled rate of 20°C/min. As expected, the endothermic peak related to water loss strongly decreases in the second scan, since major part of the water is lost during first scan.

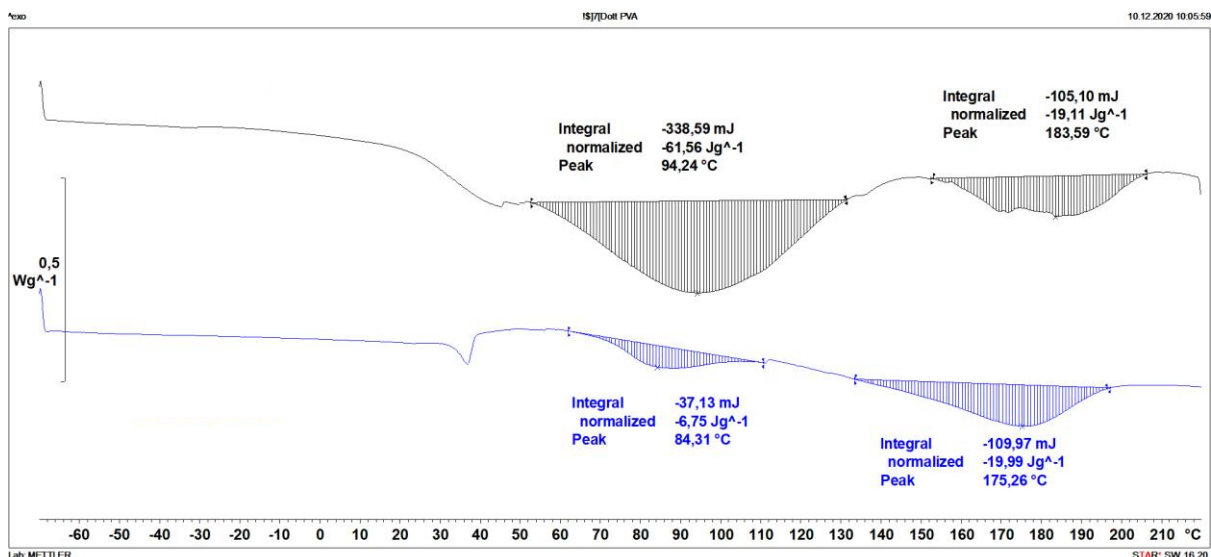


Figure 4.11: DSC curves (black, first scan; blue, second scan) of the PVA based film sample.

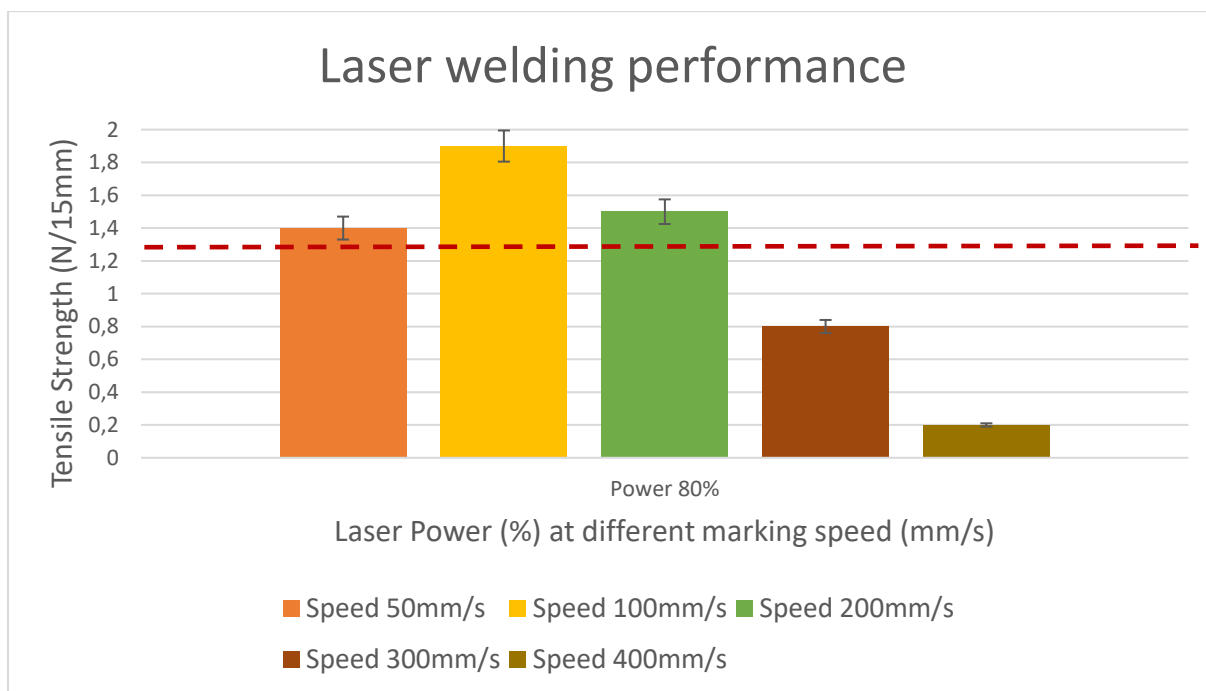


Figure 4.12: Laser welding performances of the PVA based film.

In this case the low threshold of acceptability was chosen considering the peculiar material's characteristics of water solubility, that could make the corresponding film suitable for all the applications requiring very easy end-life scenarios for very short lifetimes, avoiding production of waste for something that doesn't need high shelf life, but only an easy to dispose container. For this PVA based film, 200 mm/s maximum welding speeds are observed at 80% Power, which was chosen as most representative due to lack of sample material.

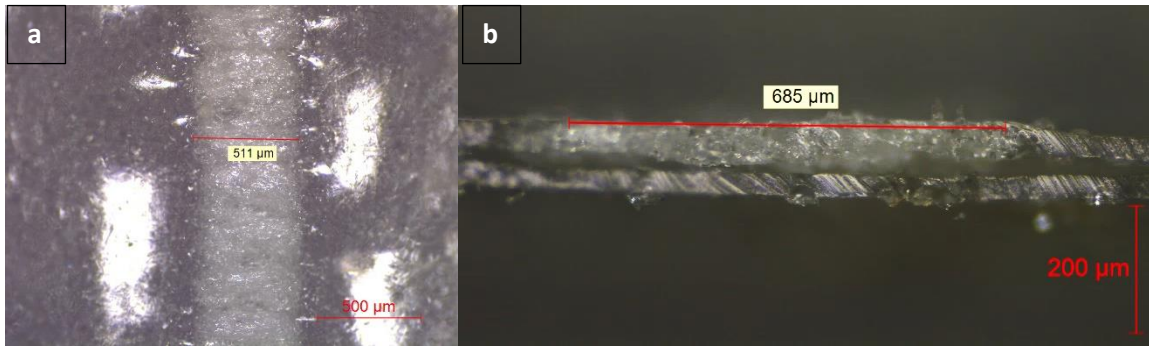


Figure 4.13: optical microscopy images of (a) joining area obtained at Power 80% and Speed 300mm/s from the top; (b) joining area obtained at Power 100% and Speed 300mm/s from the side.

The low seal strength is well represented by the cross-section observation of the seal via optical microscopy (Figure 4.12 b), in which the lower layer seems only slightly melted compared to the upper one. Probably the material absorption is high enough to prevent most of the radiation beam to reach the second layer, but still not enough to have burning effects.

Another observation is that the marking width of the laser is higher for the 100% power usage, having the same marking speed. This is explained by the fact that with the same speed in the same point we are giving more energy, thus more heat is created and the melted area is bigger.

4.3 Protein-based film

This kind of material was especially interesting due to its probable feature of being edible. What was observed, thus, is that it's for sure water soluble, which is already important like we already said. Again the thickness of the film was evaluated both via optical microscopy of the cross-section and digital comparator, having around 145 microns resulting thickness.

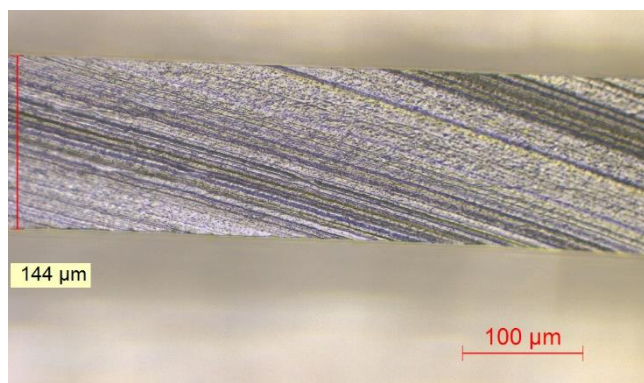


Figure 4.14: Optical microscope image of the section of the Protein based film.

The DSC curve is compatible with the one of a protein, where denaturation process is evident. FT-IR database confirmed the polymer was a protein. In particular, the database matches 82% with the spectrum of mucin, a protein present in mucoses.

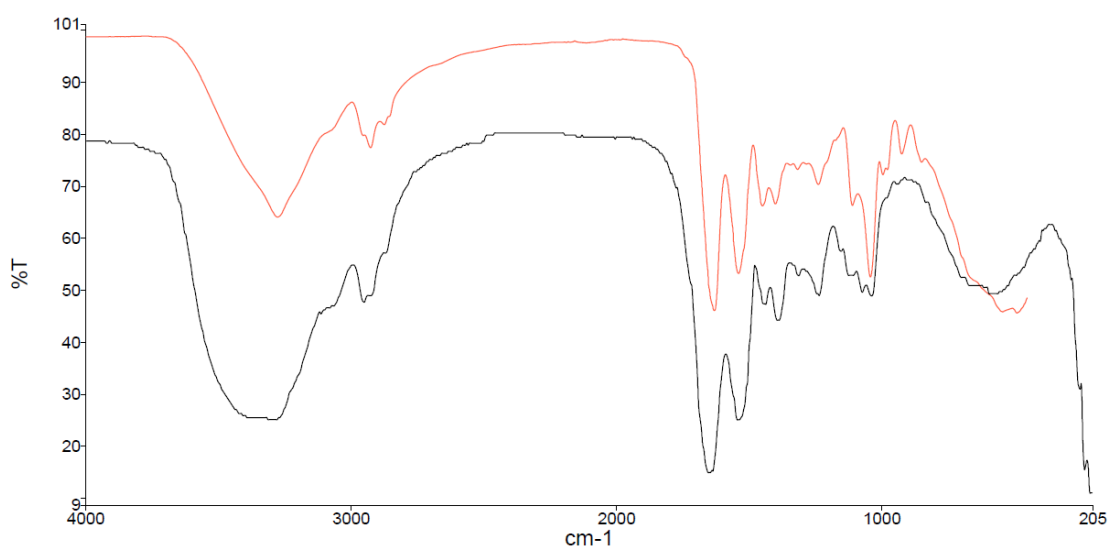


Figure 4.15: FT-IR spectra of the protein based film (red) compared to the Mucin in database (black).

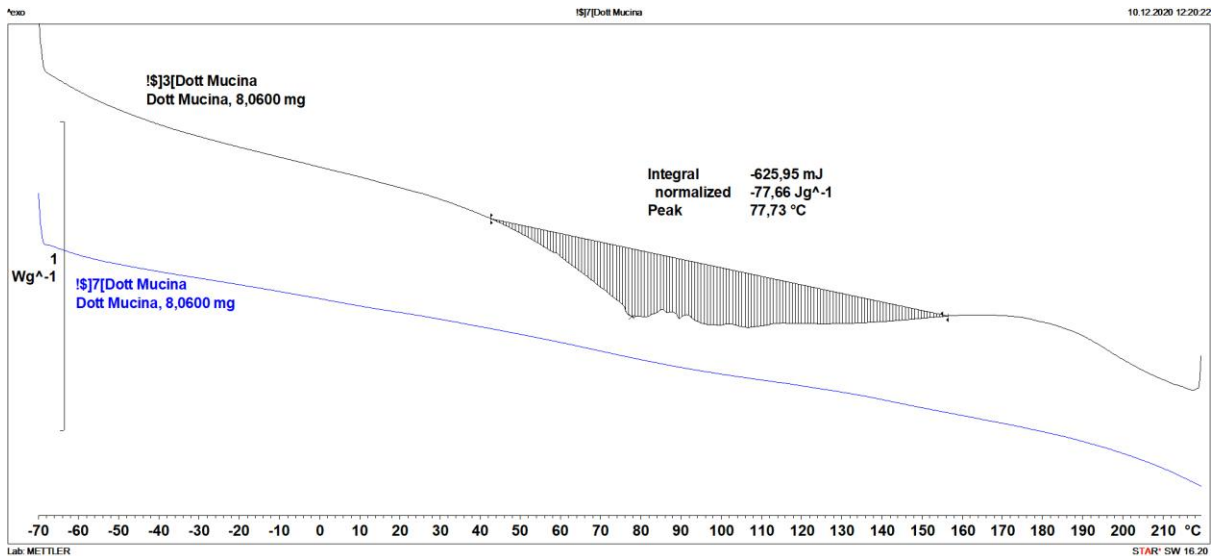


Figure 4.16: DSC curves (black, first scan; blue, second scan) of the Protein based film sample.

The protein-based film shows better performances than the previous water-soluble one, exhibiting acceptable welding capabilities even at 800 mm/s marking speed, while the seal strengths are comparable.

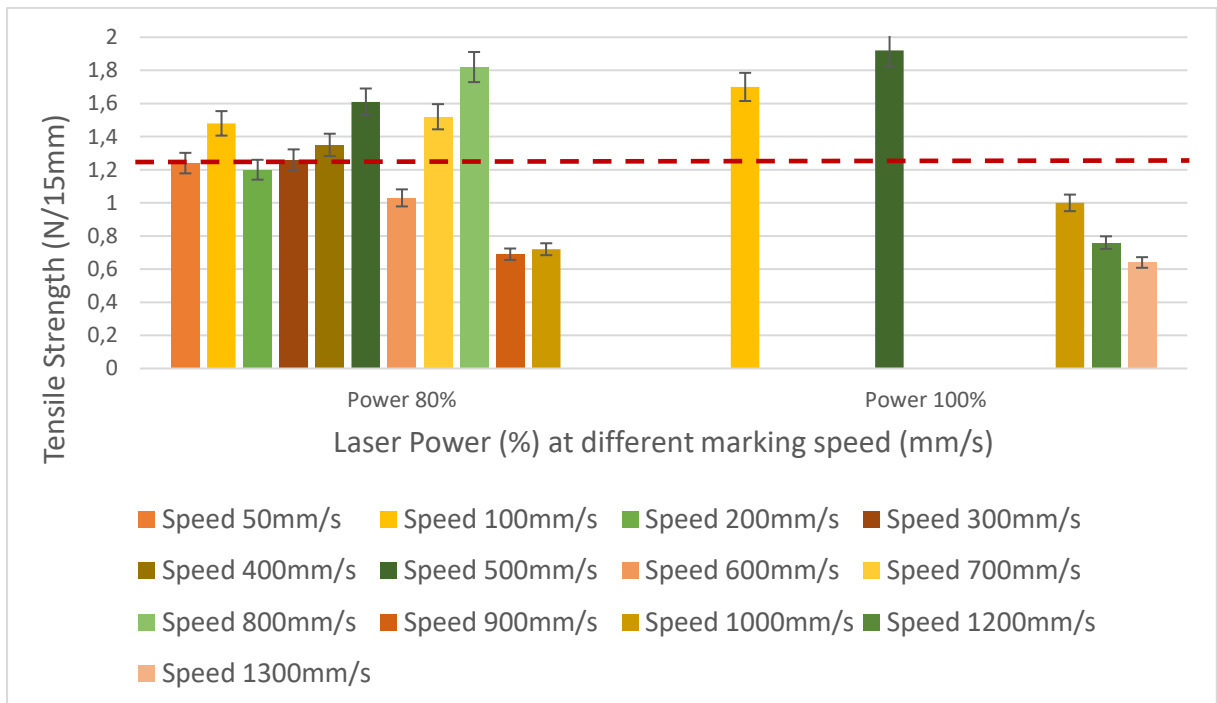


Figure 4.17: Laser welding performances of the Protein based film.

The cross-section of the joining zone (Figure 4.18b) reveals a deeper penetration of the laser, with a clearly molten material area on both layers, of course with the top layer more involved than the bottom one, proving that the material can absorb the radiation. The marking shows, as expected, a different energy distribution from the center (more intense heating) to the borders.

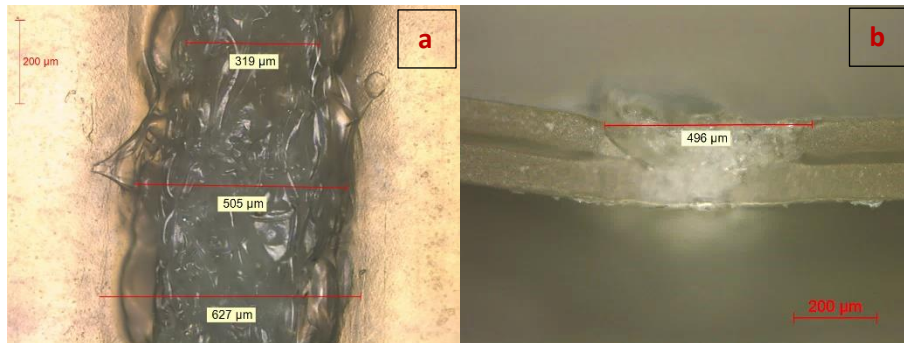


Figure 4.18: optical microscopy images of (a) joining area obtained at Power 80% and Speed 300mm/s from the top; (b) joining area obtained at Power 100% and Speed 300mm/s from the side.

In Figure 4.18a it is possible to notice the energy distribution along the marking: a central area (grey) is where the material is mostly burned, thus the energy absorption (heat) was more intense. Then there is a dark transition area that progressively fades into the normally continuous surface.

Again, same marking speed at different powers shows a wider marking in the most energetic (higher power) case.

4.4 PE/BVOHc/PE

The material was designed to have an easy recyclable barrier film. In fact, in the middle of polyethylene coextrusion is present a layer of water-soluble version of EVOH, probably a butanediol - vinyl alcohol co-Polymer. This layer is supposed to dissolve, in order to leave only PE which can be recycled by using a dedicated recycling line. In these terms, this multilayer is supposed to be eco-sustainable. Of course, further tests have been performed to verify that.

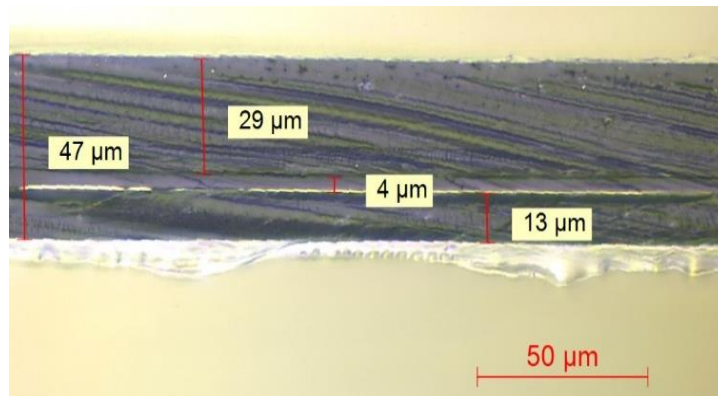


Figure 4.19: Optical microscope image of the section of the PE/BVOHc/PE film.

The total thickness of the sample is around 47 microns, always verified via both optical microscopy measure of the cross section and digital comparator direct measure.

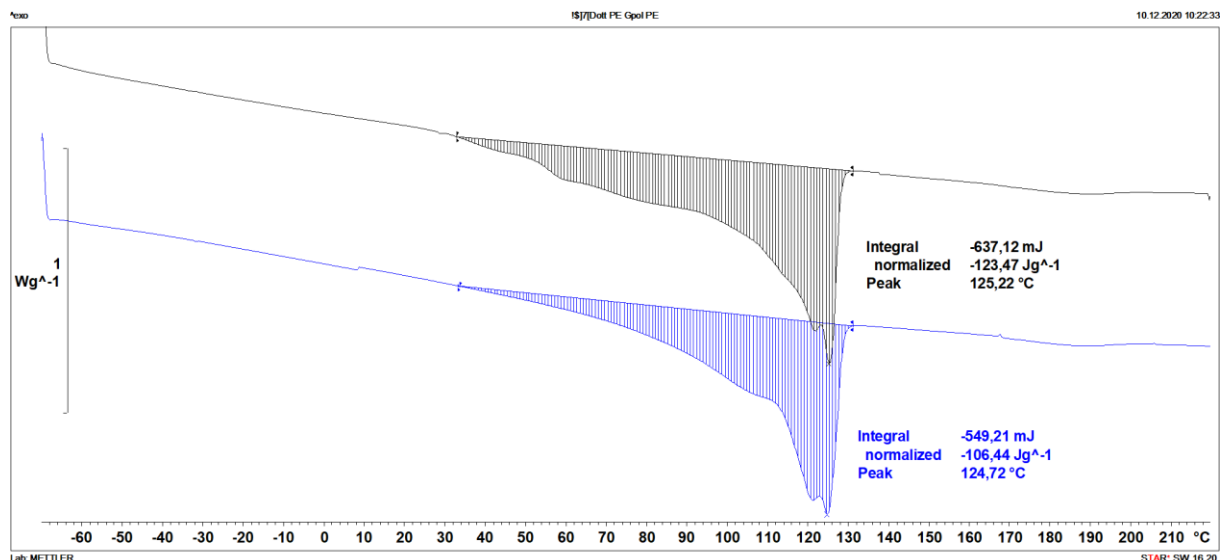


Figure 4.20: DSC curves (black, first scan; blue, second scan) of the PE/BVOHc/PE sample.

From DSC analysis, the polyethylene appears a coextruded multilayer of LDPE (melting point around 110°C, shoulder), LLDPE (melting point around 120°C) and M/HDPE (over 125°C)

melting temperature). This is quite common for industrial films that will have to withstand heat sealing conditions, with LDPE and LLDPE optimal for the sealing layer, while M/HDPE giving a slight heat and mechanical resistance. BVOHc melting temperature has a wide range of melting temperatures depending on grades, thus is not possible to precisely determine its presence. Second scan after cooling at controlled rate of 20°C/min shows as expected an abundant re-crystallization of polyethylene melt.

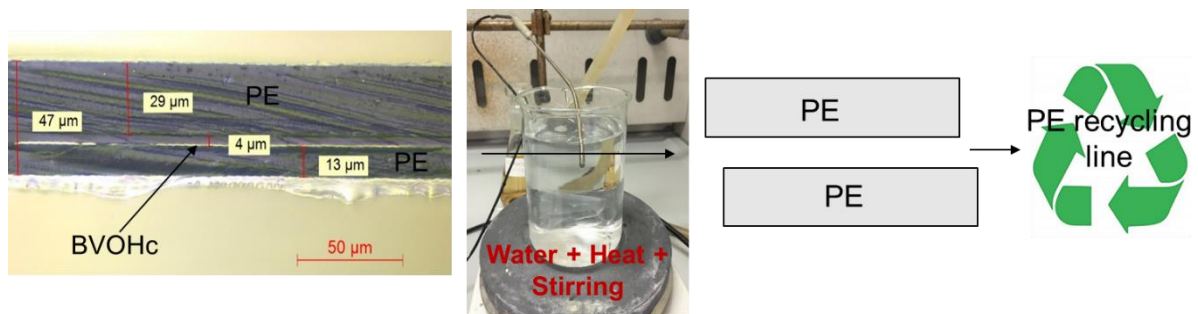


Figure 4.21: Scheme of the BVOHc water solubility evaluation process and its purpose.

The solubilisation of BVOHc in water was monitored and quantified through TGA analysis. Samples subjected to the treatment for different times were considered. As it can be seen from Figure 4.21, in all cases, the weight loss takes place in two-steps, the main one occurring at higher temperature (around 500°C) due to PE thermal degradation, the other at lower T due to BVOH layer (between 350 and 450 °C). This attribution is confirmed considering the TGA curve of BVOHc-free sample shows only the weight loss step at the highest temperature. Moreover, the weight loss corresponding to the first step occurring at lower temperature has been found regularly increasing with the time spent by the film in hot water (Figure 4.20), proving it is correlated to the fraction of BVOH solubilized in water.

The test has been repeated at different temperatures. The graph in Figure 4.21 summarizes the results obtained: only heating the water up to 80°C would lead to complete dissolution of the barrier layer within 2 hours. Those conditions are quite different from the washing conditions used to wash plastic waste. This could be the reason why this type of film did not arrive on the market.

Time (min)	Temperature (°C)	BVOH Weight Loss (%)
20-40	28	10%
1380	28	100%
20-40	37	10%
1305	37	100%
20-40	45	10%
60	45	20%
120	45	40%
310	45	65%
340	45	70%
375	45	100%
20-40	52	10%
360	52	100%
20	60	10%
250	60	100%
120	80	100%

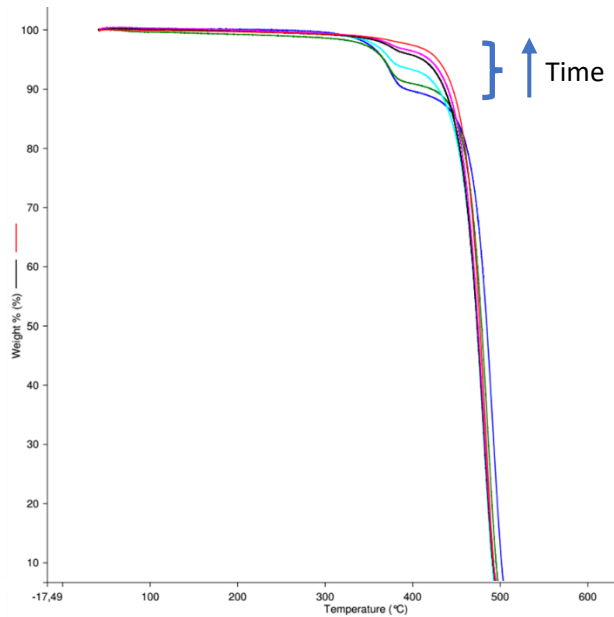


Figure 4.22: Solubility test results table and example of TGA analysis corresponding to the 45°C test run (from 0 to 375 minutes, from blue to red curve).

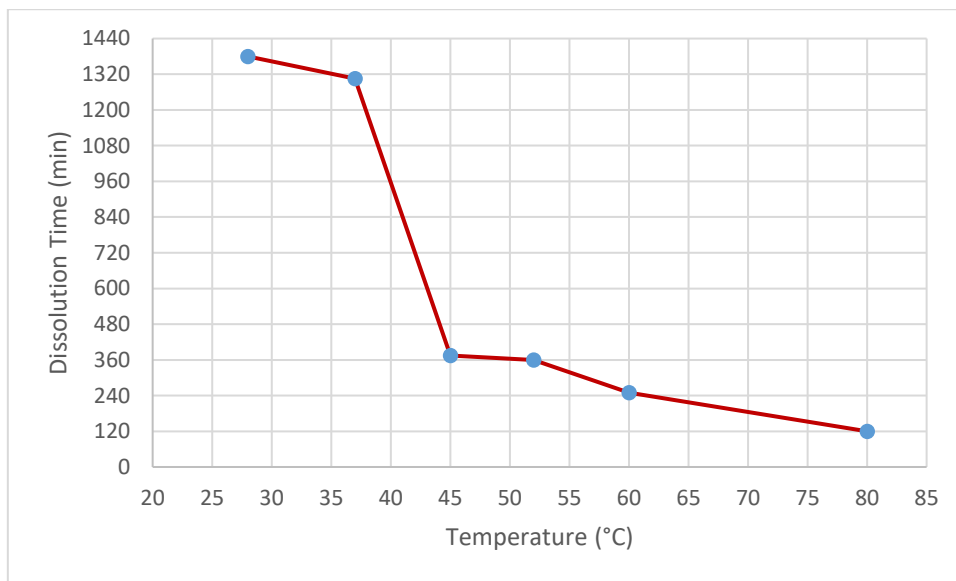


Figure 4.23: Graph of the required total dissolution time depending on the temperature set on the test run.

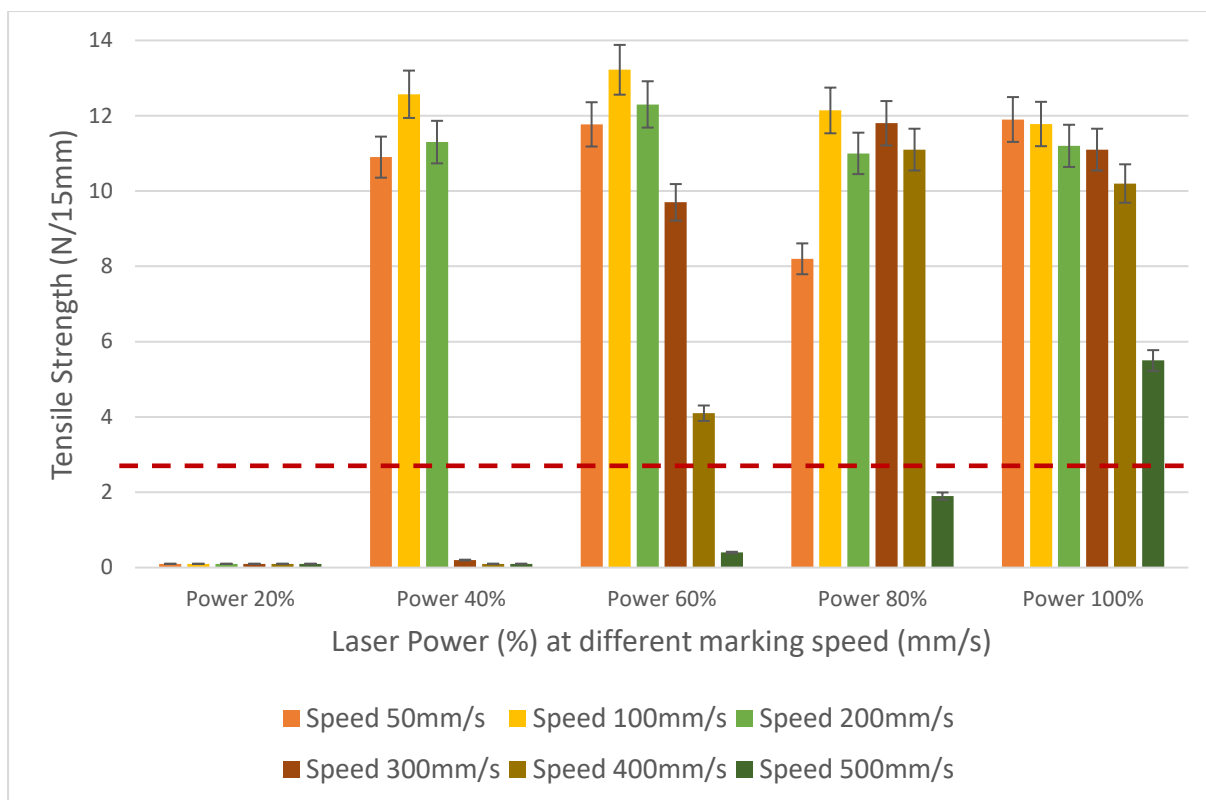


Figure 4.24: Laser welding performances of PE/BVOHc/PE film.

From now on, the threshold of the material was set to roughly 2.5N, because it is industrially speaking commonly accepted as reference value to define sealing for continuous films. In this case, the outstanding properties of polyolefins are quite explicit: seal strengths reach values above 10N, even at 400 mm/s, but performances drop after 500 mm/s welding speed.

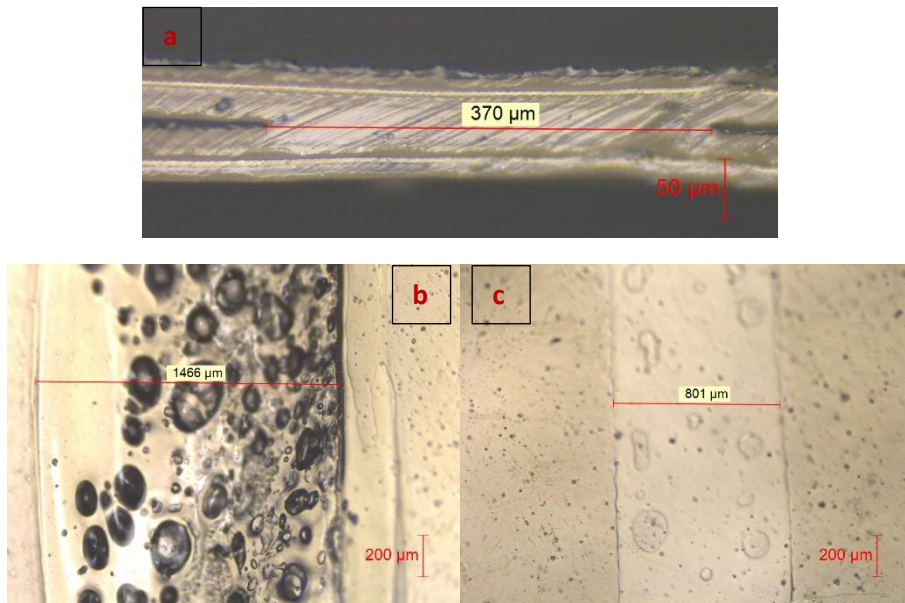


Figure 4.25 : optical microscopy images of (a) joining area from the side obtained at Power 100% and Speed 400mm/s; (b) joining area from the top obtained at Power 100% and Speed 50mm/s; (c) joining area from the top obtained at Power 100% and Speed 200mm/s.

It is also possible to observe for too low speeds (Figure 4.25b), thus too much energy in a single point, degradation phenomena along the marking (bubble of evaporation of the material, darkening due to carbonization). On the other hand, for higher speeds it is observed from the side a very good melting of the two layers (Figure 4.25a).

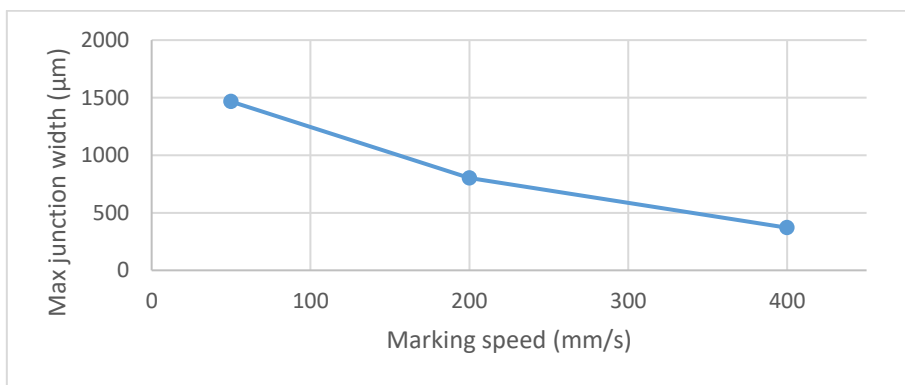


Figure 4.26: Graph of correlation between marking speed and junction width.

There is a correlation between the junction width and the marking speed (from 1466 microns at 50 mm/s to 370 microns at 400 mm/s).

4.5 PBSA + PBAT + PLA blend based film



Figure 4.27: Optical microscope image of the section of the PBSA + PBAT + PLA based film.

The material has a thickness around 30 microns, and it has been mainly characterized via DSC (Figure 4.25). In fact, the thermogram at the second scan, with more insight on the material after erasing its thermal history, shows the typical melting temperatures of PBSA ($\approx 90^\circ\text{C}$), PBAT ($\approx 120^\circ\text{C}$) and PLA ($T_m \approx 150$ and 160°C , compatible with a mixture of 90/10 (L/D,L)-PLA and 95/5 (L/D,L)-PLA). This is a typical commercially available compostable blend with sealing function.

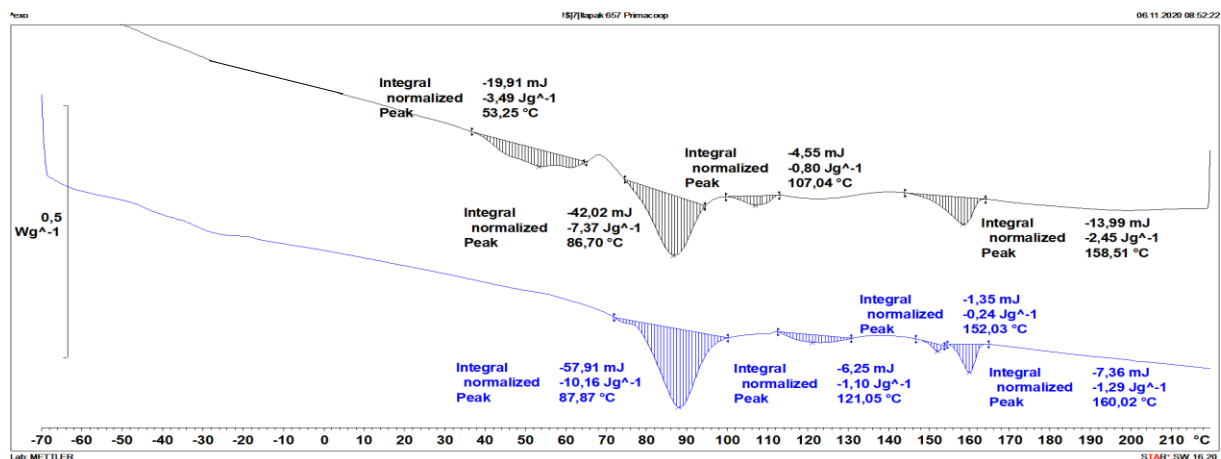


Figure 4.28: DSC curves (black first scan, blue second scan) of the PBSA + PBAT + PLA based film sample.

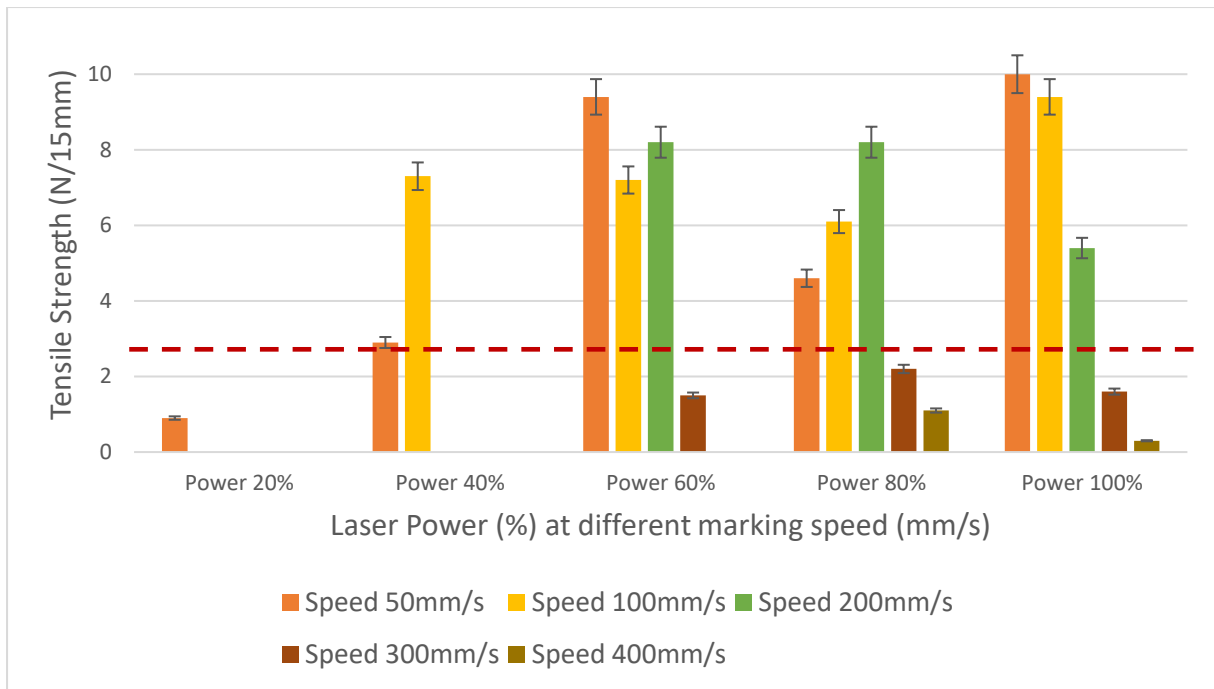


Figure 4.29: Laser welding performances of the PBSA + PBAT + PLA based film.

The good welding properties of the material are kept even using laser welding, since many tests lead to seal strengths above 6N. The best acceptable result is however at relatively low marking speed: 200mm/s.

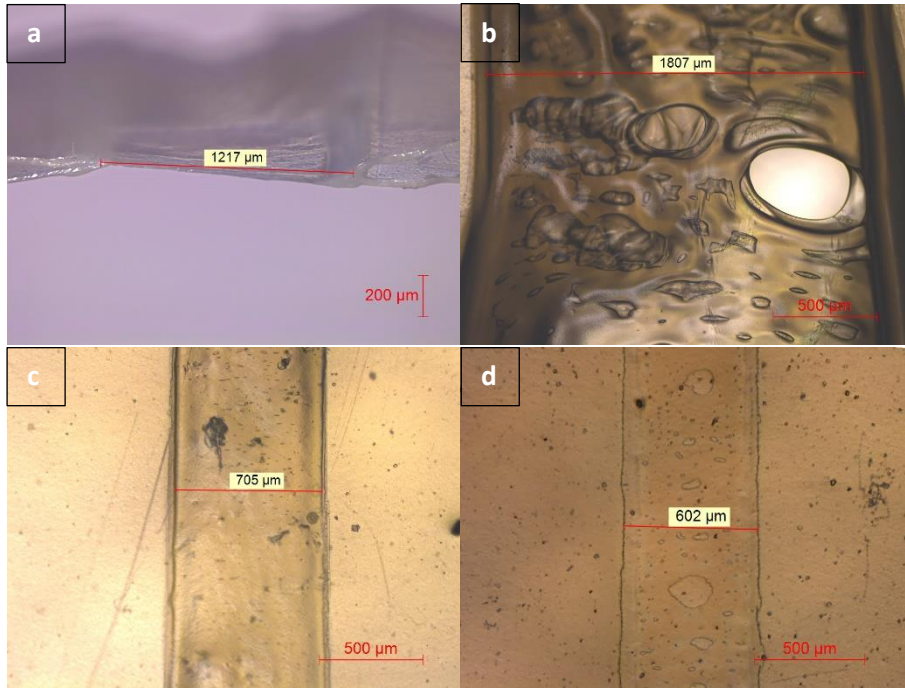


Figure 4.30: optical microscopy images of (a) joining area from the side obtained at Power 100% and Speed 100 mm/s; (b) joining area from the top obtained at Power 100% and Speed 50mm/s; (c) joining area from the top obtained at Power 100% and Speed 200mm/s; (d) joining area from the top obtained at Power 100% and Speed 400mm/s.

The observation via optical microscope (Figure 4.30) confirms the previous tendency: the higher the speed, the smaller the width of the marking (Figure 4.31, from 1807 microns at 50 mm/s to 602 microns at 400 mm/s). Please note that the marking is still present, even if the welding is not strong enough, proving that there is still a weak interaction between light and matter.

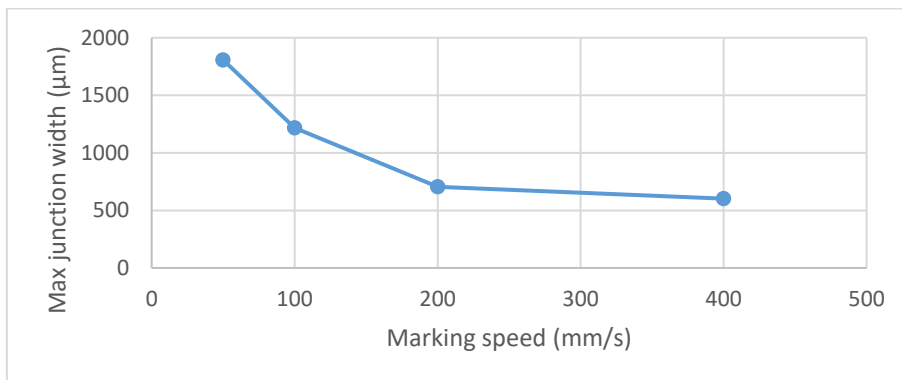


Figure 4.31: Graph of correlation between marking speed and junction width.

4.6 PBSA + PCL + PLA blend based film

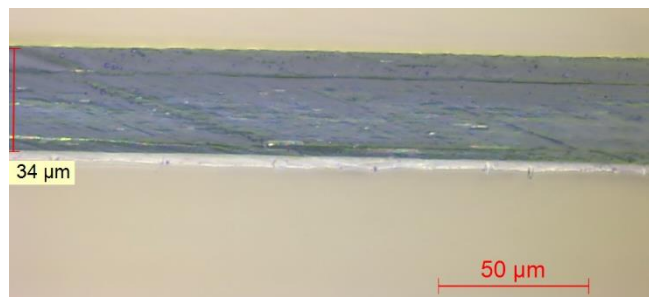


Figure 4.32: Optical microscope image of the section of the PBSA + PCL + PLA based film.

Similarly to previous case, the thickness of the film is slightly above 30 microns. Again, the main characterization consisted in DSC analysis. The DSC traces of I and II scan are reported in Figure 4.33: even in this case, we refer to the second scan. The endothermic peak at lowest temperature ($\approx 60^{\circ}\text{C}$) could be associate to the fusion of PCL; at around 87°C we observe the melting peak of PBSA and lastly at the highest temperature, about 150°C , the endothermic process due to the fusion of crystalline portion compatible to 90/10 (L/D,L)-PLA. Such crystals formed during heating scan as proved by the intense cold-crystallization peak occurring before melting one, whose heat resulted comparable to the fusion one. The result of DSC analysis is coherent with the composition of a commercially available compostable polymer blend used in packaging for sealing purposes.

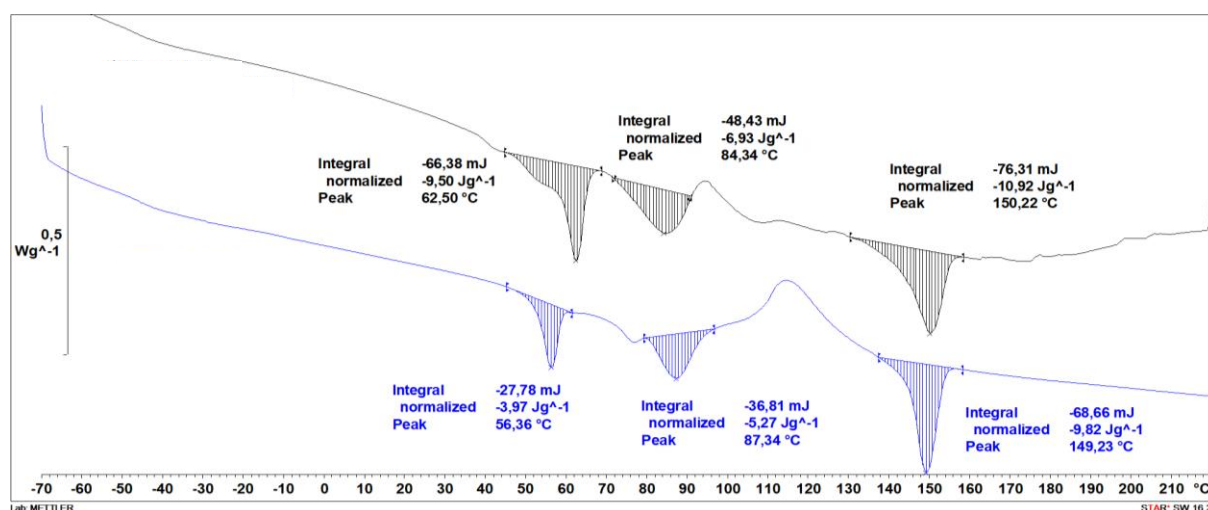


Figure 4.33: DSC curves (black first scan, blue second scan) of the PBSA + PCL + PLA based film sample.

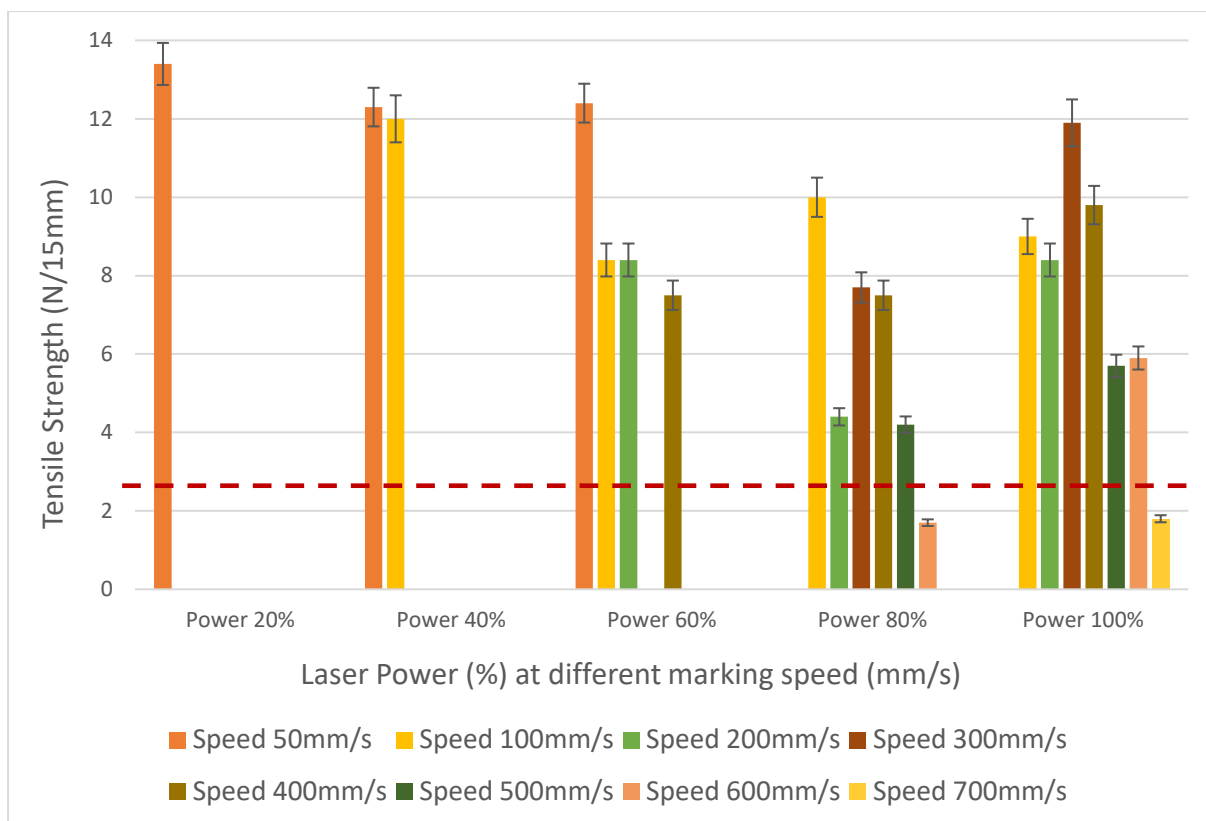


Figure 4.34: Laser welding performances of the PBSA + PCL + PLA based film.

The laser performance of this blend is better than the previous one, despite their similarities. High seal strengths are reached even at 600 mm/s of marking speed at Power 100%, while in the other case it was not possible to get over 200 mm/s. This is possibly due to the presence of PCL, which has a lower melting temperature compared to the components of the previous case, thus having a component of the blend which needs less energy to start melting.

The observations of the joining areas reveal a similar behaviour as well, even if at 100% Power and 50 mm/s (Figure 4.35a) the material appears less ruined, possibly suggesting a more efficient heat diffusion.

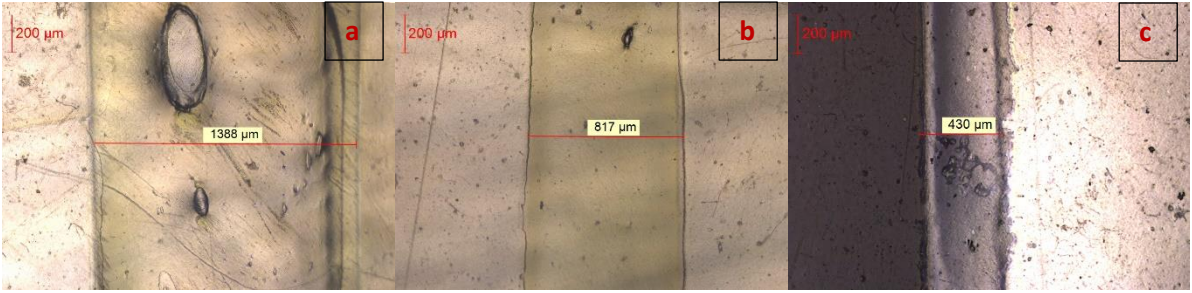


Figure 4.35: optical microscopy images of (a) joining area from the top obtained at Power 100% and Speed 50 mm/s; (b) joining area from the top obtained at Power 100% and Speed 100mm/s; (c) joining area from the top obtained at Power 100% and Speed 600mm/s.

Still, it's observed the progressive decrease of marking width, from 1388 microns at 50 mm/s to 430 microns at 600 mm/s (Figure 4.36).

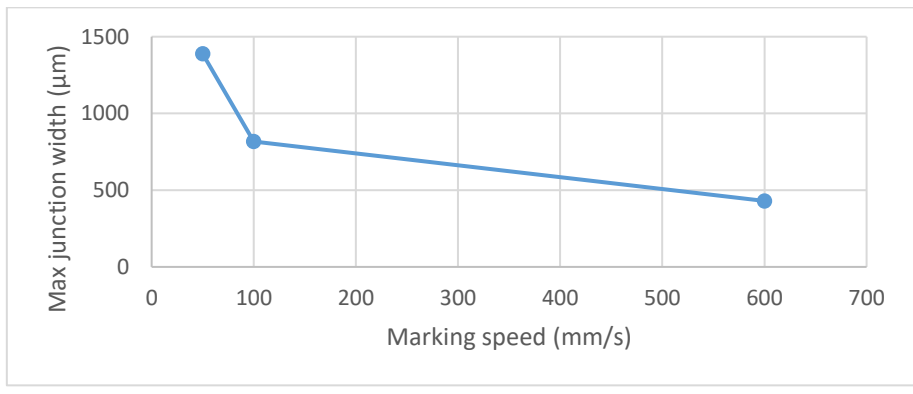


Figure 4.36: Graph of correlation between marking speed and junction width.

4.7 Cellulose Acetate + PLA multilayer

Two layers are recognizable through DSC and FT-IR formed this film: the external layer, with mechanical function, is cellulose acetate, while internal sealing layer is in PLA. In particular, the cellulose acetate layer is ca. 20 microns thick and the PLA is ca. 25 microns thick, for a total thickness around 45 microns. This material is thus compostable.

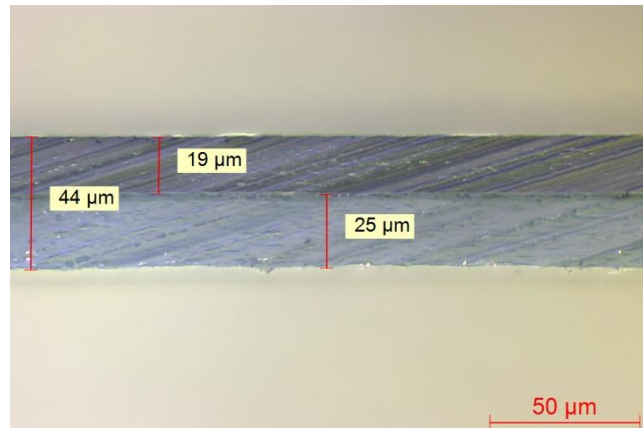


Figure 4.37: Optical microscope image of the section of the cellulose acetate-PLA multilayer.

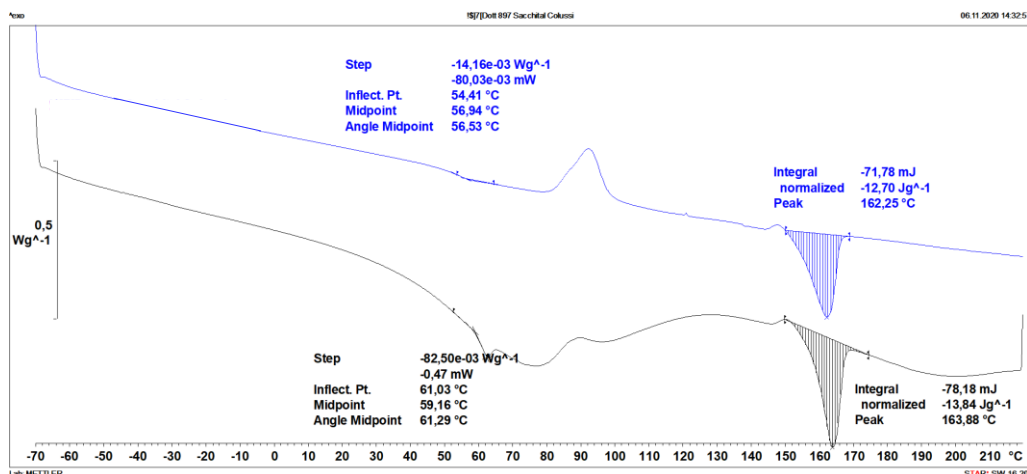


Figure 4.38: DSC curves (black first scan, blue second scan) of the cellulose acetate-PLA multilayer.

In the first scan, it's clear evident the intense and broad endothermic peak between 40 and 120 °C typical of cellulose releasing humidity absorbed thanks to its -OH groups. At higher temperature (163 °C), the melting peak, of a PLA crystalline phase. After cooling at 20°C/min

rate, the second scan only exhibits the PLA melting peak, while the cellulose water loss completely disappears as expected.

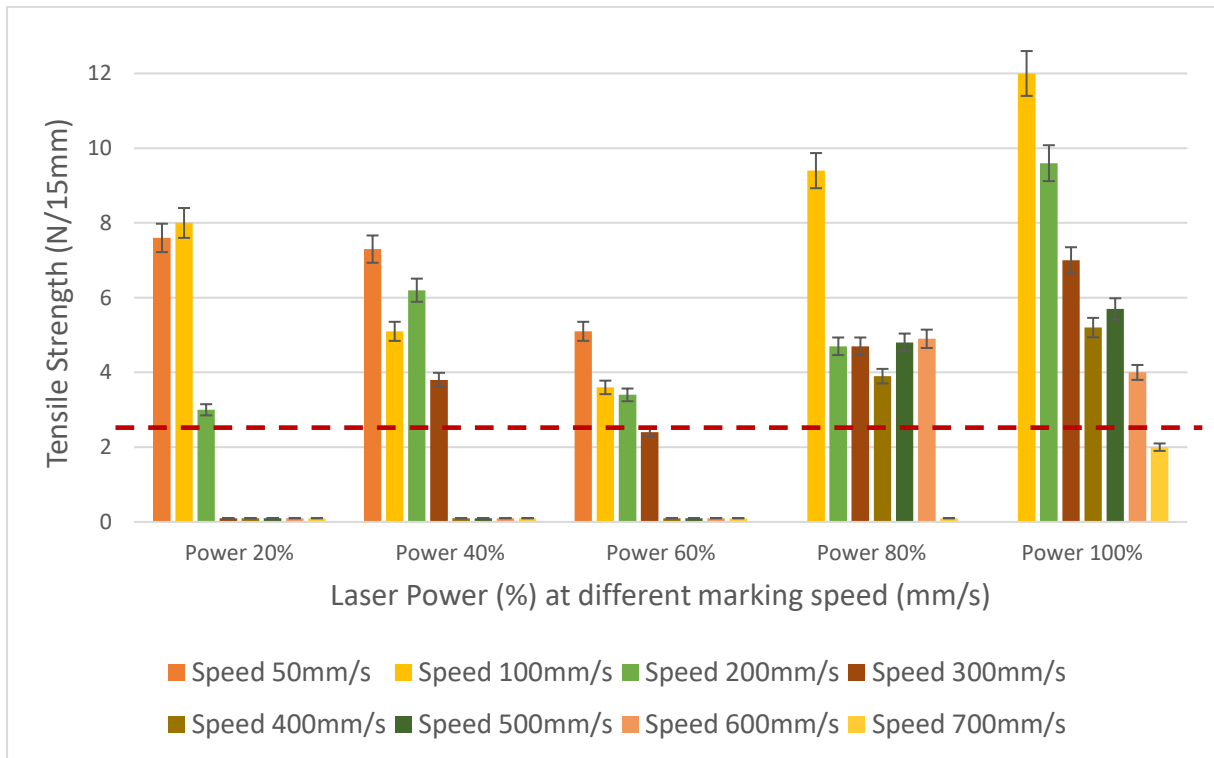


Figure 4.39: Laser welding performances of the cellulose acetate-PLA multilayer.

As to laser welding performances, these appeared quite good, with strengths above 8N under certain conditions (Speed 100-200 mm/s and Power 80-100%); moreover, acceptable seals are obtained up to 600 mm/s. It is worth noting that while cellulose is normally burned by Thulium laser radiation, when it's laminated with PLA, no detriment effect on welding capability is observed.

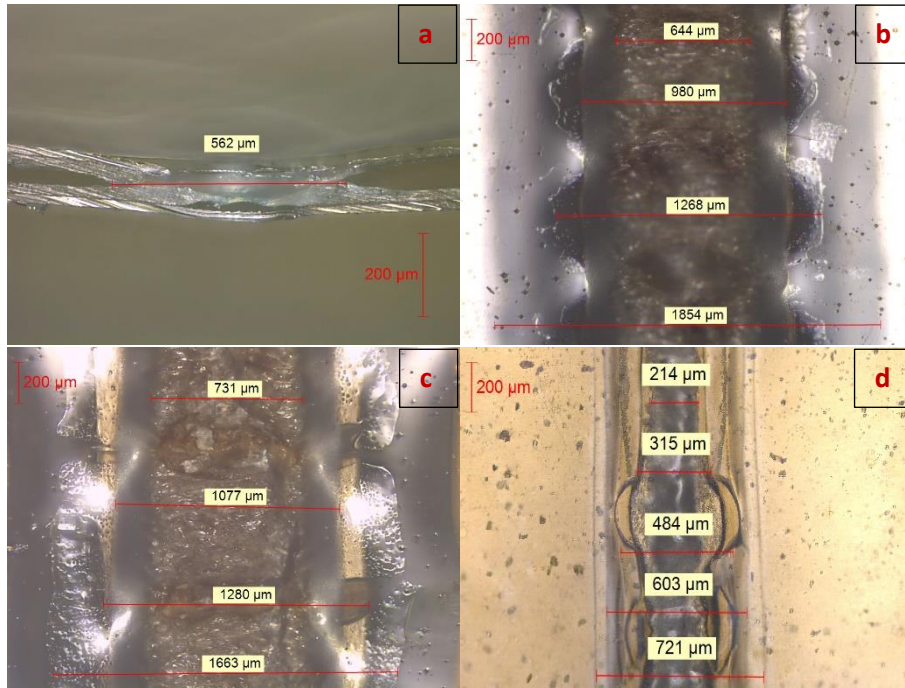


Figure 4.40: optical microscopy images of (a) joining area from the side obtained at Power 100% and Speed 300 mm/s; (b) joining area from the top obtained at Power 80% and Speed 100 mm/s; (c) joining area from the top obtained at Power 100% and Speed 100mm/s; (d) joining area from the top obtained at Power 100% and Speed 700mm/s.

The tendency of decreasing junction width by speeding up the marking velocity is still observed, confirming that the amount of energy over time is an important factor of the process and that can be tuned by changing laser power or marking speed.

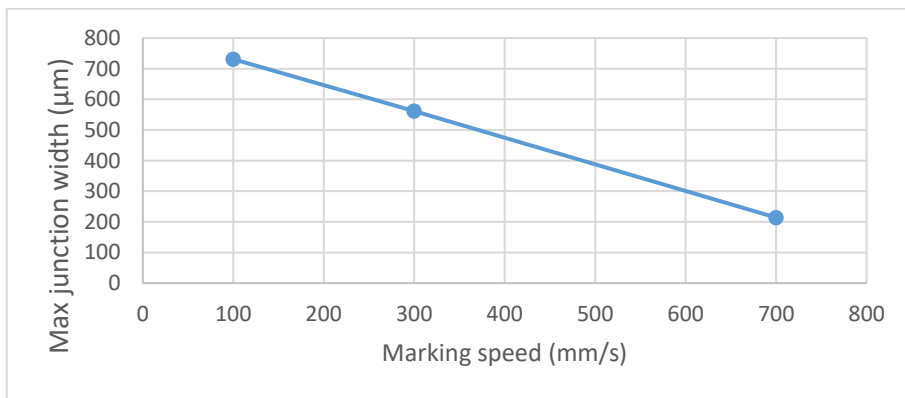


Figure 4.41: Graph of correlation between marking speed and junction width.

4.8 Cellulose Acetate + PBS multilayer

Another cellulose acetate based compostable multilayer film was characterized and tested. The cellulose acetate layer is the same thickness, but this time the sealing layer is ca. 35 microns, for a total thickness of ca. 55 microns.

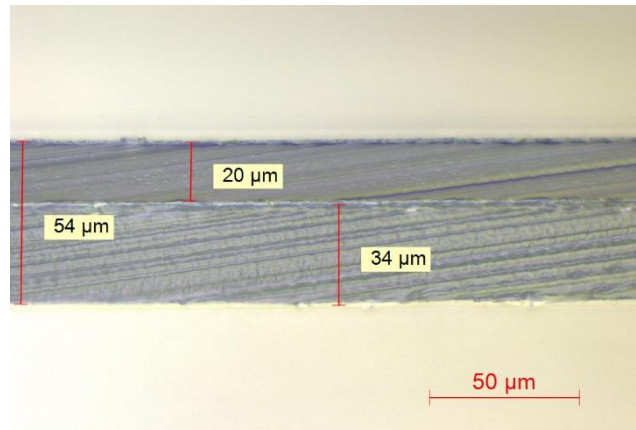


Figure 4.42: Optical microscope image of the section of the cellulose acetate-PBS multilayer.

The first scan DSC analysis shows again the cellulose humidity loss endo peak that disappears in the second scan, leaving only one endothermic peak that can be identified as melting phenomenon of PBS (112-113 °C).

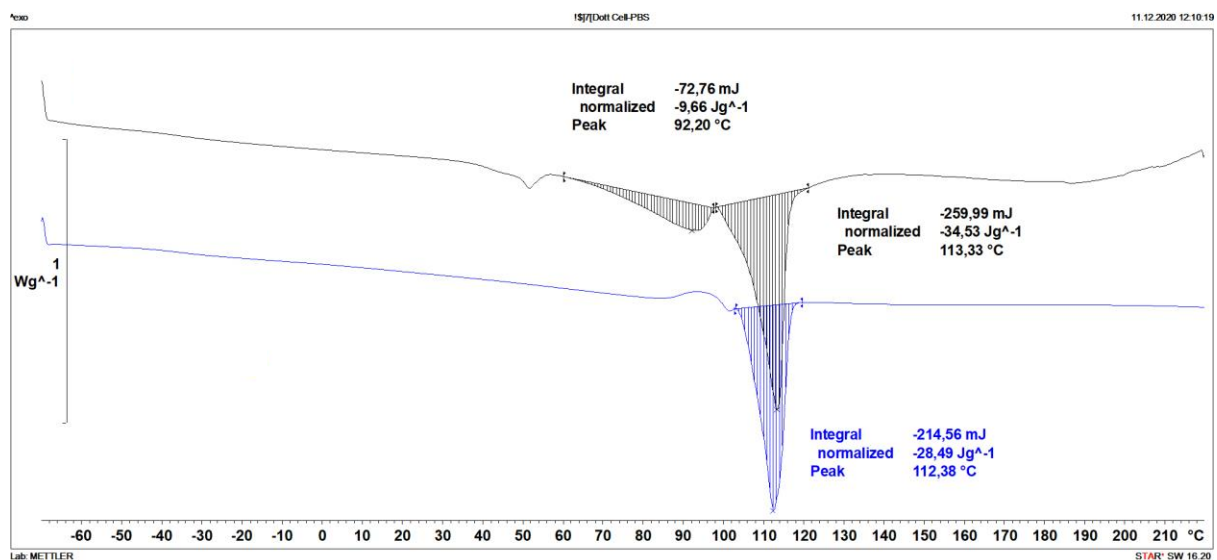


Figure 4.43: DSC curves (black first scan, blue second scan) of the cellulose acetate-PBS multilayer.

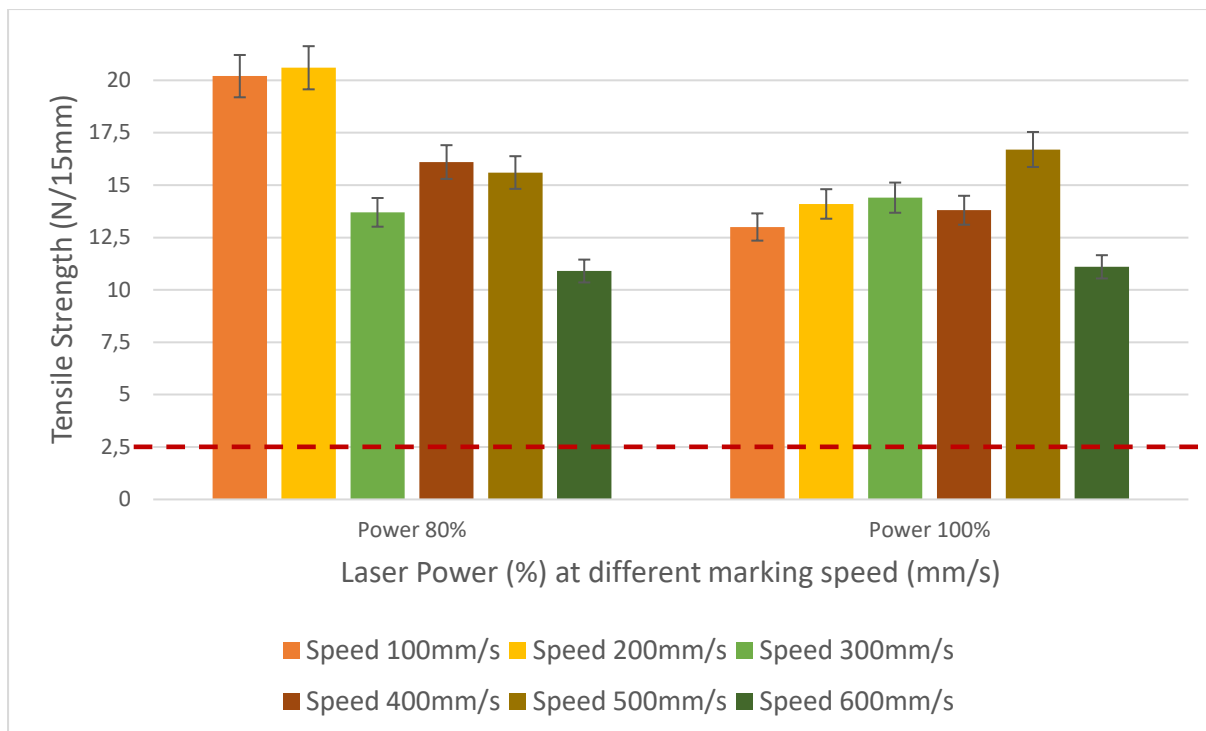


Figure 4.44: Laser welding performances of the cellulose acetate-PBS multilayer.

Laser sealing performance tests are very promising, since sealing strengths are above 10N even at 600 mm/s, while it's observed that right after this marking speed the seal strength suddenly drops and no seal is possible to be obtained. Those "drops" are a quite common behaviour, this is why probably checking an intermediate speed would lead to a more progressive diminishment of seal strength.

Having the same external cellulose layer, appearance of the laser marking is again comparable with the previous case (Figure 4.45). More images were taken in order to better build a correlation curve between junction width and marking speed (Figure 4.46).

The higher performances compared to the previous cellulose based material could be explained as due to the thicker sealing layer, which is also melting at lower temperatures, making it probably easier to weld it both with laser or more traditional methods.

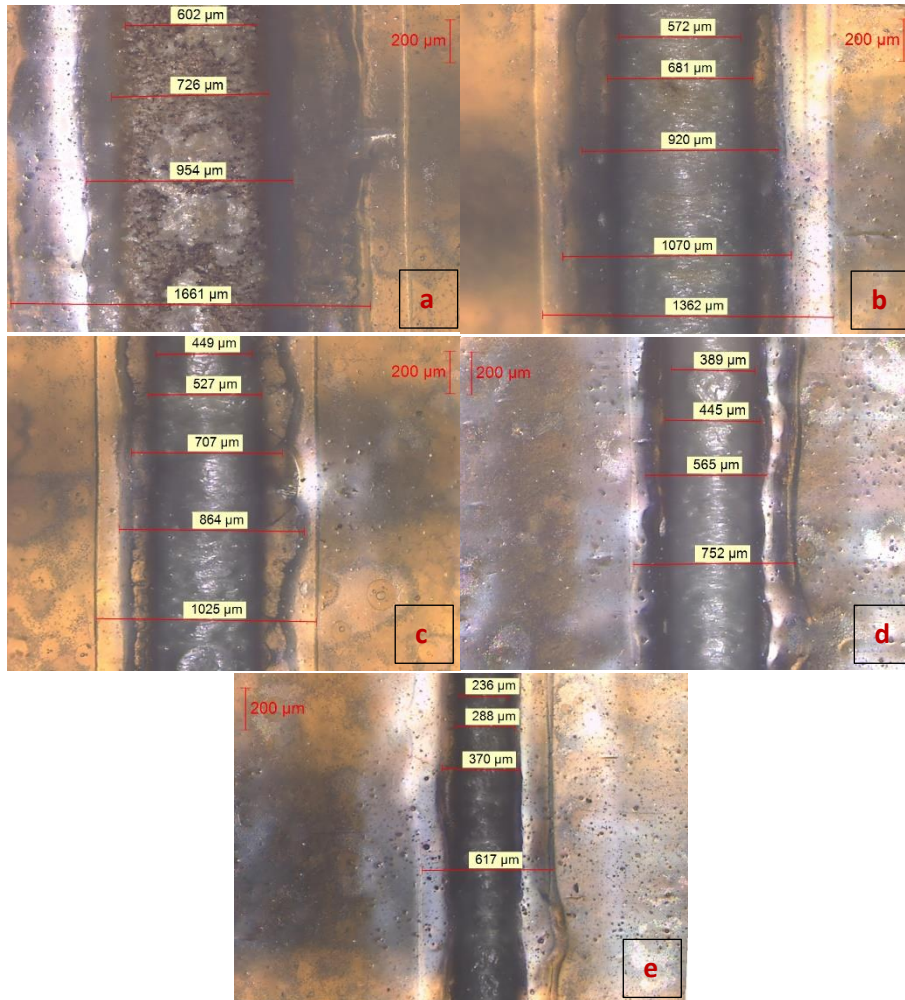


Figure 4.45: optical microscopy images of (a) joining area from the top obtained at Power 80% and Speed 100 mm/s; (b) joining area from the top obtained at Power 80% and Speed 200 mm/s; (c) joining area from the top obtained at Power 80% and Speed 300mm/s; (d) joining area from the top obtained at Power 80% and Speed 400mm/s; (e) joining area from the top obtained at Power 80% and Speed 500mm/s.

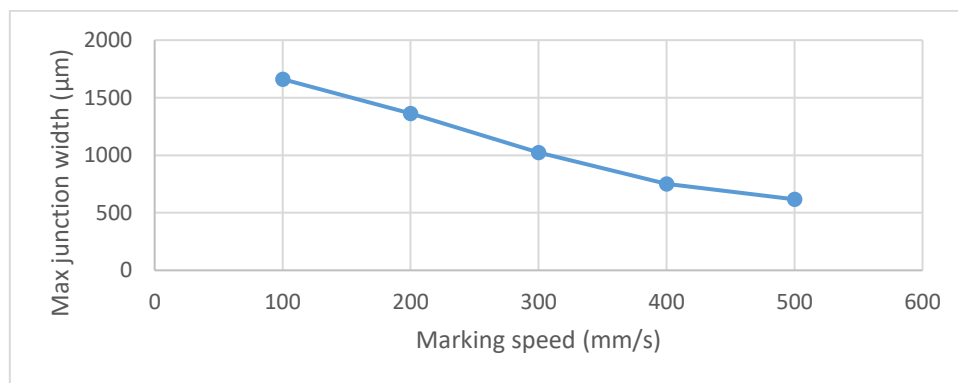


Figure 4.46: Graph of correlation between marking speed and junction width.

4.9 P (BCE_n BEPCE_m) copolymers

In this case, film thicknesses vary from 150 to 300 microns, since the films were prepared at lab scale by using compression moulding, which is a less controllable process compared to industrial films that has been taken into account up to now.

Films were fully characterized from the thermal point of view (see ref. 128), The first scan of all samples was characterized by a first small melting peak at a fix temperature, around 50°C followed by a second more intense melting phenomenon, whose temperature changed with copolymer composition, decreasing as the amount of BEPCE comonomeric units was increased. This latter peak occurred at a temperature ranging from 104 to 130°C. The parent PBCE homopolymer is a cycloaliphatic polyester melting at high temperature, around 166°C.

Due to the high thicknesses, only thinner films could be tested with the same method utilized for the other samples.

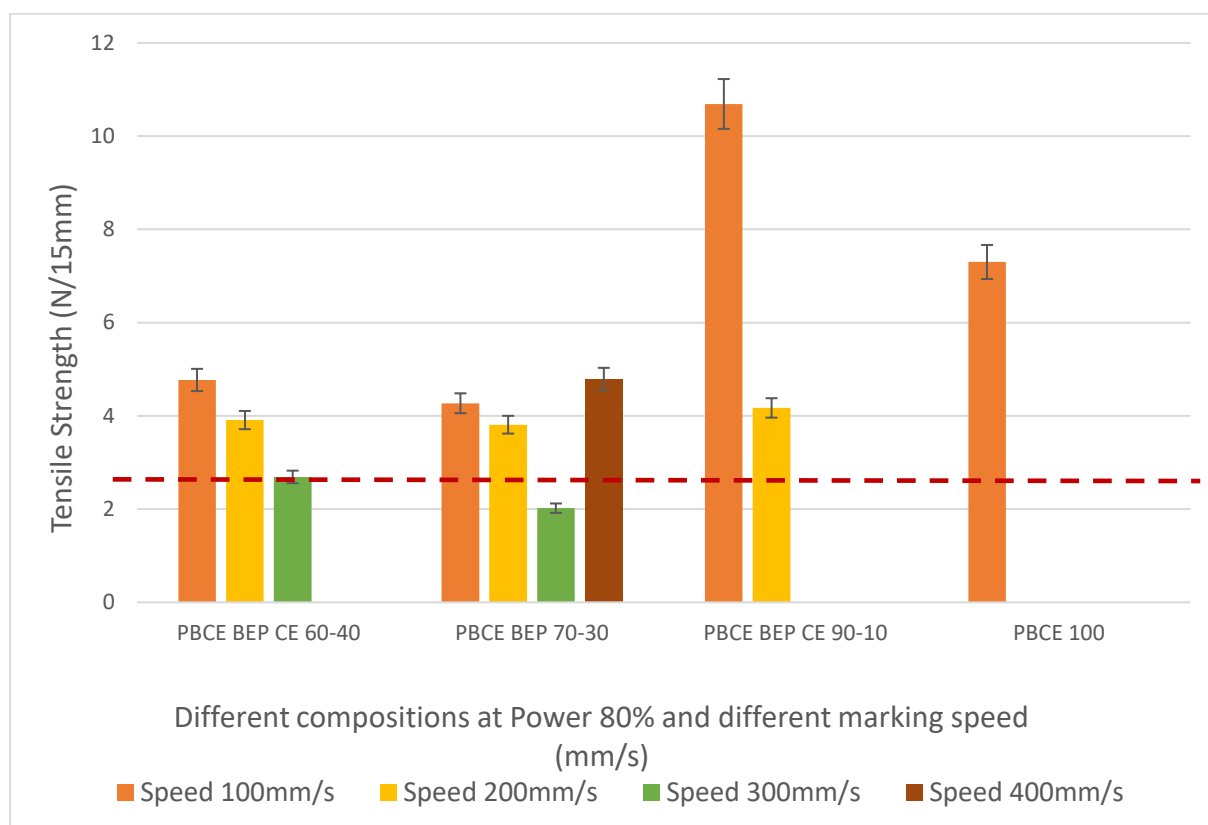


Figure 4.47: Laser welding performances of P (BCE_n BEPCE_m) copolymers

Laser welding tests show, in principle, the possibility to achieve good welding strengths. However, more homogeneously thick materials are necessary to confirm this tendency, in order to give comparable results with other materials.

On the other hand, it is probable that co-polymerization, by lowering the melting point compared to pure PBCE, makes it easier to weld the material, again both with traditional or laser welding process.

P (BCE₆₅ BEPCE₃₅) *Cis/Trans*

An interesting case is represented by the copolymer containing both *cis* (35 mol%) and *trans* isomers (65 mol%). This material is characterized by a unique melting peak at ca. 50°C, explained as due to the high irregularity of chemical structure imparted by *cis* isomer.

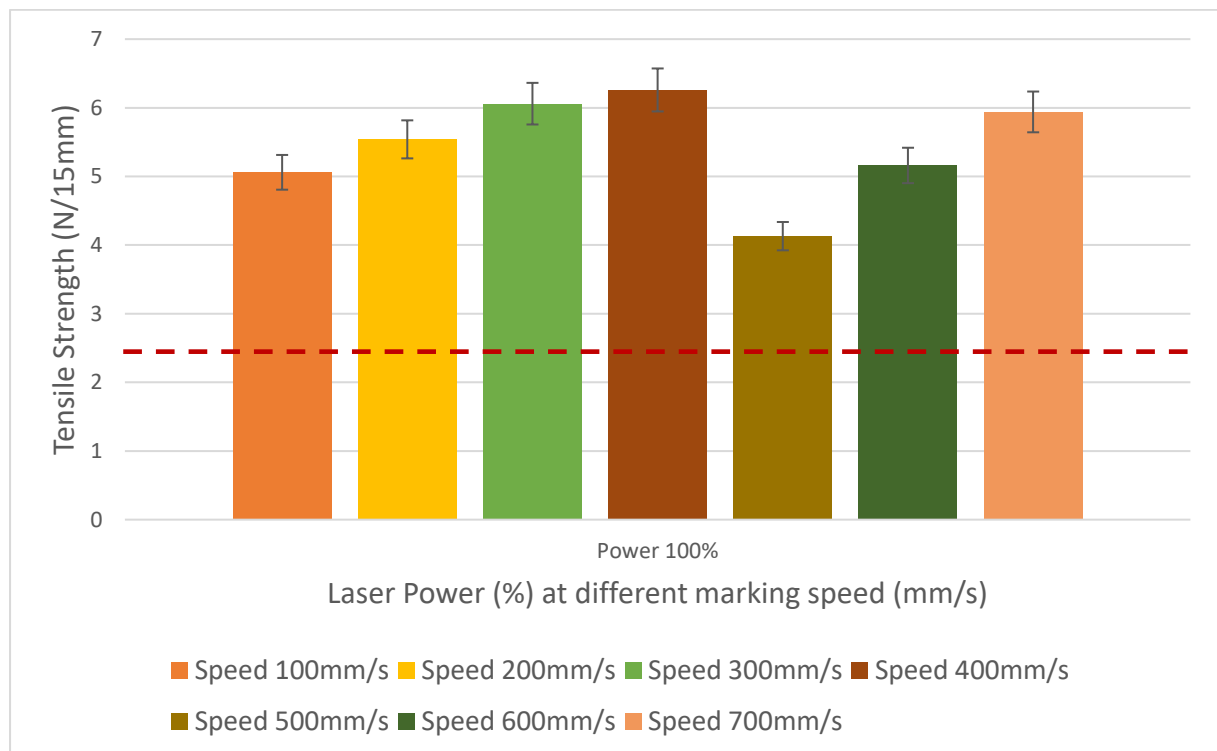


Figure 4.48: Laser welding performances of P (BCE₆₅ BEPCE₃₅) *Cis/Trans*

Laser welding performances, in facts, are well maintained up to 700mm/s marking speed. This could also depend on a less heterogeneous film thickness distribution for this particular material, thus again further testing is recommended with a more regular batch of copolymers.

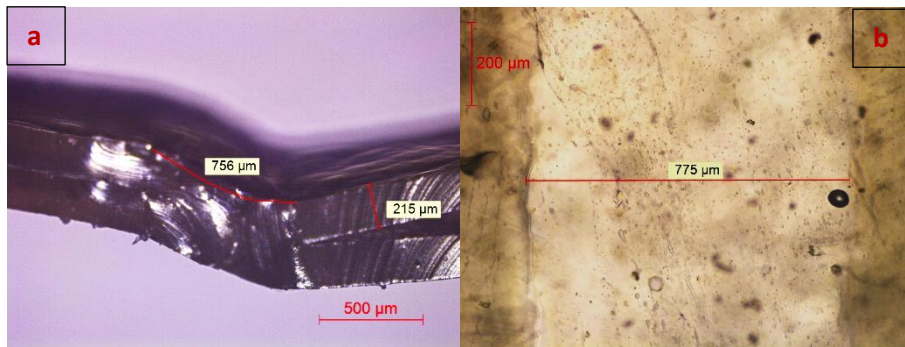


Figure 4.49: optical microscopy images of (a) joining area from the side obtained at Power 100% and Speed 200 mm/s; (b) joining area from the top obtained at Power 100% and Speed 100 mm/s;

In this case, it was possible to check on the joining area, which shows indeed a good melting between the layers. Also, the laser marking is very light, which can be an aesthetic advantage.

4.10 P (BS_n BEPS_m) copolymers

This copolymeric system was also synthesized at lab scale and characterized by Prof. Lotti's research group. The results have been published in the paper by Guidotti *et al.* (see ref. 125). The films were obtained by compression moulding, and for this reason exhibit a certain thickness variability. Anyway, it's still interesting to evaluate laser welding performances compared to other "simpler" materials.

DSC published data reveals different thermal behaviours among the copolymer containing 10 mol% BEPS co-unit and those with 20 and 30 mol%. In facts, in the first case, a single endothermic peak at 99°C was observed, while for the other two copolymers, two endothermic peaks (43-60 °C and 42-80°C for copolymers with 30 and 20 mol% BEPS co-unit, respectively) appeared in the DSC thermogram. Such multiple melting peaks can be correlated to two different crystal populations characterized by different degree of order. The low temperature melting phenomenon is due to melting of crystals with very poor degree of perfection.

Laser welding performances are less regular than in previous cases, probably again due to thickness heterogeneity, but it's clear that the poorest copolymer in BEPS co-units is better performing in terms of sealing strength up to 300 mm/s, while the other two copolymers exhibit acceptable welding resistances up to 5-700 mm/s.

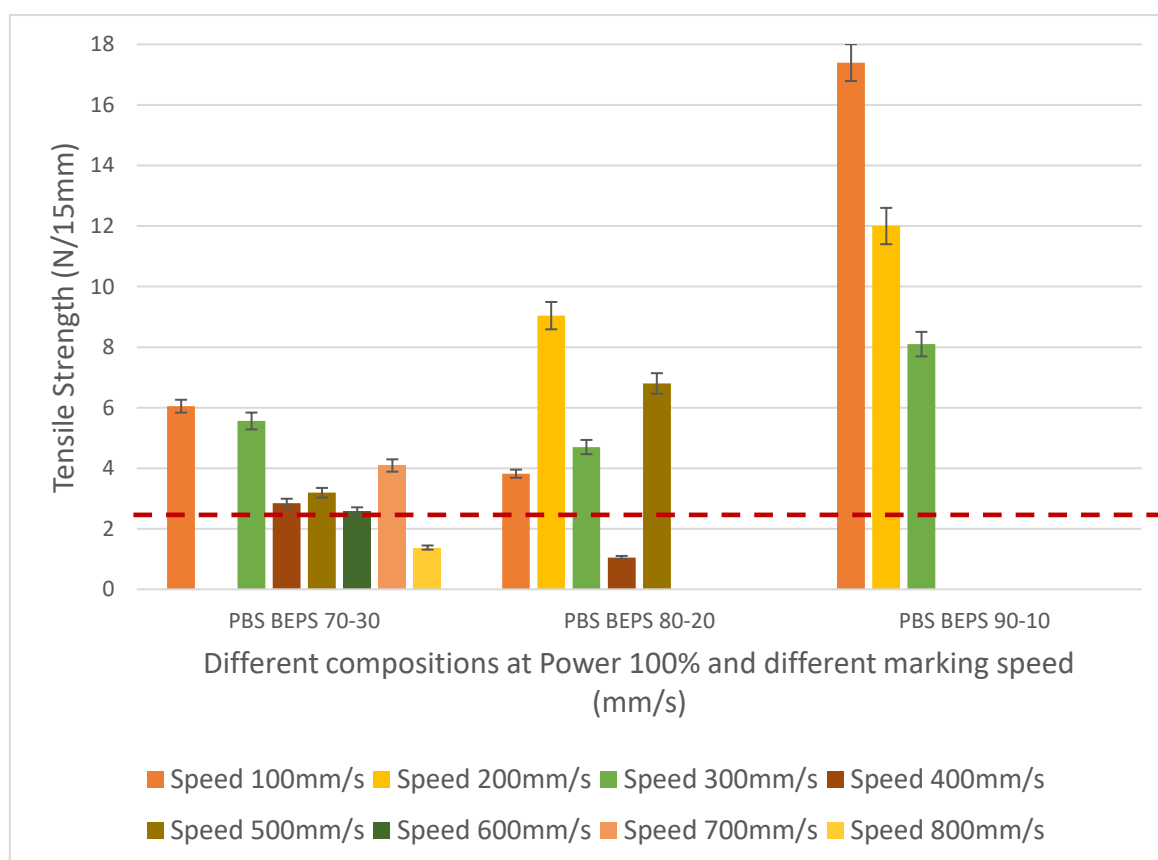


Figure 4.50: Laser welding performances of P (BS_n BEPS_m) copolymers.

Laser welding performances are less regular than other tests, probably again due to thickness heterogeneity, but it's clear that 90-10 composition is better performing in terms of sealing strength up to 300 mm/s, while it is possible for the other compositions to exhibit acceptable welding resistances up to 5-700 mm/s.

5. Conclusions

As previously stated, the aim of the work was to propose alternative technological applications for eco-friendly materials, with special focus on food packaging and industrially oriented solutions. The experimental campaign was slowed down by Covid19 emergency, which led to longer logistic and operative times.

However, more than 10 different materials were characterized and tested, some of them with special focus on their application or end-life treatment. On a certain point of view, the work was based on ready materials, not involving their important synthetic and/or filming step. On the other hand, this means that the research was deeply oriented on the development of something that is virtually market ready, with the exception of the recently published PBS copolymers, which represent more innovative materials.

The nonwovens revealed apparently suitable for tea bags laser welding and cutting application. Different fixing geometries were tested, with even higher possible marking speeds; those geometries are part of the know-how of IMA spa and may be further inspected.

An interesting aspect of the work on the recently published PBS copolymers was to suggest the idea to use new technologies to characterize new-born materials with a more final application oriented approach, adding precious information and development ideas since the very beginning of the research phase.

Another important desired consequence of the research was to stimulate the industrial interests towards eco-sustainable materials, in order to promote their use and illustrate their versatility in innovative fields. In fact, Thulium lasers are relatively new, and especially new for polymer welding applications. Obviously, these first steps can continue and spread by looking for different, even newer laser sources, which could merge a high wavelength and power with portability and flexibility.

The results showed that high speeds could be achieved by different materials: 1 m/s is considered a very high linear speed for packaging applications, and many materials could seal over 0.5 m/s with more than acceptable welding. For slower welding materials, many applications exist where speed is less important than quality of the seal e.g. doypacks for form-fill-sealing liquids that will undergo sterilization.

The innovative stimulus apparently was a success, since not only tea bags machines, but also horizontal form-fill-seal machines sector found laser technology as a possible problem solver for transversal sealing in pillow pouches. This will lead to further industrial research towards this way of thinking a known application for new fields. Next steps will be, as said, the development of new geometries for fixing the samples and in general the smartest way to install the laser on-line, in order to evaluate a real test on running industrial machinery.

6. Acknowledgments

Passiamo all'italiano per questo penultimo capitolo, visto che non tutti i diretti interessati parlano l'inglese. Voglio ringraziare tutte le persone con cui ho avuto a che fare all'Università di Bologna negli ultimi 3 (anzi 4) anni. In particolare i miei Supervisor: la Professoressa Nadia Lotti ed il Professor Maurizio Fiorini. E' stato un periodo difficile, specialmente l'ultima parte, per svariati motivi, ma sono sicuro di essere stato fortunato di aver potuto contare sul vostro consiglio e supporto. Con loro, anche i membri dei loro gruppi di ricerca che ho avuto il piacere di conoscere: il Professor Ingegnere Andra Munari, il Dott. Stefano Oradei, il Dott. Alberto Marcolongo, il Dott. Emanuele D'Angelo, la Dottoressa Elisabetta Rotante, la Dottoressa Giulia Guidotti e la Dottoressa Michelina Soccio. Ognuno di voi ha dato un contributo all'accrescimento del mio sapere ed alla crescita di questo progetto di Tesi, ed una buona parte di voi ha rappresentato una parola amica in situazioni sia serie che facete. Ultime ma non ultime, le mie giovani colleghe di Dottorato, sempre parte dell'ala di Ingegneria dei Materiali al DICAM: Silvia Quattrosoldi e Greta Giacobazzi. Spero di aver lasciato qualcosa a voi come voi l'avete lasciato a me, nel parlare delle difficoltà quotidiane di questo percorso che abbiamo affrontato, mi piace pensare di essere stato a volte come un fratello maggiore, come voi siete state per me sorelle minori (di età solamente).

Doveroso è il secondo ringraziamento a I.M.A. spa, Industria Macchine Automatiche, che ha non solo finanziato questo progetto di Dottorato, ma ha anche mostrato grande disponibilità ed interesse verso di questo, specialmente nelle persone dell'Ing. Davide Baraccani, l'Ing. Dario Rea e il Dott. Davide Paltrinieri. Non posso che sentirmi privilegiato di potervi chiamare oggi miei colleghi.

Il mio terzo ringraziamento va ai miei amici, sempre meno frequentabili, sempre più lontani, ma senza i quali la vita sarebbe decisamente più noiosa. Elencarvi tutti è impossibile, per cui ne nominerò due a caso: Luca e Giulia, miei testimoni di nozze, visto che questi ultimi tre anni hanno portato anche questa grande novità. Oltre a loro, che come pochi altri mi sono stati vicini e mi hanno cercato anche quando ero meno avvicinabile, ringrazio Michele, Piergiorgio, Federica e ancora troppi per continuare la lista senza fare torto a qualcuno.

Il penultimo ringraziamento va alla mia famiglia, che nell'ultimo anno si è improvvisamente allargata, fra suoceri e altri parenti acquisiti che mi hanno accolto (in verità da qualche anno ormai). Grazie Aldo e Mirella per aver "adottato" questo burbero genero, grazie ad Andrea e Adriana, con i miei nipoti Serena e Daniele, come pure grazie a Roberta e Dario, con le mie nipotine Giulia e Irene. Grazie a mia nonna Rosanna, perché nonostante il nonno Renato non ci sia più da qualche mese, combatti ancora e so che entrambi siete stati fra le persone che più mi hanno amato al mondo. Grazie a mia nonna Bruna, che se n'è andata il giorno prima del mio compleanno nel 2018, ma che era una delle persone con lo spirito più vivo e forte che io conoscessi, nonostante tutti gli acciacchi, ti invidierò sempre questo tuo carattere, nonostante le troppe chiacchiere.

Grazie papà Claudio, per le tue lezioni di vita (non ho detto se tramite esempi da seguire o evitare accuratamente), perché nonostante tutto quello che vuoi farci credere sei una persona buona, nobile e generosa e, per quanto tu sappia farci arrabbiare, ti vogliamo bene. Spero tu sappia ormai smussare e filtrare le mie parole, come io penso di saper smussare e filtrare le tue, per capire che alla fine il nostro rapporto padre-figlio c'è, c'è sempre stato, ed è unico.

Grazie mamma Antonella, perché sei una delle persone che più ammiro al mondo, nonostante le tue ansie e paure che a volte ti fanno esagerare. Le difficoltà della vita che stai affrontando come una leonessa sono per me fonte di ispirazione, mi dispiace solo del troppo poco aiuto che ti ho dato. Non ti dico mai abbastanza quanto bene ti voglia e quanto tu sia sempre una roccia per me, nonostante sia più grande e grosso di te dalle scuole medie ormai.

Dulcis in fundo, come per fortuna ho già avuto modo di scrivere nei ringraziamenti della tesi di laurea magistrale (7 anni fa!), il mio ultimo e più grande ringraziamento va a te: Laura. In 7 anni sono cambiate molte cose, prima fra tutte quella coppia di anelli che portiamo al dito anulare. Ci vorrebbero interi capitoli per provare anche solo lontanamente ad esprimere quello che rappresenti per me, quindi ovviamente cercherò di distillarlo in poche parole: sei l'amore della mia vita. Ho la fortuna di averti accanto ogni giorno, di condividere un progetto di una nuova famiglia, di fare mille piani e di ridere e piangere per ognuno di questi. Ogni difficoltà diventa meno spaventosa con un tuo semplice sorriso, mi dai la forza ed il coraggio di affrontare le nuove sfide che ci aspettano. Grazie di avermi accompagnato fino a questo traguardo, ma soprattutto grazie per tutta la strada che ci aspetta, cercherò sempre la tua mano per percorrerla insieme.

7. Bibliography

1. Vert, M.; Aliphatic Polyesters: Great Degradable Polymers That Cannot Do Everything; *Biomacromolecules*, **6** (2), 538-546 (2005).
2. Browne, M.A.; Dissanayake, A.; Galloway, T.S.; Lowe, D.M.; Thompson, R.C.; Ingested Microscopic Plastic Translocates to the Circulatory System of the Mussel, *Mytilus edulis* (L.); *Environmental Science & Technology*, **42** (13), 5026-5031 (2008).
3. Geissdoerfer, M.; Savaget, P.; Bocken, N.M.P. and Hultink, E.J.; The Circular Economy – A new sustainability paradigm?; *Journal of Cleaner Production*, **143**, 757–768 (2017).
4. Invernizzi, D.C.; Locatelli, G.; Velenturf, A.; Love, P.E.D.; Purnell, P.; Brookes, N.J. Developing policies for the end-of-life of energy infrastructure: Coming to terms with the challenges of decommissioning. *Energy Policy*. **144**, 111677 (2020).
5. Towards the Circular Economy: an economic and business rationale for an accelerated transition; *Ellen MacArthur Foundation*, p.24 (2012).
6. Municipal sector grapples with plastic realities; *Plastics Recycling Update* (2019).
7. Taddonio, P.; Plastics Industry Insiders Reveal the Truth About Recycling; *PBS.org, Frontline* (2020).
8. Sedaghat, L.; 7 Things You Didn't Know About Plastic (and Recycling); *National Geographic Blog* (2018).
9. Advancing Sustainable Materials Management: Facts and Figures Fact Sheet *EPA.gov* (2018).
10. www.paprec.com
11. Kaskey, J.; These companies are trying to reinvent recycling; www.bloomberg.com (2019).
12. Kreiger, M.; Anzalone, G.C.; Mulder, M.L.; Glover, A.; Pearce, J.M; Distributed Recycling of Post-Consumer Plastic Waste in Rural Areas; *MRS Online Proceedings Library*, **1492**, 91–96 (2013).
13. Staub, C.; Commercial plastics-to-fuel plant receives financing; *Plastics Recycling Update* (2019).
14. Ignatyev, I.A.; Thielemans, W.; Van der Beke, B.; Recycling of Polymers: A Review; *ChemSusChem.*, **7** (6), 1579–1593 (2014).
15. Creton, C.; Molecular stitches for enhanced recycling of packaging; *Science*, **355** (6327), 797–798 (2017).
16. Eagan J.M.; Xu, J.; Di Girolamo, R.; Thurber, C.M.; Macosko, C.W.; LaPointe, A.M.; Bates, F.S.; Coates, G.W.; Combining polyethylene and polypropylene: Enhanced performance with PE/iPP multiblock polymers; *Science*, **355** (6327), 814–816 (2017).
17. www.european-bioplastics.org
18. Lucas, N.; Bienaime, C.; Belloy, C.; Queneudec, M.; Silvestre, F.; Nava-Saucedo, J.E.; Polymer biodegradation: mechanisms and estimation techniques; *Chemosphere*, **73**, 429 (2008).

19. Luckachan, G.E.; Pillai, C.K.S.; Biodegradable Polymers- A Review on Recent Trends and Emerging Perspectives; *Journal of Polymers and the Environment*, **19**, 637-676 (2011).
20. Gross, R.A. and Kalra, B.; Biodegradable polymers for the environment; *Science*, **297**, 803-807 (2002).
21. Mark, H.; Whitby, G. S.; *Collected Works of Wallace Hume Carothers on High Polymeric Substances*, (Interscience Publishers, New York, 1940).
22. Achillas, S.; Bikiaris, D.N.; *Biodegradable Polyesters*, cap.4, (Wiley-VCH Verlag GmbH & Co.KGaA, 2015).
23. Okada, M.; Chemical syntheses of biodegradable polymers; *Prog. Polym. Sci.*, **27**, 87-133 (2002).
24. Albertsson, A.C.; Varma, I.K.; *Aliphatic Polyesters: Synthesis, Properties and Applications*; in *Advances in Polymer Science* (Springer, Berlin, Heidelberg, 2002).
25. Stillinger, F. H.; Translation-rotation paradox for diffusion in fragile glass-forming liquids; *Phys. Rev.*, **50**, 2064-2068 (1994).
26. Perez, J. Quasi-punctual defects in vitreous solids and liquid-glass transition; *Solid State Ionics*, **39**, 69-79 (1990).
27. Ediger, M. D.; Inoue, T.; Cicerone, M. T.; Blackburn, F. R.; Probe rotation near and below T_g: relationship to viscoelasticity and physical aging; *Macromol. Symp.*, **101**, 139–146 (1996).
28. Chan, R. K.; Pathmanathan, K.; Johari, G. P.; Dielectric relaxations in the liquid and glassy states of glucose and its water mixtures; *J. Phys. Chem.*, **90**, 6358-6362 (1986).
29. Roudaut, G.; Simatos, D.; Champion, D.; Contreras-Lopez, E.; Le Meste, M.; Molecular mobility around the glass transition temperature: A mini review; *Innov. Food Sci. Emerg. Technol.*, **5**, 127–134 (2004).
30. Parker, M. J.; *Test Methods, Nondestructive Evaluation, and Smart Materials*; in *Comprehensive Composite Materials* (Zweben, A. K. and C., 2000).
31. Struik, L.C.E.; Effect of thermal history on secondary relaxation processes in amorphous polymers; *Polymer (Guildf)*, **28**, 57–68 (1987).
32. Tiemblo, P.; Guzman, J.; Riande, E.; Mijangos, C.; Reinecke, H.; Erratum: Effect of physical aging on the gas transport properties of PVC and PVC modified with pyridine groups; *Polymer (Guildf)*, **42**, 8321 (2001).
33. Lotz, B.; *Phase Transitions and Structure Of Crystalline Polymers*, Institut Charles Sadron, France.
34. Soccio, M.; Lotti, N.; Gigli, M.; Finelli, L.; Gazzano, M.; Munari, A.; Reactive blending of poly(butylene succinate) and poly(triethylene succinate): characterization of the copolymers obtained; *Polym. Int.*, **61**, 1163-1169 (2012).
35. Fabbri, M.; Soccio, M, Gigli, M., Guidotti, G., Gamberini, R., Gazzano, M., Siracusa, V., Rimini, B., Lotti, N., Munari, A.; Design of fully aliphatic multiblock poly(ester urethane)s displaying thermoplastic elastomeric properties; *Polymer*, **83**, 154-161 (2016).
36. Gigli, M., Lotti, N., Gazzano, M., Finelli, L., Munari, A. Novel eco-friendly random copolyesters of poly(butylene succinate) containing ether-linkages. *React. Funct. Polym.* **72**, 303–310 (2012).

37. M. Gigli, N. Lotti, M. Gazzano, L. F. and A. M. Synthesis and Characterization of Novel Poly(butylenesuccinate)-Based Copolyesters Designed as Potential Candidates for Soft Tissue Engineering. *POLYM ENG SCI.*, **53**, 491–501 (2013).
38. Gigli, M.; Negroni, A.; Zanaroli, G.; Lotti, N.; Fava, F.; Munari, A.; Environmentally friendly PBS-based copolyesters containing PEG-like subunit: Effect of block length on solid-state properties and enzymatic degradation; *React. Funct. Polym.*, **73**, 764-771 (2013).
39. Soccio, M.; Lotti, N.; Gigli, M.; Finelli, L.; Gazzano, M.; Reactive blending of poly(butylene succinate) and poly(triethylene succinate): characterization of the copolymers obtained; *Polym. Int.*, **63**, 1163 (2012).
40. Alison, J.; Scott, A.P.; *Reference Module in Chemistry, Molecular Sciences and Chemical Engineering*; (Elsevier, 2017).
41. Nicholas, P.; *Condensed Encyclopedia of Polymer Engineering Terms*; (Elsevier, 2001).
42. Lodge, T. P.; Block copolymers: Past successes and future challenges; *Macromol. Chem. Phys.*, **204**, 265–273 (2003).
43. Müller A.J.; Arnal M.L.; Balsamo V.; Crystallization in Block Copolymers with More than One Crystallizable Block. In: Reiter G., Strobl G.R. (eds) *Progress in Understanding of Polymer Crystallization. Lecture Notes in Physics*, **714**, (Springer, Berlin, Heidelberg, 2007).
44. Zheng, Y.; Yanful, E. K.; Bassi, A. S.; A review of plastic waste biodegradation; *Crit. Rev. Biotechnol.*; **25**, 243–250 (2005).
45. Singh, B.; Sharma, N.; Mechanistic implications of plastic degradation; *Polym. Degrad. Stab.*, **93**, 561–584 (2008).
46. Sivasamy, P.; Palaniandavar, M.; Vijayakumar, C.T.; The role of β -hydrogen in the degradation of polyesters; *Polym. Degrad. Stab.*, **38**, 15–21 (1992).
47. Zimmermann H.; Chu D.D.; *Developments in Polymer Degradation* (1986).
48. Chrissafis, K.; Paraskevopoulos, K. M.; Bikiaris, D. N.; Thermal degradation mechanism of poly(ethylene succinate) and poly(butylene succinate): Comparative study; *Thermochim. Acta*, **435**, 142–150 (2005).
49. Landel R.F.; Nielsen L.E.; *Mechanical Properties of Polymers and Composites* (Boca Raton, 1993).
50. Ward I.M.; Sweeney J.; *Mechanical Properties of Solid Polymers*; (Wiley, UK, 2013).
51. Jakobsen, M.; Bertelsen, G.; CO₂ and Its Effect on Chemical, Quality Changes in the Meat : a Review; *Journal of Muscle Foods*, **13**, 143–168 (2001).
52. Tharanathan, R.N.; Biodegradable films and composite coatings: Past, present and future; *Trends Food Sci. Technol.*, **14**, 71–78 (2003).
53. Lagaron, J.M.; Catalá R.; Gavara R.; Structural characteristics defining high barrier properties in polymeric materials; *Materials science and technology*, **20**, 1-7 (2004).
54. Sano, T.; Hasegawa, M.; Kawakami, Y.; Yanagishita, H.; Separation of methanol/methyl-tert-butyl ether mixture by pervaporation using silicalite membrane; *Journal of membrane science*, **107**, 193-196 (1995).
55. Minelli, M.; Sarti, G.C.; Gas transport in glassy polymers: Prediction of diffusional time lag; *Membranes (Basel)*, **8**, 1-15 (2018).
56. Duda J.L.; *Diffusion in Polymers* (ed. P. Neogi, Marcel Dekker, US, 1996).

57. Singh A.; Koros W. J.; *Polymers* (San Francisco, 1998).
58. Weinkauff, D.H.; Paul D.R.; *Barrier Polymers and Structures* (American Chemical Society, 1990).
59. Göpferich, A.; Mechanisms of polymer degradation and erosion; *Biomaterials*, **17**, 103-114 (1996).
60. Ikada, Y.; Tsuji, H.; Biodegradable polyesters for medical and ecological applications; *Macromol. Rapid Commun.*, **21**(3), 117-132 (2000).
61. Hakkarainen, M.; *Adv. Polym. Sci.*, 2002, 157, 113–138
62. Van der Zee, M.; Structure-biodegradability relationship of polymeric material; *Dissertation University of Twente*, Enschede, The Netherlands, 213, (1997).
63. Von Burkersroda, F.; Schedl, L.; Göpferich, A.; Why degradable polymers undergo surface erosion or bulk erosion; *Biomaterials*, **23**, 4221-4231 (2002).
64. Li D.; Xia Y.N.; Electrospinning of Nanofibers: Reinventing the Wheel?; *Advanced Materials*, **16**, 1151-1170 (2004).
65. Mochizuki, M.; Hirami M.; Structural Effects on the Biodegradation of Aliphatic Polyesters; *Polym. Adv. Technol.*, **8**, 203-209 (1997).
66. Grima, S.; Bellon-Maurel, V.; Feuilloley, P.; Silvestre, F.; Aerobic Biodegradation of Polymers in Solid-State Conditions: A Review of Environmental and Physicochemical Parameter Settings in Laboratory Simulations; *Journal of Polymers and the Environment*, **8**(4), 183-195 (2000).
67. Suyama, T.; Tokiwa, Y.; Ouichanpagdee, P.; Kanagawa, T.; Kamagata, Y.; Phylogenetic Affiliation of Soil Bacteria That Degrade Aliphatic Polyesters Available Commercially as Biodegradable Plastics; *Applied and Environmental Microbiology*, **64**, 5008-5011 (1998).
68. Bastioli, C.; *Handbook of Biodegradable Polymers*; (Rapra Technology, 2005).
69. Dorsch R.R.; Miller R.W.; Tuomela M.; Degradation of lignin and other ¹⁴C-labelled compounds in compost and soil with an emphasis on white-rot fungi; *Academic dissertation in microbiology*, (Helsinki, 2002).
70. Rudnik E.; *Compostable Polymer Materials*, Elsevier, Amsterdam, 2008.
71. Albertsson, A.C.; Varma, I.K.; *Advances in Polymer Science*, 157 (Springer-Verlag, Berlin Heidelberg, 2002).
72. Diaz, A.; Katsarava, R.; Puiggali, J.; Synthesis, properties and applications of biodegradable polymers derived from diols and dicarboxylic acids: from polyesters to poly(ester amide)s; *Int. J Mol. Sci.*, **15**, 7064-7123 (2014).
73. Sokolsky-Papkov, M.; Agashi, K.; Olaye, A.; Shakesheff, K.; Domb, A.J.; Polymer carriers for drug delivery in tissue engineering; *Adv. Drug Deliv. Rev.*, **59**, 187–206 (2007).
74. Zhang, Y; Liu, Z.; Starch-based edible films, in *Environmentally Compatible Food Packaging*; E. Chiellini, Ed., (Woodhead Publishing Limited, Cambridge, UK, 2008).
75. Chang, P.R.; Jian, R.; Yu, J.; Ma, X.; Fabrication and characterisation of chitosan nanoparticles/plasticised-starch composites; *Food Chemistry*, **120**, 736-740 (2010).
76. Buono, D.; Luzi, F.; Benincasa, P.; Kenny, M.; Torre, L. and Puglia, D.; Extraction of nanostructured starch from purified granules of waxy and non- waxy barley cultivars; *Industrial Crops and Products*, **130**, 520-527 (2019).

77. Cannarsi, M.; Baiano, A.; Marino, R.; Sinigaglia, M. and Del Nobile, M. A.; Use of biodegradable films for fresh cut beef steaks packaging; *Meat Science*, **70**(2), 259-265 (2005).
78. Siracusa, V.; Rocculi, P.; Romani, S. and Rosa, M.D.; Biodegradable Polymers for Food Packaging: A Review; *Trends in Food Science & Technology*, **19**(12), 634–643 (2008).
79. Yokesahachart, C.; Yoksan, R.; Effect of amphiphilic molecules on characteristics and tensile properties of thermoplastic starch and its blends with poly(lactic acid); *Carbohydrate Polymers*, **83**, 22–31 (2011).
80. Imre, B.; García, L.; Puglia D.; Vilaplana F.; Reactive compatibilization of plant polysaccharides and biobased polymers: Review on current strategies, expectations and reality; *Carbohydr Polym*, **209**, 20-37 (2019).
81. Soccio, M.; Dominici, F.; Quattrosoldi, S.; Luzi, F.; Munari, A.; Torre, L. and Puglia, D.; PBS-Based Green Copolymer as an Efficient Compatibilizer in Thermoplastic Inedible Wheat Flour/Poly (butylene succinate) Blends; *Biomacromolecules*, **21**(8), 3254-3269 (2020).
82. Vieira, M.; Altenhofen, M.; Oliveira, L.; and Masumi, M.; Natural-based plasticizers and biopolymer films: A review; *Eur. Polym. J*, **47**, 254–263 (2011).
83. Di Franco, C.R.; Cyras, V. P.; Busalmen, J. P.; Ruseckaite, R. A. and Vazquez, A.; Degradation of polycaprolactone/starch blends and composites with sisal fibre; *Polymer Degradation and Stability*, **86**(1), 95-103 (2004).
84. Ortega-Toro, R.; Contreras, J.; Talens, P.; Chiralt, A.; Physical and structural properties and thermal behaviour of starch-poly(ϵ -caprolactone) blend films for food packaging; *Food packaging and shelf life*, **5**, 10-20 (2015).
85. Dominici, F.; Gigli, M.; Armentano, I.; Genovese, L.; Luzi, F.; Torre, L.; Munari, A. and Lotti, N.; Improving the flexibility and compostability of starch/poly(butylene cyclohexanedicarboxylate)-based blends; *Carbohydrate polymers*, **246**, 116631 (2020).
86. Zhang, J.; Sun, X.; Mechanical properties of poly (lactic acid)/starch composites compatibilized by maleic anhydride; *Biomacromolecules*, **5**, 1446–1451 (2004).
87. Olivato, J.B., Grossmann M.V.E.; Yamashita F.; Eiras D.; Pessan L.A.; Citric acid and maleic anhydride as compatibilizers in starch/poly(butylene adipate-co-terephthalate) blends by one-step reactive extrusion; *Carbohydrate Polymers*, **87**, 2614–2618 (2012).
88. Genovese, L; Dominici, F.; Gigli, M.; Armentano, I; Lotti, N.; Fortunati, E.; Siracusa, V.; Torre, L.; Munari, A.; Processing, thermo-mechanical characterization and gas permeability of thermoplastic starch/poly(butylene trans-1,4-cyclohexanedicarboxylate) blends; *Polymer Degradation and Stability*, **157**, 100-107 (2018).
89. Behjat, T.; Cellulose-Based Polymers for Packaging Applications, in *Lignocellulosic Polymer Composites*, Vijay Kumar Thakur (Ed.), 477-498 (2014).
90. Puglia, D.; Tomassucci, A.; Kenny, J.M.; Processing, Properties and Stability of Biodegradable Composites Based on Mater-Bi® and Cellulose Fibers; *Polym. Adv. Technol.*, **14** (11-12) 749-756 (2003).
91. Puglia, D.; Fortunati, E. and Kenny, J.M.; *Multifunctional Polymeric Nanocomposites Based on Cellulosic Reinforcements*, Ed. William Andrew (2016)

92. Fortunati, E.; Armentano, I.; Zhou, Q.; Puglia, D.; Terenzi, A.; Berglund, L.A.; Kenny, J.M.; Microstructure and nonisothermal cold crystallization of PLA composites based on silver nanoparticles and nanocrystalline cellulose; *Polymer Degradation and Stability*, **97**(10), 2027-2036 (2012).
93. Luzi, F.; Fortunati, E.; Puglia, D.; Lavorgna, M.; Santulli, C.; Kenny, J. M.; Torre, L.; Optimized extraction of cellulose nanocrystals from pristine and carded hemp fibres; *Industrial Crops and Products*, **56**, 175-186 (2014).
94. Cai, J.; Liu, C.; Cai, M.; Zhu, J.; Zuo, F.; Hsiao, B.; Gross, R. A.; Effects of molecular weight on poly (ω -pentadecalactone) mechanical and thermal properties; *Polymer*, **51**, 1088-1099 (2010).
95. Liu, C.; Liu, F.; Cai, J.; Xie, W.; Long, T. E.; Turner, S. R.; Lyons, A.; Gross, R. A.; Polymers from fatty acids: Poly(ω -hydroxyl tetradecanoic acid) synthesis and physico-mechanical studies; *Biomacromolecules*, **12**, 3291-3298 (2011).
96. Pepels, M.P.F.; Hansen, M.R.; Goossens, H.; Duchateau, R.; From Polyethylene to Polyester : Influence of Ester Groups on the Physical Properties; *Macromolecules*, **46**, 7668-7677 (2013).
97. Menges, M.G.; Penelle, J.; Le Fevere de Ten Hove, C.; Jonas, A.M.; Schmidt-Rohr, K.; Characterization of Long-Chain Aliphatic Polyesters: Crystalline and Supramolecular Structure of PE22,4 Elucidated by X-ray Scattering and Nuclear Magnetic Resonance; *Macromolecules*, **40**, 8714-8725 (2007).
98. Stempfle, F.; Ortmann, P.; Mecking, S.; Which Polyesters Can Mimic Polyethylene?; *Macromol. Rapid Commun.*, **34**, 47-50 (2013).
99. Trzaskowski, J.; Quinzler, D.; Baehrle, C.; Mecking, S.; Aliphatic Long-Chain C20 Polyesters from Olefin Metathesis; *Macromol. Rapid Commun.*, **32**, 1352-1356 (2011).
100. Vilela, C.; Silvestre, A.J.D.; Meier, M.A.R.; Plant Oil-Based Long-Chain C₂₆ Monomers and Their Polymers; *Macromol. Chem. Phys.*, **213**, 2220-2227 (2012).
101. Chrissafis, K.; Paraskevopoulos, K. M.; Bikiaris, D. N.; Thermal degradation mechanism of poly(ethylene succinate) and poly(butylene succinate): Comparative study; *Thermochim. Acta*, **435**(2), 142-150 (2005).
102. Gigli, M.; Fabbri, M.; Lotti, N.; Gamberini, R.; Rimini, B.; Munari, A.; (Poly(butylene succinate)-based polyesters for biomedical applications: A review in memory of our beloved colleague and friend Dr. Lara Finelli; *Eur. Polym. J.*, **75**, 431-460 (2016).
103. Gan, Z.; Abe, H.; Doi, Y.; Crystallization, Melting, and Enzymatic Degradation of Biodegradable Poly(butylene succinate-co-14 mol ethylene succinate) Copolyester; *Biomacromolecules*, **2**, 313-321 (2001).
104. Gualandi, C.; Soccio, M.; Saino, E.; Focarete, M. L.; Lotti, N.; Munari, A.; Visai, L.; Easily synthesized novel biodegradable copolyesters with adjustable properties for biomedical applications; *Soft Matter*, **8**, 5466-5476 (2012);
105. Gigli, M.; Lotti, N.; Vercellino, M.; Visai, L.; Munari, A. Novel ether-linkages containing aliphatic copolyesters of poly(butylene 1,4-cyclohexanedicarboxylate) as promising candidates for biomedical applications; *Mater. Sci. Eng. C*, **34**, 86-97 (2014).
106. <http://www.showadenko.com>.
107. <http://www.m-kagaku.co.jp>.

108. Quattrosoldi, S.; Soccio, M.; Gazzano, M.; Lotti, N.; Fully biobased, elastomeric and compostable random copolyesters of poly(butylene succinate) containing Pripol 1009 moieties: structure-property relationship; *Pol Deg Stab Accept.* (2020).
109. Varadarjan, S.; Miller, D.J.; Catalytic Upgrading of Fermentation-Derived Organic Acids; *Biotechnol. Progr.*, **15**, 845–854 (1999).
110. Soccio, M.; Lotti, N.; Finelli, L.; Gazzano, M.; Munari, A.; Influence of transesterification reactions on the miscibility and thermal properties of poly(butylene/diethylene succinate) copolymers; *Eur. Polym. J.*, **44**, 1722–1732 (2008).
111. Yoo, E.S.; Im, S.S.; Melting behavior of poly(butylene succinate) during heating scan by DSC; *J. Polym. Sci. Polym. Phys.*, **37**, 1357–1366 (1999).
112. Xu, J.; Guo, B.H.; Poly(butylene succinate) and its copolymers: Research, development and industrialization; *Biotechnol. J.*, **5**, 1149–1163 (2010).
113. Miyata, T.; Masuko, T.; Crystallization behaviour of poly(tetramethylene succinate); *Polymer*, **39**, 1399–1404 (1998).
114. Papageorgiou, G.Z.; Bikiaris, D.N.; Crystallization and melting behavior of three biodegradable poly(alkylene succinates). A comparative study; *Polymer*, **46**, 12081–12092 (2005).
115. Fabbri, M.; Gigli, M.; Gamberini, R.; Lotti, N.; Gazzano, M.; Rimini, B.; Munari, A.; Gas permeability, mechanical behaviour and compostability of fully-aliphatic bio-based multiblock poly(ester urethane)s; *Polym. Degrad. Stab.*, **108**, 223–231 (2014).
116. Fujimaki, T.; Processability and properties of aliphatic polyesters, 'BIONOLLE', synthesized by polycondensation reaction; *Polym. Degrad. Stab.*, **59**, 209–214 (1998).
117. Guidotti, G.; Soccio, M.; García-Gutiérrez, M. C.; Ezquerro, T.; Siracusa, V.; Gutiérrez-Fernández, E.; Lotti, N.; Fully Biobased Superpolymers of 2,5-Furandicarboxylic Acid with Different Functional Properties: From Rigid to Flexible, High Performant Packaging Materials; *ACS Sustain. Chem. Eng.*, **8**, 9558–9568 (2020).
118. Soccio, M.; Lotti, N.; Gazzano, M.; Govoni, M.; Giordano, E.; Munari, A.; Molecular architecture and solid-state properties of novel biocompatible PBS-based copolyesters containing sulphur atoms; *React. Funct. Polym.*, **72**, 856–867 (2012);
119. Gigli, M.; Negroni, A.; Soccio, M.; Zanaroli, G.; Lotti, N.; Fava, F.; Munari, A.; Influence of chemical and architectural modifications on the enzymatic hydrolysis of poly(butylene succinate); *Green Chem.*, **14**, 2885–2893 (2012).
120. Siracusa, V.; Lotti, N.; Munari, A.; Poly(butylene succinate) and poly(butylene succinate-co-adipate) for food packaging applications: Gas barrier properties after stressed treatments; *Polym. Degrad. Stab.*, **119**, 35–45 (2015).
121. Genovese, L.; Lotti, N.; Gazzano, M.; Siracusa, V.; Dalla Rosa, M.; Munari, A.; Novel biodegradable aliphatic copolyesters based on poly(butylene succinate) containing thioether-linkages for sustainable food packaging application. *Polym. Degrad. Stab.*, **132**, 191–201 (2016).
122. Siracusa, V.; Genovese, L.; Munari, A.; Lotti, N.; How stress treatments influence the performance of biodegradable poly(butylene succinate)-based

- copolymers with thioether linkages for food packaging applications. *Materials*, **10**, 1009 (2017).
123. Buchholz, V.; Agrawal, S.; Greiner, A.; Synthesis and enzymatic degradation of soft aliphatic polyesters; *Macromol. Biosci.*, **16**, 207–213 (2016).
124. Kint, D.P.R.; Martínez de Ilarduya, A.; Sansalvadó, A.; Ferrer, J.; Iribarren, J.I.; Muñoz-Guerra, S.; Structural characterization and thermal properties of poly(ethylene terephthalate) copolymers containing 2-Butyl-2-ethyl-1,3-propanediol; *J. Appl. Polym. Sci.*, **86**, 1077–1086 (2002).
125. Guidotti, G.; Soccio, M.; Siracusa, V.; Gazzano, M.; Salatllelli, E.; Munari, A.; Lotti, N.; Novel Random PBS-Based Copolymers Containing Aliphatic Side Chains for Sustainable Flexible Food Packaging; *Polymers*, **9**, 724 (2017).
126. Siracusa, V.; Genovese, L.; Ingraio, C.; Munari, A.; Lotti, N.; Barrier properties of poly(propylene cyclohexanedicarboxylate) random eco-friendly copolyesters; *Polymers (Basel)*, **10**(5), 502 (2018).
127. Gigli, M.; Lotti, N.; Gazzano, M.; Siracusa, V.; Finelli, L.; Munari, A.; Dalla Rosa, M.; Fully aliphatic copolyesters based on poly(butylene 1,4-cyclohexanedicarboxylate) with promising mechanical and barrier properties for food packaging applications; *Ind. Eng. Chem. Res.* **52**, 12876–12886 (2013).
128. Guidotti, G.; Soccio, M.; Siracusa, V.; Gazzano, M.; Munari, A.; Lotti, N.; Novel random copolymers of poly(butylene 1,4-cyclohexane dicarboxylate) with outstanding barrier properties for green and sustainable packaging: Content and length of aliphatic side chains as efficient tools to tailor the material's final performance; *Polymers (Basel)*, **10**, 866 (2018).
129. Soccio, M.; Martínez-Tong, D. E.; Alegría, A.; Munari, A.; Lotti, N.; Molecular dynamics of fully biobased poly(butylene 2,5-furanoate) as revealed by broadband dielectric spectroscopy; *Polymer (Guildf)*, **128**, 24–30 (2017).
130. Soccio, M.; Costa, M.; Lotti, N.; Gazzano, M.; Siracusa, V.; Salatllelli, E.; Munari, A.; Novel fully biobased poly(butylene 2,5-furanoate/diglycolate) copolymers containing ether linkages: Structure-property relationships; *Eur. Polym. J.*, **81**, 397–412 (2016).
131. Guidotti, G.; Soccio, M.; García-Gutiérrez, M. C.; Gutiérrez-Fernández, E.; Ezquerro, T. A.; Siracusa, V.; Lotti, N.; Evidence of a 2D-Ordered Structure in Biobased Poly(pentamethylene furanoate) Responsible for Its Outstanding Barrier and Mechanical Properties; *ACS Sustain. Chem. Eng.*, **7**, 17863–17871 (2019).
132. Guidotti G.; Soccio M.; Lotti N.; Siracusa V.; Gazzano M.; Munari A.; New multi-block copolyester of 2,5-furandicarboxylic acid containing PEG-like sequences to form flexible and degradable films for sustainable packaging; *Polym. Degrad. Stab.*, **169**, (2019).
133. Guidotti, G.; Soccio, M.; García-Gutiérrez, M.C.; Ezquerro, T.; Siracusa, V.; Gutiérrez-Fernández, E.; Lotti, N.; Fully Biobased Superpolymers of 2,5-Furandicarboxylic Acid with Different Functional Properties: From Rigid to Flexible, High Performant Packaging Materials; *ACS Sustain. Chem. Eng.*, **8**, 9558–9568 (2020).
134. Soccio, M.; Martínez-Tong, D. E.; Guidotti, G.; Robles-Hernández, B.; Munari, A.; Lotti, N.; Alegría, A.; Broadband dielectric spectroscopy study of biobased

- poly(alkylene 2,5-furanoate)s' molecular dynamics; *Polymers (Basel)*, **12**, 1–16 (2020).
135. Guidotti, G.; Soccio, M.; Lotti, N.; Gazzano, M.; Siracusa, V.; Munari, A.; Poly(propylene 2,5-thiophenedicarboxylate) vs. Poly(propylene 2,5-furandicarboxylate): Two examples of high gas barrier bio-based polyesters; *Polymers (Basel)*, **10**(7), 785 (2018).
 136. Guidotti, G.; Genovese, L.; Soccio, M.; Gigli, M.; Munari, A.; Siracusa, V.; Lotti, N.; Block copolyesters containing 2,5-furan and trans-1,4-cyclohexane subunits with outstanding gas barrier properties; *Int. J. Mol. Sci.*, **20**, 1–15 (2019).
 137. Gualandi, C.; Soccio, M.; Govoni, M.; Valente, S.; Lotti, N.; Munari, A.; Focarete, M.L.; Poly(butylene/diethylene glycol succinate) multiblock copolyester as a candidate biomaterial for soft tissue engineering: Solid-state properties, degradability, and biocompatibility; *J. Bioact. Compat. Polym.*, **27**, 244–264 (2012).
 138. Genovese, L.; Soccio, M.; Gigli, M.; Lotti, N.; Gazzano, M.; Siracusa, V.; Munari, A.; Biodegradable aliphatic copolyesters containing PEG-like sequences for sustainable food packaging applications; *Polym. Degrad. Stab.*, **105**, 96–106 (2014).
 139. Genovese, L.; Soccio, M.; Gigli, M.; Lotti, N.; Gazzano, M.; Siracusa, V.; Munari, A.; Gas permeability, mechanical behaviour and compostability of fully-aliphatic bio-based multiblock poly(ester urethane)s; *RSC Adv.*, **6**, 55331–55342 (2016).
 140. Gigli, M.; Lotti, N.; Siracusa, V.; Gazzano, M.; Munari, A.; Dalla Rosa, M.; Effect of molecular architecture and chemical structure on solid-state and barrier properties of heteroatom-containing aliphatic polyesters; *Eur. Polym. J.*, **78**, 314–325 (2016).
 141. Gualandi, C.; Soccio, M.; Saino, E.; Focarete, M. L.; Lotti, N.; Munari, A.; Moroni, L.; Visai, L.; Easily synthesized novel biodegradable copolyesters with adjustable properties for biomedical applications; *Soft Matter*, **8**, 5466–5476 (2012).
 142. Genovese L.; Lotti N.; Gazzano M.; Finelli L.; Munari A.; New eco-friendly random copolyesters based on poly(propylene cyclohexanedicarboxylate): Structure-properties relationships; *Express Polym. Lett.*, **9**, 972–983 (2015).
 143. Gupta, B.; Revagade, N.; and Hilborn, J.; Poly(lactic acid) fiber: An overview; *Prog. Polym. Sci.*, **32** (4), 455-482 (2007).
 144. Rasal, R.M.; Janorkar, A.V. and Hirt, D.E.; Poly(lactic acid) modifications; *Progr. Polym. Sci.*, **35**, 338–356 (2010).
 145. Gross R.A., Kalra B.; Biodegradable polymers for the environment; *Science*, **297**, 803-807 (2002).
 146. Lunt, J.; Large-scale production, properties and commercial applications of polylactic acid polymers; *Polym. Degrad. Stab.*, **59**, 145-152 (1998).
 147. Madhavan Nampoothiri, K.; Rajendran Nair, N.; John, R.P.; An overview of the recent developments in polylactide (PLA) research; *Bioresour. Technol.*, **101**, 8493 –8501 (2010).
 148. Auras, R.; Harte, B.; Selke, S.; An Overview of Polylactides as Packaging Materials; *Macromol. Biosci.*, **4**, 835–864 (2004).

149. Chen, G.-Q.; Patel, M.K.; Plastics derived from biological sources: present and future: a technical and environmental review; *Chem. Rev.*, **112**, 2082-2099 (2012).
150. Drumright, R.E.; Gruber, P.R.; Henton, D.E.; Polylactic acid technology; *Adv. Mater.*, **12**, 1841-1846 (2000).
151. Ingraio, C.; Tricase, C.; Cholewa-Wójcik, A.; Kawecka, A.; Rana R.; Siracusa, V.; Polylactic acid trays for fresh-food packaging: A Carbon Footprint assessment; *Science of the Total Environment*, **537**, 385–398 (2015).
152. Genovese, L.; Soccio, M.; Lotti, N.; Gazzano, M.; Siracusa, V.; Salatelli, E.; Balestra, F.; Munari, A.; Design of biobased PLLA triblock copolymers for sustainable food packaging: Thermo-mechanical properties, gas barrier ability and compostability; *Eur. Polym. J.*, **95**, 289–303 (2017).
153. Armentano, I.; Bitinis, N.; Fortunati, E.; Mattioli, S.; Rescignano, N.; Verdejo, R.; Lopez-Manchado M.A.; Kenny J.M.; Multifunctional nanostructured PLA materials for packaging and tissue engineering; *Progress in Polymer Science*, **38** (10–11), 1720-1747 (2013).
154. Fortunati, E.; Peltzer, M.; Armentano, I.; Torre, L.; Jiménez, A.; Kenny, J.M.; Effects of modified cellulose nanocrystals on the barrier and migration properties of PLA nano-biocomposites; *Carbohydrate Polymers*, **90**(2), 948-956 (2012).
155. Fortunati, E.; Peltzer, M.; Armentano, I.; Torre, L.; Jiménez, A.; Kenny, J.M.; Effects of modified cellulose nanocrystals on the barrier and migration properties of PLA nano-biocomposites; *Carbohydrate Polymers*, **90**(2), 948-956 (2012).
156. Burgos, N.; Armentano, I.; Fortunati, E.; Dominici, F.; Luzi, F.; Fiori, S.; Cristofaro, F.; Visai, L.; Jiménez, A.; Kenny, J.M.; Functional Properties of Plasticized Bio-Based Poly(Lactic Acid)_Poly(Hydroxybutyrate) (PLA_PHB) Films for Active Food Packaging; *Food Bioprocess Technol*, **10**, 770–780 (2017).
157. Lizundia, E.; Fortunati, E.; Dominici, F.; Vilas, J.L.; León, L.M.; Armentano, I.; Torre, L.; Kenny, J.M.; PLLA-grafted cellulose nanocrystals: Role of the CNC content and grafting on the PLA bionanocomposite film properties; *Carbohydrate Polymers*, **142**, 105-113 (2016).
158. Armentano, I.; Fortunati, E.; Burgos, E.; Dominici, F.; Luzi, F.; Fiori, S.; Jiménez, A.; Yoon, K.; Ahn, J.; Kang, S.; Kenny, J.M.; Bio-based PLA_PHB plasticized blend films: Processing and structural characterization; *LWT - Food Science and Technology*, **64**(2), 980-988 (2015).
159. Aluigi, A.; Tonetti, C.; Rombaldoni, F.; Puglia, D.; Fortunati, E.; Armentano, I.; Santulli, C.; Torre, L. and Kenny, J.M.; Keratins extracted from Merino wool and Brown Alpaca fibres as potential fillers for PLLA-based biocomposites; *J Mater Sci*, **49**, 6257–6269 (2014).
160. Armentano, I.; Bitinis, N.; Fortunati, E.; Mattioli, S.; Rescignano, N.; Verdejo, R.; Lopez-Manchado, M.A.; Kenny, J.M.; Multifunctional nanostructured PLA materials for packaging and tissue engineering; *Progress in Polymer Science*, **38** (10–11), 1720-1747 (2013).

161. Armentano, I.; Fortunati, E.; Burgos, N.; Dominici, F.; Luzi, F.; Fiori, S.; Jiménez, A.; Yoon, K.; Ahn, J.; Kang, S.; Kenny, J. M.; Processing and characterization of plasticized PLA/PHB blends for biodegradable multiphase systems; *EXPRESS Polymer Letters*, **9**(7), 583–596 (2015).
162. De Azeredo, H. M. C.; Nanocomposites for food packaging applications; *Food Research International*, **42**(9), 1240-1253 (2009).
163. Davis, G.; and Song, J. H.; Biodegradable packaging based on raw materials from crops and their impact on waste management; *Industrial Crops and Products*, **23**(2), 147-161 (2006).
164. Sorrentino, A.; Gorrasi, G.; and Vittoria, V.; Potential perspectives of bio-nanocomposites for food packaging applications; *Trends in Food Science & Technology*, **18**(2), 84-95 (2007).
165. Siracusa, V.; Blanco, I.; Romani, S.; Tylewicz, U.; Rocculi, P.; Dalla Rosa, M.; Poly(lactic acid)-Modified Films for Food Packaging Application: Physical, Mechanical, and Barrier Behavior; *J. Appl. Polym. Sci.*, **125**, E390-E401 (2012).
166. López, O.V.; Castillo, L.A.; García, M.A.; Villar, M.A.; Barbosa, S.E.; Food Packaging Bags Based on Thermoplastic Corn Starch Reinforced with Talc Nanoparticles; *Food Hydrocolloids*, **43**, 18-24 (2015).
167. Amanatidou, A.; Slump, R. A.; Gorris, L. G. M. and Smid, E. J. ; High Oxygen and High Carbon Dioxide Modified Atmospheres for Shelf-life Extension of Minimally Processed Carrots; *J. Food. Sci.*, **65**, 61–66 (2000).
168. Barry-Ryan, C. and Beirne, D. O.; Effects of peeling methods on the quality of ready-to-use carrot slices; *Int J. Food Sci. Technol.*, **35**, 243–254 (2000).
169. Sandhya, S.; Modified atmosphere packaging of fresh produce: Current status and future needs; *LWT-Food. Sci. Technol.*, **43**, 381–392 (2010).
170. Russo, G. M.; Simon, G. P.; and Incarnato, L.; Correlation between Rheological, Mechanical, and Barrier Properties in New Copolyamide-Based Nanocomposite Films; *Macromolecules*, **39**(11), 3855-3864 (2006).
171. Hotchkiss, J. H.; Safety considerations in active packaging. In: *Active Food Packaging* (Springer US, 1995).
172. Pasha, I.; Saeed, F.; Tauseef Sultan, M.; Rafiq Khan M.; Rohi, M.; Recent Developments in Minimal Processing: A Tool to Retain Nutritional Quality of Food; *Critical Reviews in Food Science and Nutrition*, **54**, 340–351 (2014).
173. Ohlsson, T. and Bengtsson, N.; *Minimal Processing Technologies in the Food Industry*, 1st ed. (CRC Press, Washington, DC, 2002).
174. Farber, J. N.; Harris, L. J.; Parish, M. E.; Beuchat, L. R.; Suslow, T. V.; Gorney, J. R.; Garrett, E. H. and Busta, F. F.; Microbiological Safety of Controlled and Modified Atmosphere Packaging of Fresh and Fresh-Cut Produce; *Rev. Food Sci. Food Safety*, **2**, 142–160 (2003).
175. Xing, Y.; Li, X.; Xu, Q.; Jiang, Y.; Yun, J. and Li, W.; Effects of chitosan-based coating and modified atmosphere packaging (MAP) on browning and shelf life of fresh-cut lotus root (*Nelumbo nucifera* Gaerth); *Innovat. Food Sci. Emerg. Technol.*, **11**, 684–689 (2010).
176. Scott, G.; “Green” Polymers; *Polymer Degradation and Stability*, **68**, 1-7 (2000).

177. Halek, G.W.; Relationship between polymer structure and performance in food packaging applications; *American Chemical Society*, **16**, 195-202 (1988).
178. Conn, R.E.; Kolstad, J.J.; Borzelleca, J.F.; Dixler, D.S.; Filer, Jr. L.J.; LaDu, Jr. B.N.; Pariza, M.W.; Safety assessment of polylactide (PLA) for use as a food-contact polymer; *Food and Chemical Toxicology*, **33**(4), 273-283 (1995).
179. Wilson, A.; in: *Applications of Nonwovens in Technical Textiles*. Chapman, R. ed. (Woodhear Publishing Ltd., Cambridge, 2010).
180. <http://www.freedoniagroup.com/DocumentDetails.aspx?ReferrerId=FG-01&studyid=2983>.
181. Bhat G. and Parikh D.V.; in: *Applications of Nonwovens in Technical Textiles*. Chapman, R. ed. (Woodhear Publishing Ltd., Cambridge, 2010).
182. Stojko, M.; Włodarczyk, J.; Sobota, M.; Karpeta-Jarząbek, P.; Pastusiak, M.; Janeczek, H.; Dobrzyński, P.; Starczynowska, G.; Orchel, A.; Stojko, J.; Batoryna, O.; Olczyk, P.; Komosińska-Vassev, K.; Olczyk, K.; Kasperczyk, J.; Biodegradable Electrospun Nonwovens Releasing Propolis as a Promising Dressing Material for Burn Wound Treatment; *Pharmaceutics*, **12**(9), 883 (2020).
183. Balkan, O.; Demirer, H.; Ezdeşir, A. and Yıldırım, H; Effects of welding procedures on mechanical and morphological properties of hot gas butt welded PE, PP, and PVC sheets; *Polymer Engineering and Science*, **48**(4), 732 (2008).
184. Grewell, D.; Rooney, P.; Kagan, V.A.; Relationship between optical properties and optimized processing parameters for through-transmission laser welding of thermoplastics; *Journal of Reinforced Plastics and Composites*; **23**(3), 239–47 (2004).
185. Olowinsky, A.; Boglea, A.; Gedicke, J.; Innovative laser welding processes; *Laser Technik Journal*, **5**(3), 48–51 (2008).
186. Horn, W.; Strategies for polymer welding with high-power diode lasers; *Key Engineering Materials*, **447–448**: 277–81 (2010).
187. Jaeschke, P.; Herzog, D.; Haferkamp, H.; Peters, C.; Herrmann, A.S.; Laser transmission welding of high-performance polymers and reinforced composites - a fundamental study; *Journal of Reinforced Plastics and Composites*, **29**(20), 3083–94 (2010).
188. Hilton, P.A.; Jones, I.A.; Kennish, Y.; Transmission laser welding of plastics; *Proc. SPIE*, First International Symposium on High-Power Laser Macroprocessing, **4831**, 44 (2003).
189. Troughton; M.J.; *Handbook of Plastic Joining - A Practical Guide*. (William Andrew Publishing, 2008).
190. Ruotsalainen, S.; Laakso, P.; Kujanpää, V.; Laser Welding of Transparent Polymers by Using Quasi-simultaneous Beam Off-setting Scanning Technique; *Physics Procedia*, **78**, 272–284 (2015).
191. Tres, P.A.; Welding Techniques for Plastics; in: *Designing Plastic Parts for Assembly (eighth ed.)*, (München: HANSER, 2017).
192. Grewell, G.A.; Benatar, A.; Park, J.; *Plastics and Composites Welding Handbook*. (München: HANSER, 2003).

193. Benatar, A.; Plastics Joining; in: *Handbook of Applied Plastics Engineering (second ed.)*, (Library of Plastics Architecture, 2017).
194. Troughton, M.J.; *Plastic Joining Manual - A Practical Guide*; (William Andrew Publishing, 2008).
195. PDL Staff; Laser Welding; in: *Handbook of Plastics Joining* (Plastics Design Library, 1997).
196. Acherjee, B.; Kuar, A.S.; Mitra, S.; Misra, D.; Effect of carbon black on temperature field and weld profile during laser transmission welding of polymers: A FEM study; *Optics & Laser Technology*, **44** (3), 514-521 (2012).
197. Pagano, N.; Campana, G.; Fiorini, M.; Morelli, R.; *Optics & Laser Technology*, **91**, 80-84 (2017).
198. Mc Comb, T.S.; Sims R.A.; Willis C.C.C.; Kadwani P.; Sudesh V.; Shah L. and Richardson, M.; High-power widely tunable thulium fiber lasers; *Applied Optics*, **49**(32): 6236–6242 (2010).
199. Mingareev, I; Weirauch, F.; Olowinsky, A; Shah, L.; Kadwani, P; Richardson, M.; Welding of polymers using a 2 μ m thulium fiber laser; *Optics & LaserTechnology*, **44**, 2095–2099 (2012).